Universidade de Aveiro Departamento de Química
ANO 2014

CARLA MARIA BATISTA GONÇALVES

PROPRIEDADES DE BARREIRA DE FILMES BASEADOS EM POLI(ÁCIDO LÁCTICO)

BARRIER PROPERTIES OF POLY(LACTIC ACID) BASED FILMS

Universidade de Aveiro Departamento de Química
ANO 2014

CARLA MARIA BATISTA GONÇALVES

PROPRIEDADES DE BARREIRA DE FILMES BASEADOS EM POLI(ÁCIDO LÁCTICO)

BARRIER PROPERTIES OF POLY(LACTIC ACID) BASED FILMS

Tese apresentada à Universidade de Aveiro para cumprimento dos requisitos necessários à obtenção do grau de Doutor em Engenharia Química, realizada sob a orientação científica da Doutora Isabel Maria Delgado Jana Marrucho Ferreira, Investigadora Coordenadora do Instituto de Tecnologia Química e Biológica António Xavier da Universidade Nova de Lisboa e do Professor Doutor João Manuel da Costa Araújo Pereira Coutinho, Professor Catedrático do Departamento de Química da Universidade de Aveiro.

Apoio financeiro do POCTI no âmbito do III Quadro Comunitário de Apoio.

Apoio financeiro da FCT e do FSE no âmbito do III Quadro Comunitário de Apoio.

Dedico este trabalho à minha mãe.

o júri

presidente

Doutor Luís Filipe Pinheiro de Castro
professor catedrático da Universidade de Aveiro

Doutor Adélio Miguel Magalhães Mendes
professor associado com agregação da Faculdade de Engenharia da Universidade do Porto

Doutor Nelson Simões Oliveira
professor adjunto do Instituto Politécnico de Leiria

Doutora Ana Maria Antunes Dias
investigadora auxiliar da Faculdade de Ciências e Tecnologia da Universidade de Coimbra

Doutor João António Baptista Pereira de Oliveira
professor associado da Universidade de Aveiro

Doutora Isabel Maria Delgado Jana Marrucho Ferreira
investigadora coordenadora do Instituto de Tecnologia Química e Biológica Antonio Xavier da Universidade Nova de Lisboa

agradecimentos

À Universidade de Aveiro e, em particular, ao Departamento de Química e ao CICECO, pelas condições e meios proporcionados para a execução do presente trabalho. À Fundação para a Ciência e a Tecnologia (FCT), pelo financiamento dos meus estudos através de uma bolsa de doutoramento (SFRH/BD/23455/2005) e apoios associados.

À Doutora Isabel Marrucho e ao Professor Doutor João Coutinho por me integrarem na sua equipa de investigação, pelo apoio e confiança.

Ao Professor Doutor Adélio Mendes e à Lúcia Brandão pela ajuda na construção do equipamento de time-lag.

Ao Professor Doutor João Oliveira pelos esclarecimentos sobre a técnica de QCM

A todos os colegas e amigos que estão sempre por perto e que têm demonstrado ao longo destes anos uma verdadeira amizade.

Ao pessoal da Enarpur, em especial ao Hugo e ao Sérgio, por me auxiliarem nestes últimos meses para finalização desta dura etapa.

Ao Gil, ao "Gilinho" e à Inês ….eles sabem porquê!!!

palavras-chave

Poliácido láctico, PLA, embalagem activa, α-tocoferol, BHT, TBHQ, microbalança de cristais de quartzo, QCM, time-lag, sorção, permeabilidade, solubilidae e difusão.

resumo

Nos últimos anos temos assistido à procura de produtos amigos do ambiente. Um dos maiores desafios tem sido a procura de materiais biodegradáveis que possam substituir materiais vulgarmente designados por "plástico". Se há dezenas de anos o plástico veio, por exemplo, substituir o marfim nas bolas de bilhar, salvando vidas de milhares de elefantes, hoje, procuramos um substituto para esse plástico, de forma a preservar as condições ambientais que nos permitem viver harmoniosamente com a restante fauna e flora, e que a espécie humana tem, nos últimos anos, vindo a destruir. O plástico é um derivado do petróleo, cujo preço tem vindo a crescer exponencialmente, devido ao facto de ser barato e possuir propriedades que permitem desenhar produtos essenciais à vida quotidiana. Por isso, precisamos de sair da era petroquímica e entrar numa nova era ambientalmente sustentável, baseada em materiais biodegradáveis provenientes de fontes renováveis. Esta mudança para rotas "verdes", só será possível com o apoio de grandes empresas, e medidas governamentais drásticas. O poliácido láctico, PLA, produzido a partir da lactose presente no amido ou no açúcar, tem sido intensivamente estudado nos últimos anos e possui potencial para substituir os tradicionais polímeros derivados do petróleo, se forem melhoradas algumas propriedades necessárias ao processamento por extrusão. O PLA, é muito frágil, pouco resistente e pouco flexível. Neste trabalho foram adicionados antioxidantes naturais (alfa-tocoferol) e sintéticos (BHT e TBHQ) ao PLA com o objetivo não só de melhorar as suas propriedades mecânicas, mas também de criar uma embalagem ativa que prolongue o prazo de validade dos alimentos e melhore as suas propriedades organoléticas prevenindo alterações ou perda de sabor. O impacto da adição destes antioxidantes nas propriedades originais do PLA a nível mecânico, térmico e de barreira foi estudado pela utilização das técnicas de FTIR, DSC, SEM, AFM, DMA, TGA, QCM e *time-lag*.

keywords

Poly(lactic acid), PLA, active packaging, α-tocopherol, BHT, TBHQ, quartz crystal microbalance, time-lag, sorption, permeability, solubility and diffusivity.

abstract

In recent years, the search for a environmentally friendly products has increased. One of the major challenges has been the demand for biodegradable materials that can replace plastic. If a few decades ago, plastic replaced, for example, the ivory in billiard balls, and in other products, saving the lives of thousands elephants, nowadays a replacement for that plastic is being searched, to prevent the change of the environmental conditions, essential to life in harmonly with the fauna and flora that the human specie has, in recent years, destroyed. Plastic is a petroleum derivate, whose price has been growing exponentially, mainly due to the fact of beind a cheap material and also to enable the production of products that are essential to modern life. Therefore, the petrochemical era is going to come to an end and a new environmentally sustainable era, based on biodegradable materials from renewable sources, will follow. The change to green routes only will be possible with the support of the major companies, and the implementation of drastic governmental law.

Poly(lactic acid), PLA, is produced from the lactose present in the corn or sugarcane and has been intensively studied in recent years because if some limitants properties required its extrusion are overcome, it has the potential to replace the traditional polymers. PLA have high brittleness, low toughness and low tensile elongation. In this work, natural antioxidant (alpha-tocopherol) and synthetics antioxidants (BHT ant TBHQ) were added to the PLA with the aim not only to improve their flexibility, but also to create an active packaging to extend the shelf life of the foods and improve the organoleptic properties by preventing food losses. The impact of the addition of antioxidants into the PLA films, in its mechanical, thermal and barrier properties were studied by FTIR, DSC, SEM, AFM, DMA, TGA, QCM and time-lag techniques.

Contents

List of Figures

List of Tables

Nomenclature

aTC -α-tocopherol,

BHT - 2,6-bis(1,1-dimethylethyl)-4-methylphenol

C - solubility of the gas in polymer

D – diffusion coefficient

DMSM - dual-mode sorption model

E_D - activation energy for gas diffusion

E_P – activation energy for gas permeation

E_S - activation energy for gas sorption

MAP - modified atmosphere packaging

New- DMS – New dual-mode sorption model

P - octanol-water partition coefficient

P – permeation coefficient

PA - polyamide

PBS – polybutadiene styrene

PC – polycarbonate

PE - Polyethylene

PEG - poly(ethylene glycol)

PEN – Polyethylene napthalene,

PET - polyethylene terephthalate

PHB-co-V-

PLA – Poly(lactic acid)

PLA (98:2)- PLA (% L: % D)

PP - polypropylene

PS - polystyrene

PVC - polyvinylchloride

S – sorption coefficient

TBHQ- 2-(1,1-Dimethylethyl)-1,4-benzenediol or *tert*-Butylhydroquinone

T_C – Crystallization temperature

Tg - Transition temperature

Tm – melting temperature

1. Introduction

1.1. Context

Since their pioneering days over a hundred years ago, plastics have greatly improved human living conditions and are indispensable and irreplaceable in modern everyday life. As a result of their resource, efficient production processes, facile processing, and high versatility in terms of tunable properties and broad range of applications, these materials render high technologies affordable for all humankind.[1] Plastics are versatile materials potentially indestructible, ideal for a number of commercial and domestic applications. Every day thousands of tones of plastic are used and disposed in the form of disposable cups to thin cellular packing. Statistics show that about 85 % of these plastics are sent to landfill or dumped elsewhere.[2] Every year in Europe, 10 million tones of post-consumer plastic waste are buried in landfills[3], that are quickly reaching their capacities, and consequently new landfills are opened, generating great environmental threat in the coming years. Although plastics take long time to break down, only about 5 % of plastics used are currently being recycled.[2] Plastics make our life easier and better, e.g. when used as packaging they can safely protect from damage and leaking and deliver a product unalterable from the manufacturer to the consumer, in a world where one more day of shelf life matters and simultaneously safety cannot be compromised. The world's plastic consumption has increased incredibly in recent decades, generating more and more plastic waste, thus increasing the public concern.[4] Petrochemical-based plastics such as Polyethylene (PE) polypropylene (PP), polyvinylchloride (PVC), polystyrene (PS) and polyethylene terephthalate (PET) and polyamide (PA) have been increasingly used as packaging materials due not only to their large availability at relatively low cost, but also to their good mechanical performance such as tensile and tear strength, good barrier to oxygen, carbon dioxide and aroma compound, heat sealability, and so on. [5]

Worldwide plastics production increased 4 % in 2011, with more than 10 million tons of plastics produced. Polyolefins, PP, PVC, PET and PS account for about 70 % of the total global demand, i.e. 200 million tons. From 2010 to 2016, global plastics consumption is expected to grow by an average of about 4 % each year. The world will consume 540 million tons of plastic in 2020.[6] Figure 1 present the estimates of worldwide production by 2016. [4]

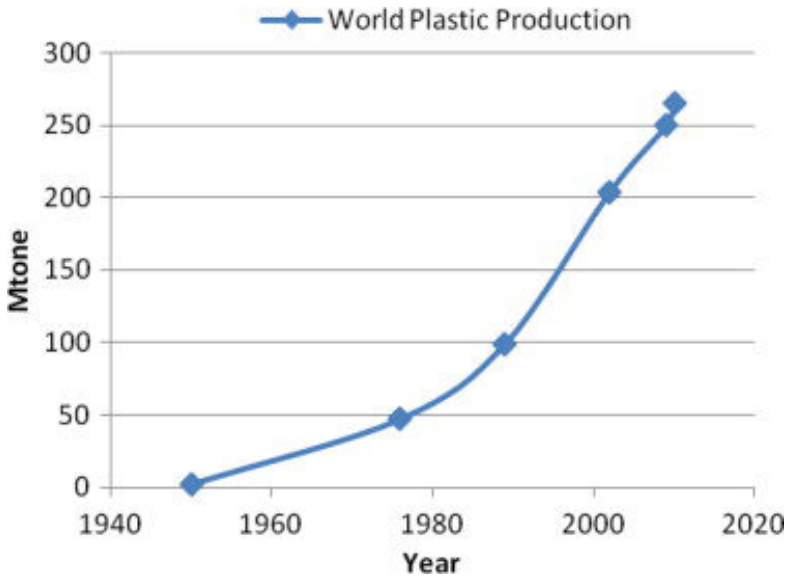

Figure 1 - Estimates of the worldwide production of plastics. [4]

During the 20th century, a great variety of synthetic polymers became available at industrial scale. This was mainly due to the petrochemistry, a strong technology emerging since the 1950s. Exploitation of oil and gas as fossil raw materials for the chemical industry and polymer production greatly improved cost-effectiveness and simplified manufacturing of macromolecular materials. Since then, the attractive combination of low cost with facile processing and innovation represents the key feature of plastics. In the 1990s, new recycling technologies enabled the effective reuse of polymer products that had completed their first lifecycle.[1]

Polymer wastes can thus become a valuable source of raw materials and energy. In today's highly efficient industrial polymerization processes, polymers are tailored to be stiff, soft or rubbery, conducting or insulating, optically transparent or opaque, permeable or impermeable, stable or (bio)degradable. Prominent examples of polymer applications include food and medical packaging materials, lightweight engineering plastics in the automotive and aerospace industries, damage-tolerant construction materials for modern architecture, high-strength fibers for textiles and composite materials, printed circuit boards and photoresists for microelectronics, solvent-free coatings for corrosion protection, adhesives, and new materials for biomedical applications such as wound dressing, membranes for artificial kidneys and water purification, dental fillings, drug delivery systems, artificial hearts, and implants. Plastics have become essential components of

virtually any kind of consumer product, meeting the highly diversified demands of human society.[1] Despite the many applications that a wide diversity of plastics find in different sectors, the packaging industry is by far the one that shows the highest use of these materials, as depicted in Figure 2.[6]

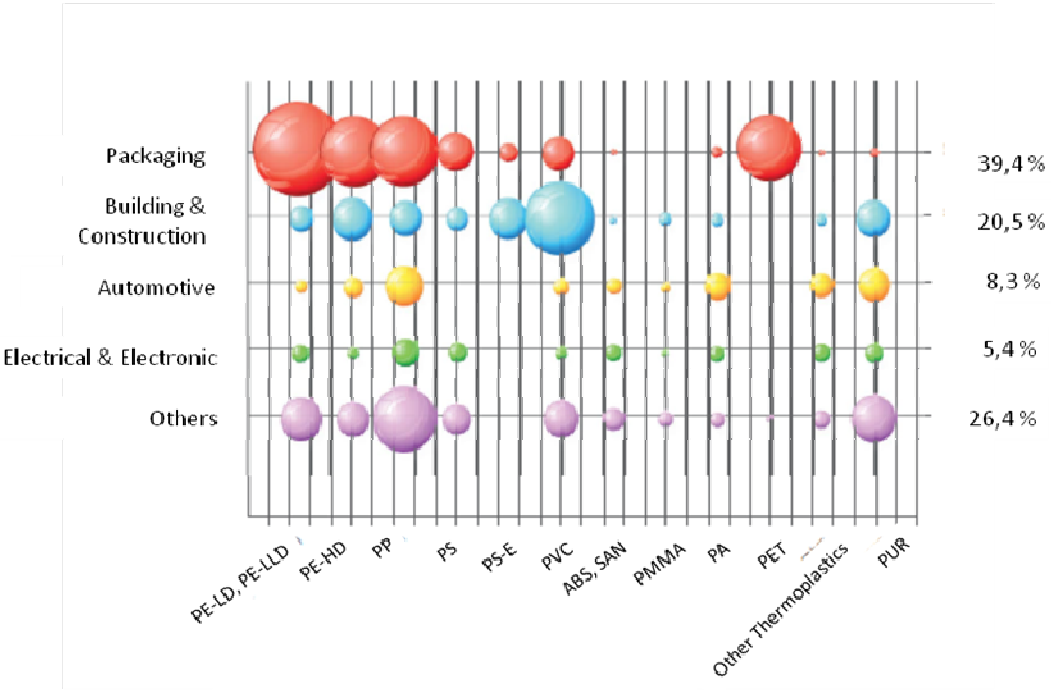

Figure 2 – European Plastics demand and its sectors of application.[6]

Food packaging is a necessary part of exchanging goods around a country and the world, securing the food supply chain. The way consumers buy goods demands protection and preservation.[5] In industrialized countries, polymer packaging secures the food supply chain, whereas in developing countries around half the food is lost in transportation.[1]

For a long time polymers have supplied most of common packaging materials because they are able to present several key features like softness, lightness and transparency. However, increased use of synthetic packaging has led to serious ecological problems due to their total non-biodegradability.[5] Figure 3 illustrates the different types of plastics used in the different packaging applications.

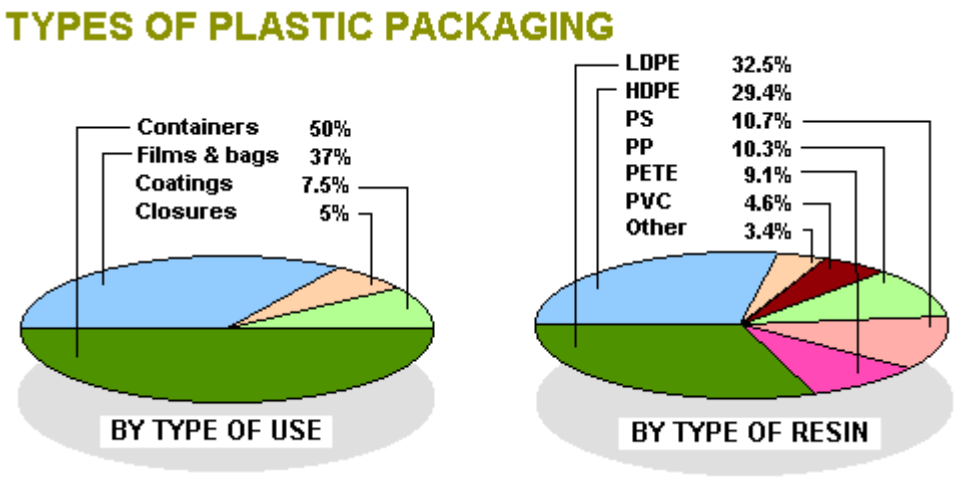

Figure 3 – Types of plastic packaging divided by type of use and type of resin.[7]

It is widely accepted that the use of long-lasting polymers from petrochemicals in products with a short life-span, such as engineering applications packaging, catering, surgery, and hygiene, is not adequate. Persistent polymers generate significant sources of environmental pollution, harming wildlife when they are dispersed in nature.[8] Moreover, incineration of plastic waste presents severe environmental issues since it yields toxic emissions (e.g., dioxins).[8] Although their complete replacement with eco-friendly packaging films is just impossible to achieve, at least for specific applications, like food packaging, the use of bioplastics is clearly the future.[5]

Today the world is quickly coming to realize the impact of packaging on human life. The world is beginning to see the effects of our existence on the planet. This has sparked a major movement towards maintaining society's thirst for goods while improving the footprint left on our planet.[5] The past few years, marked by the paradigm of sustainable development, have brought about a renewed interest in biodegradable polymers originating from renewable resources. The most important market for those novel polymers will be the packaging sector, within which food packaging represents approximately 65 % in volume.[9] Bio-based polymers offer important contributions by reducing the dependence on fossil fuels and through the related positive environmental impacts such as reduced carbon dioxide emissions.[10] The first generation of bio-based polymers focused on deriving polymers from agricultural feedstocks such as corn, potatoes, and other carbohydrate feedstocks. However, the focus has shifted in recent years due to a desire to move away from food-based resources and also significant breakthroughs in biotechnology.[10] Bio-

based polymers similar to conventional polymers are produced by bacterial fermentation processes synthesis of the building blocks (monomers) from renewable resources, including lignocellulosic biomass (starch and cellulose), fatty acids, and organic waste.[10] Natural bio-based polymers are the other class of bio-based polymers which are found in nature, such as proteins, nucleic acids, and polysaccharides (collagen, chitosan, etc.). These bio-based polymers have shown enormous growth in recent years in terms of technological developments and their commercial applications.[10]

The terms bio-based polymers and biodegradable polymers are used extensively in the literature.[10] Biodegradable polymers are defined as materials whose physical and chemical properties undergo deterioration and completely degrade when exposed to microorganisms, carbon dioxide (aerobic) processes, methane (anaerobic processes), and water (aerobic and anaerobic processes).[10] Bio-based polymers can be biodegradable (e.g., polylactic acid) or nondegradable (e.g., biopolyethylene). Similarly, while many bio-based polymers are biodegradable (e.g., starch and polyhydroxyalkanoates), not all biodegradable polymers are bio-based (e.g., polycaprolactone).[10] There are three principal ways to produce bio-based polymers as shown in Figure 4:

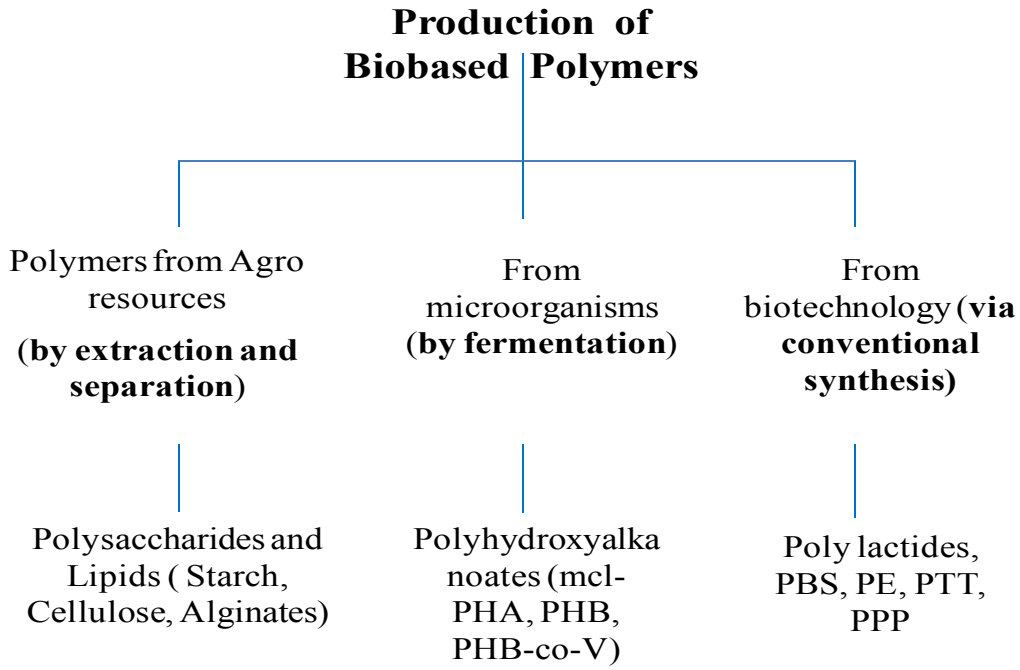

Figure 4 – Bio-based polymers produced by different processes.[11]

Bio-based polymers hold a tiny fraction of the total global plastic market. Recent data show that the production of bio-based polymers should increase from 1.5 % in 2011 to 3 % in 2020. Figure 5 shows the evolution of production capacities of bio-based polymers.[12]

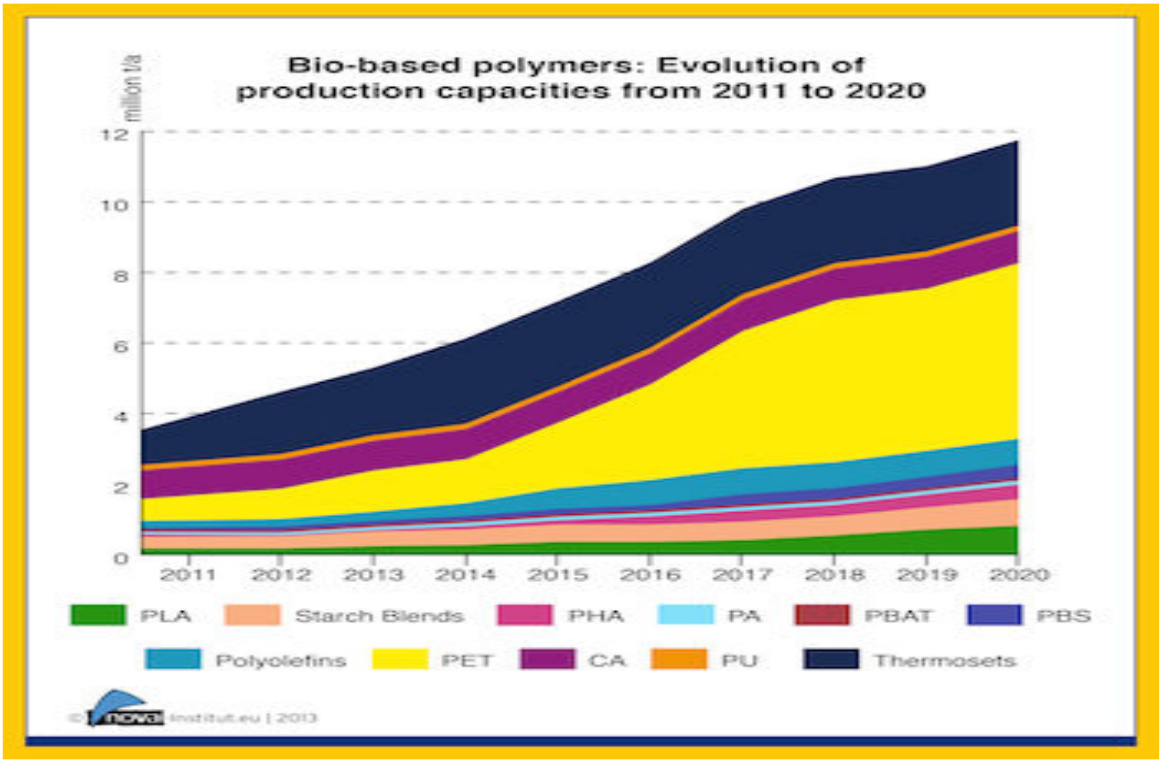

Figure 5 – Evolution of production capacities of bio-based polymers.[12]

The worldwide interest in bio-based polymers has accelerated in recent years due to the desire and need to find non-fossil fuel-based polymers as shown in Figure 6.[10] Several synthetic polymers are biodegradable and compostable like natural carbon-based polymers, such as starch, cellulose and lignin. In the same way some bioplastics based on natural monomers, can lose biodegradability through chemical modifications, like polymerization, such as for example Nylon 9 types polymers obtained from polymerization of oleic acid monomer or Polyamid 11 obtained from the polymerization of castor oil monomer.[5]

Synthetic and natural polymers stand at the opposite ends of a spectrum of properties: i) polyolefins are hydrocarbon hydrophobic polymers, resistant to peroxidation

and biodegradation, highly resistant to hydrolysis, which is their main attribute for the application in packaging. To make polyolefins biodegradable it is necessary to introduce pro-oxidant additives which promote the oxo-biodegradation by producing low molar mass oxidation compounds bioassimilable by the microorganisms; ii) natural compounds, like cellulose, starch and so on, are hydrophilic polymers, water wettable or swellable and consequently biodegradable. They are not technologically useful for food packaging where water resistance is required. Between these two extremes are the hydro-biodegradable aliphatic polyesters such as polylactic acid (PLA) and the poly(hydroxyacid) (PHA).[5] Among bio-source-based polymers emerging on the food market, the semi-crystalline polyester poly(lactic acid) (PLA) is one of the most applied.[9]

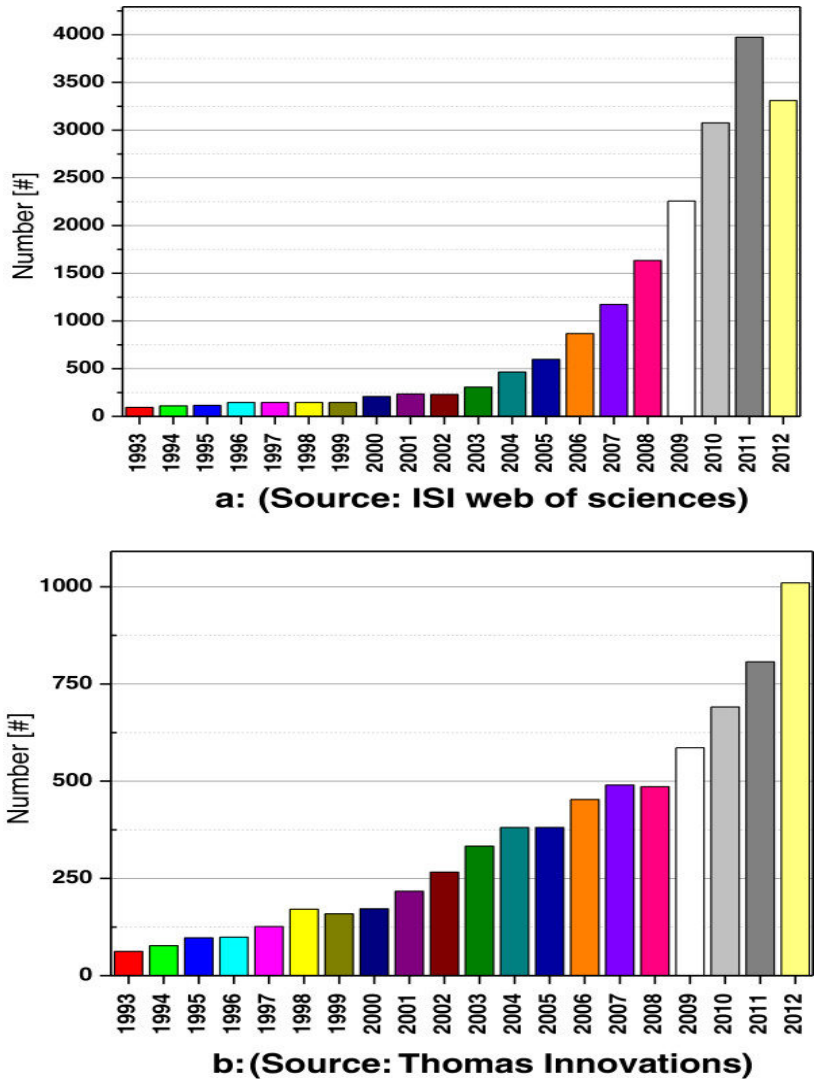

Figure 6 – Citation trends of (a) publications and (b) patents on bio-based polymers in recent years.[10]

1.2. Poly(lactic acid)

Lactic acid (2-hydroxy propionic acid) is a molecular compound with a chiral carbon atom and exists in two enantiomeric forms (Figure 7). The lactide monomer, from which PLA is made of, comes from lactic acid, that has two enantiomers, L and D[13] (Figure 7).[14] Control of the (L:D) monomer ratio is a very important feature in PLA, since it has a large effect on material properties, including the degradation time,[13] melting temperature, degree of crystallinity, and barrier properties. Generally, higher L-lactide content should result in higher barrier properties of the polymer because of greater stereochemical purity.[15] The L-type is the most abundant naturally.[15] The chiral nature of lactic acid results in distinct forms of polylactide, namely, poly(L-lactide) (PLLA), poly(D-lactide) (PDLA), and poly(DL-lactide) (PDLLA), which are synthesized from the L-, D- and DL-lactic acid monomers, respectively, or from the corresponding L,L-lactide, D,D-lactide, and DL-lactide, respectively.[15]

The future widespread availability of PLA raises interesting and important questions regarding its application.[13]

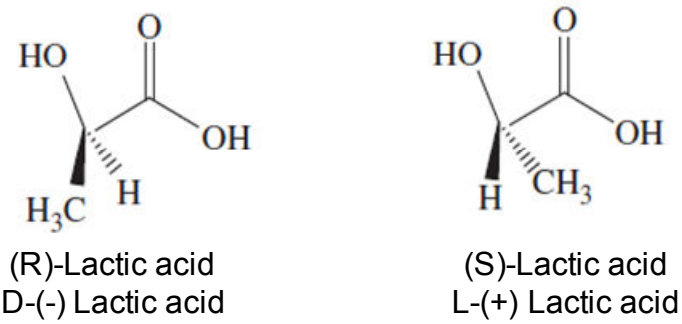

Figure 7 – Chemical structure of L - and D - lactic acid and the enantiomeric forms of lactic acid: (S) - and (R) – 2- hydroxypropionic acid.[15]

The lactic acid molecule has a hydroxyl and an acid functional group, which may result in intermolecular and intramolecular esterification reactions.[14] Almost all lactic acid available in the market is produced by fermentation. During fermentation, a suitable carbohydrate is converted to lactic acid by microorganisms. [14]

The first step of the polymerization is the formation of a linear dimer (lactoyl lactic acid). This condensation reaction can proceed to higher oligomers and is promoted by elimination of water. Also a cyclic dimer, lactide, is formed in small amounts. Lactide can be formed by intramolecular esterification of lactoyl lactic acid or by breakdown of higher oligomers. All reactions are equilibrium reactions (Figure 8).[15]

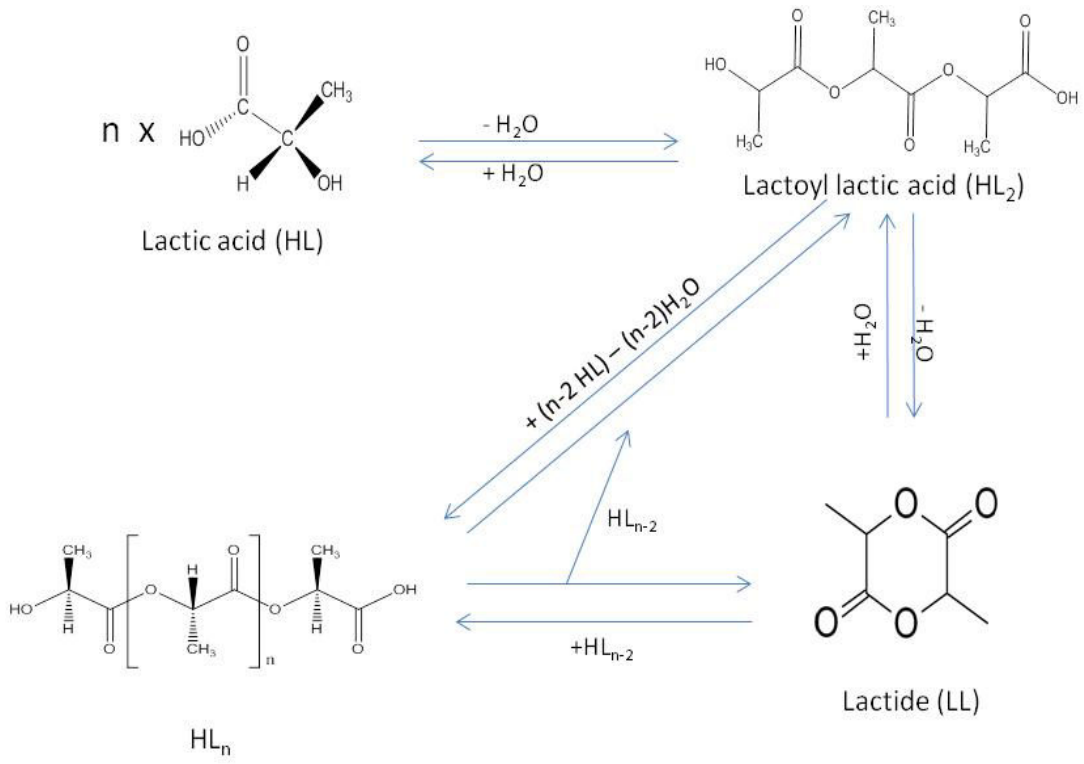

Figure 8 – Lactic acid condensation reactions-interchange between lactide, oligomers, and poly(lactic acide).[15]

Lactic acid can form PLA by means of the reaction of the hydroxyl and carboxylic acid groups of lactic acid. By removing the water formed during this condensation reaction, the reaction proceeds towards the product side, PLA. The preparation of PLA from lactic acid by direct condensation can be divided into three principal stages: i) removal of the free water content, ii) oligomer polycondensation, and iii) melt polycondensation of high molecular weight PLA.[15]

High molecular mass PLA is obtained either by the polycondensation of lactic acid or by ring-opening polymerization (ROP) of the cyclic dimer 2,6-dimethyl-1,4-dioxane-

2,5-dione commonly referred to as dilactic or lactide. The generally applied ROP process for polylactides involves three separate steps: polycondensation, lactide manufacturing, and ring-opening polymerization.[15]

Commercial PLA is usually prepared from L-lactic (LLA), because the resulting polymer poly(L-lactic acid) (PLLA) is semicrystalline with a relatively high melting and glass transition temperature (Tg).

Polylactides have been known for several decades but only recently have these polymers gained commercial significance as a leading environmentally benign plastic available from renewable resources. The production of lactic acid started in the United States in the 1880s, and, unfortunately the process of fermentation of vegetable sugars was not very sucessful.[15] In 1950, the first commercial production of synthetic lactic acid started in Japan.[15] In 1966 occurred the first application of polylactides as implants, sutures and orthopedic fixation, with advantage over nondegradable biomaterials eliminating the need to remove implants and providing long-term biocompatibility, furthermore, it was observed that the degradation of PLLA powder implanted had a nontoxic tissue response.[15]

Only in 1990, the use of poly (lactic acid) (PLA) in packaging and other commercial ends started (Table 1).[15]

Table 1 – Historical trend in market development of PLA.[15]

	Early 1990s	Latter 1990s	2000s
Concept	Biodegradability	Plant origin Biodegradability	Plant origin
Target application	Fishline, net, Compostable material, Agricultural film	Packaging container Agricultural and engineering Compostable material	Packaging container Durables Fibers
Social topics keyword	Landfill life, Dumping of plastic articles		

Poly(lactic acid) (PLA) is a biodegradable thermoplastic polyester that has been the subject of intensive research due to its intrinsic characteristics, such as biodegradability and sustainability, since it is made from natural resources like corn, sugar beet and wheat. PLA exhibits many properties that are equivalent or superior to those of many petroleum-based plastics, which makes it suitable for a large variety of applications. [16]

Figure 9 presents a comparison of the physical properties of PLA to other commodity thermoplastics. It is seen that PLA compares favourably with polystyrene, (PS), a widely used plastic based on non-renewable resources. It should be noted though, that PLA has a glass transition temperature that is significantly lower, $T_g \approx 59$ ºC, than polystyrene, $T_g \approx 100$ ºC. This translates into a lower heat distortion temperature and limits the applicability of PLA for applications requiring better heat resistance. [17]

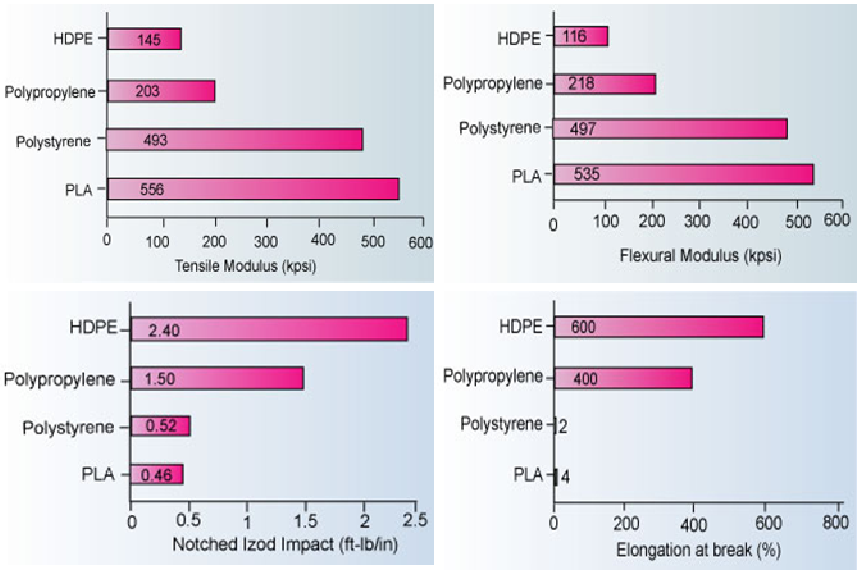

Figure 9 – Physical properties of PLA compared to other common plastics.[17]

Packages made with plastic, in contrast to glass or metal packaging material, are permeable, at different degrees, to small molecules like gases, water vapour, and organic vapour and to other low molecular weight compounds like aromas, flavour, and additives present into food.[18] The knowledge of the solution/diffusion/permeation behaviours of these molecules through the polymer film has become increasingly important in recent years, especially for polymers used in the food packaging field where contamination from external environment has to be avoided and the shelf life of the food controlled by the use of modified atmosphere packaging (MAP) techniques.[18]

PLA is currently used for single or multilayer films, trays, cups, and bottles, and can be manufactured by extrusion, thermoforming, injection and blow molding processes for packaging applications. PLA is also suitable for the production and use of functional membranes.[19] It has been reported that PLA is more suitable than polyethylene or

polystyrene as packaging material for juices, yoghurt, salad dressing and sour cream. Nevertheless, when tested with cheese, a moisture loss of 10 times higher than of the reference packaging (PET) material was observed.[20]

Despite PLA shows good physical properties, similar to those of PS and poly(ethylene terephthalate, PET, the relatively high oxygen permeability of PLA and its brittleness are main drawbacks for flexible packaging applications, namely foods and/or pharmaceuticals products susceptible to oxidation.[19] The fact that PLA has higher carbon dioxide and oxygen permeability than polystyrene, low density polyethylene, LDPE, and poly(ethylene terephthalate), clearly indicates that the development of PLA packaging requires further efforts.

1.3. Active packaging

Important functionalities of packaging are not only to ensure food safety, but also to guarantee the organoleptic quality of the packed product during its shelf- life. Shelf-life is defined as the time during which the food product will: i) remain safe; ii) be certain to retain desired sensory, chemical, physical and microbiological characteristics; iii) comply with any label declaration of nutritional data, when stored under the recommended conditions.[21] Many factors can influence shelf-life, and can be categorized into intrinsic and extrinsic factors. Intrinsic factors are influenced by variables such as raw material type and quality, and product formulation and structure.

They include the following:

- Water activity (*a*w) (available water).
- pH value and total acidity; type of acid.
- Redox potential (*E*h).
- Available oxygen.
- Nutrients.
- Natural microflora and surviving microbiological counts.
- Natural biochemistry of the product formulation (enzymes, chemical reactants).
- Use of preservatives in product formulation (e.g. salt).

Extrinsic factors are those the final product encounters as it moves through the food chain. They include the following:

• Time–temperature profile during processing; pressure in the headspace.
• Temperature control during storage and distribution.
• Relative humidity (RH) during processing, storage and distribution.
• Exposure to light (UV and IR) during processing, storage and distribution.
• Environmental microbial counts during processing, storage and distribution.
• Composition of atmosphere within packaging.
• Subsequent heat treatment (e.g. reheating or cooking before consumption).
• Consumer handling.

All these factors can operate in an interactive and often unpredictable way, and the possibility of cross-interactions must be investigated. A particularly useful type of interaction occurs when factors such as reduced temperature, mild heat treatment, antioxidant action and controlled atmosphere packaging operate in synergy to restrict microbial growth, the so-called 'hurdle effect'. This way of combining factors which, individually, are unable to prevent microbial growth but, in combination, provide a series of hurdles, allows manufacturers to use milder processing techniques which retain more of a product's sensory and nutritional properties.[21]

The interaction of such intrinsic and extrinsic factors inhibits or stimulates a number of processes which limit the product shelf-life. These processes can be classified as microbiological, chemical, physical and temperature related. [21]

Table 2 shows some examples of processes associated to the deterioration of several food classes. In composite foods the factors limiting shelf-life can be quite different from those that limit the shelf-life of the individual components. For example, an important factor limiting shelf-life in breakfast cereals containing a mixture of cereal and dried fruit is the hardening of the fruit from moisture migration into the cereal. In contrast, the limiting factors for the individual fruit and cereal components would be flavor changes arising from chemical reactions, and moisture uptake and softening of the cereal. There are many factors to be considered in choosing the optimal packaging form and material for any particular product, including the product characteristics, processing considerations, shelf-life required and overall cost. In many cases, packaging is an integral part of the processing stage. Advances in packaging materials and techniques have increased the options available for maintaining quality and for improving the shelf-life of foods.[21]

Table 2 – Examples of factors limiting shelf-life of some food products.[21]

Product	Deterioration processes	Limiting changes
Fruit and vegetables (Soft fruit, Hard fruit, Coleslaw, prepared salads)	Moisture loss; Enzymic action; Mould growth; fat oxidation	Textural softening; dry appearance; Loss of crispness; microbial growth; rancidity
Meat products (fresh red meat, fresh poultry, fresh bacon, canned ham)	Oxidation; microbial growth; chemical reactions	Loss of red color; rancidity; off-odors and flavors; freezer burn; microbial; gas generation
Cereal and other dry products (bread, cakes, dried pasta, breakfast cereals)	Starch retrogradation; moisture migration; moisture uptake; oxidation; starch changes; protein change	Stable texture and flavor; dry texture; mould growth; drying and hardening; mould formation; rancidity
Beverages (carbonated beverages, beer; coffee; fruit juices, tea, wine)	Gas evolution, hydrolysis/oxidation; microbial growth; volatile loss; enzymic reactions	Carbonation loss: flavor loss; rancidity; turbidity; nutrient loss; flavor loss
Dairy products (ice-cream, butter, cheese, yoghurt)	Moisture migration; oxidation; hydrolysis reactions; microbial growth; lactose crystallization; syneresis	Ice crystal formation; rancidity; gritty texture; mould production; serum separation;

Modified Atmosphere Packaging (MAP), which involves replacing the air in the headspace of a packaged product with a single or mixture of special gases, has made the greatest impact on the shelf-life of chilled products. The gases commonly used are carbon dioxide and nitrogen. Carbon dioxide is used to suppress microbial growth, but its effectiveness is very much dependent on the sensitivity of different classes of microorganisms to this gas. Nitrogen is used as a inert filler, since oxygen is to be excluded to prevent aerobic spoilage. One special case, however, is that of fresh fruit and vegetables, where a delicate balance of carbon dioxide and oxygen is necessary to allow aerobic respiration to continue at a very low rate and thereby extend shelf-life. One of the requirements of food packaging is that it should play a passive role, remaining inert and not interacting with the food it contains. [21] However, as a result of new consumer trends, a demand for better fresh-like quality using convenient food products intensifiers made traditional packaging concepts outdated. Besides the protection of the foods shape and texture, preservation of flavors and odours, shelf-life extension and control of the water or moisture content of foods, the packaging industry has been developing a new innovative concept: active packaging. [22–24]

This is a type of packaging where changes in the packaging atmosphere are promoted in order to fulfil one or more specific objectives, such as the extension of its shelf-life and the increase of the packaged foods safety and quality. [22]

Active packaging systems can be regarded as active scavenging/releasing systems. While in the first type undesired compounds such as oxygen, ethylene, carbon dioxide or moisture are removed, in the last compounds such as carbon dioxide, water, antioxidants or preservatives are added. The most studied of these compounds are undoubtly oxygen and carbon dioxide. Although CO_2 has a beneficial effect in microbiological control and in the storage of foods such as meat, cheese or fish, an excess of CO_2 may cause package collapse, promoting anaerobic metabolism, pH reduction and flavor change. Micro-perforation is the most used method to control CO_2 content inside the package, due the deterioration or respiration reactions, by increasing the permeability of the gas through the packaging material. [25,26]

On the other hand, oxygen is responsible for several undesirable chemical reactions in foods, promoting the growth of aerobic microbes and the spoilage of many foods by microbial attack. Nonetheless, oxygen inhibits the growth of anaerobic micro-organisms.[25,26] The mould growth control and the delay in the rancidity development of vegetable oils are the most important application of oxygen scavenging systems in food packaging.[26] Usually, these active packaging technologies make use of sachets with active compounds, such as iron powder, ascorbic acid, photosensitive dyes and enzymes but these approaches meet some resistance due to the accidental spill and consumption of sachet contents.[24,25]

There is a growing interest in bioactive packaging through the use of natural compounds incorporated into the polymer wall of the package in order to increase the foods shelf-life and, at same time, prevent the oxidation of polymer by thermal degradation. Antioxidants are widely used as food additives to improve the stability of lipids to oxidation and to prolong shelf-life of dried products and oxygen sensitive foods. They have also been incorporated in small concentrations into plastic films to obtain additional stability under processing conditions.[27–29]

Therefore, the barrier properties of the packaging polymer against the transfer of small gaseous molecules, such as O_2, CO_2 or H_2O, are important[9], and should prevent food degradation and oxidation, preserving aromas and flavours[13]. In particular, oxygen is an

excellent oxidizing agent of lipids which can cause deterioration of product quality. Moreover, barrier properties against light, water vapor, atmospheric gases and larger volatile molecules, such as aroma compounds, need to be assessed since the transfer of these compounds into the polymer could cause a modification of the aroma formulation of the packaged food leading to a deterioration of its quality.[9]

1.4. Scope

The central idea behind this thesis was to develop a biodegradable poly(lactic acid) (PLA)-based packaging system that can provide an extended shelf life for foods and improve food safety, improving its barrier properties. PLA, was selected for this study since it is obtained from natural renewable resources and presents mechanical properties comparable to hydrocarbon based polymers and with excellent flavor and odor barrier.[30,31,32] PLA is already used as a packaging material for the storage of fresh-fruits and vegetables or foods with short shelf-life. In order to improve PLA's barrier properties, antioxidants (natural and artificial) were incorporated in films of PLA. The objective of this study is to evaluate the impact of the addition of three antioxidants α-tocopherol, 2,6-bis(1,1-dimethylethyl)-4-methylphenol or (Butylated hydroxytoluene), BHT, and 2-(1,1-Dimethylethyl)-1,4-benzenediol or *tert*-Butylhydroquinone (TBHQ) (Figure 12) in PLA films. For that purpose, films with different quantities of antioxidant were prepared and thermal, mechanical and barrier properties were measured so that their suitability as a polymer materials for food packaging can be assessed.

2. Antioxidants Poly(lactic acid) Composite Films Characterization

2.1. Introduction

The selection of a polymeric material for certain application depend on the performance of the membrane and specially of the glass transition temperature, T_g, and the crystallinity which are important parameters and affect directly the transfer of small molecules through the membrane. These parameters are determined by structural factors such as chain flexibility, chain interaction, chain symmetry, presence of lateral chains, extent of polymer chain unsaturation, presence of polar groups in the polymer backbone, orientation of the polymer chains and degree of crosslinking, cohesive energy of the polymer and molecular weight and presence of additives.[33,34] The knowledge of T_g is essential in the selection of materials for various applications. In general, values of T_g well below room temperature define the domain of elastomers and values above room temperature define rigid and structural polymers, i.e., the mechanical and physical properties change drastically over a relatively small temperature interval covering the glass transition temperature. The glassy state of a polymer can be considered as a frozen state with a highly restricted chain mobility.[33] However, in the presence of some substances, depression of the glass transition may occur due to an increase on the free volume.

Most of the dense materials used as food packaging are made up of semi-crystalline polymers (PE, PP, PET) in which both phases can be distinguished: an amorphous phase and a crystalline phase (Figure 10). When the crystallization occurs in solution, the polymeric chains fold back and forth, forming folded chain lamellar crystals, connected to the amorphous regions by polymer chains.

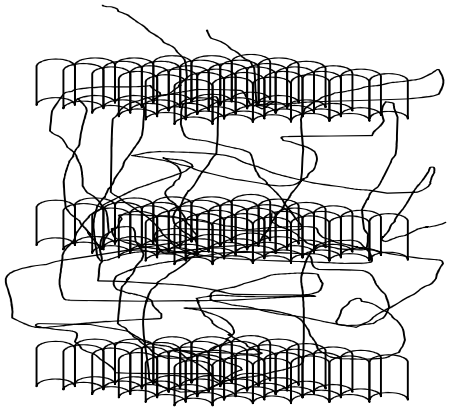

Figure 10 – Semi-crystalline polymer structure presenting lamellar crystals connected by polymer chains (amorphous regions).

In the melted state, the polymer chains are highly entangled therefore the folding of chains during the nucleation and crystallization process is hindered.[35] Crystallization from the melted polymer results in the formation of spherical crystal aggregates, the so-called spherulites, notably at isothermal crystallization at low supercooling.[35]

Typically, polymer crystals are not in thermal equilibrium since their formation is strongly complicated and hindered due to the connectivity of the segments, involving co-operative movements of a large number of connected monomers.[35] Although the free energy would be lowest for fully extended crystalline molecules, long polymers usually form much thinner lamellae ("chain-folding"). Therefore, polymer crystals represent meta-stable states with a significant degree of disorder, mainly characterized by the degree of chain foldind.[35]

Three parameters whose role is essential when dealing with mass transfer through polymeric matrices are free volume, glass transition temperature, and crystallinity of the polymer, which are also function of previously given factors.[34] Diffusion in semicrystalline polymers is complicated by the presence of crystallites. Crystalline zones are excluded volumes where molecules cannot sorb and increase the path that diffusing molecules must pass in the membrane because they increase tortuosity and may also decrease the mobility of the amorphous polymeric chains because chain ends could be trapped in the neighboring crystalline lamellae.[34] In the amorphous part, the diffusion mechanism is different according to whether the membrane is in a rubbery or a glassy state at the temperature of use (above or below of T_g).[34] Membranes in the glassy state are actually not in equilibrium because the time necessary for a polymer in the glassy state to relax, i.e., for its structure to rearrange in response to external changes, is long. Membranes in the rubbery state are at equilibrium and do not contain fixed regions of non equilibrium excess volume because the structure rearranges promptly in response to external changes.[34]

The concept of free volume is useful for explaining aspects of the chain mobility and permeability of polymers. Free volume (microvoids), including its nanostructure characteristics (mean size and size distribution of microcavities, their spatial arrangement and topology), determines many properties of glassy polymers and in particular, the transport parameters of membrane materials such as permeability and diffusion coefficients of gases.[36] The relation between the free volume and the polymer mobility is frequently studied by measuring the diffusion properties of small molecules in polymers. As a general

rule, gases solubility, diffusivity and permeability increase with the increase in free volume. In semi-crystalline polymers (PP, PE, PET…), free volume is linked to Tg of the amorphous part.[34] Conceptually, permeation of small gas molecules through a glassy polymer is viewed as proceeding by jump motion whereby a permeant molecule spends most of the time in free-volume cavities and occasionally jumps to a neighboring cavity.[37] The jump motion proceeds by formation of a channel between two neighboring holes. Thus gas permeation depends on the number and size of cavities in the polymer matrix (static free volume) and the frequency of channel formation (dynamic free volume). Static free volume is essentially independent of thermally accessible motions of the polymer chains and relates to gas sorption, S. Dynamic free volume derives from accessible conformational changes and segmental motions of the polymer chain and relates to gas diffusivity, D.[37]

In recent years many efforts have been devoted to the development, formulation and characterization of new ecologically friendly and sustainable plastic materials that can overcome the major environmental problems created by the extensive use of petrochemical based plastics. In particular, PLA has been playing a dominant role among biorenewable resources plastics. As we mentioned in the previous section, many important properties of PLA are controlled by ratio of *D*- to *L*- enantiomers used and the sequence of arrangement of the enantiomers in the polymers. PLLA constitutes the main fraction of PLA derived from renewable sources since the majority of lactic acid obtained from biological sources exists as LLA. PLA with PLLA content higher than 90 % tends to be crystalline while that with lower optical purity is amorphous. The melting temperature, T_m, glass transition temperature, T_g, and crystallinity of PLA decrease with decreasing amounts of PLLA.[15]

Thermoplastic polymers exhibit many properties ideal for use in packaging and other consumer products, such as light weight, low process temperature (compared to metal and glass), variable barrier properties to match endues applications, good printability, heat sealable, and ease of conversion into different forms.[38] Similar to many thermoplastics polymers, semicrystalline PLA exhibits T_g and T_m. Above Tg (~58 ºC) PLA is rubbery, while below T_g, it becomes a glass. Figure 11 displays the T_g and T_m of thermoplastics polymers.[38]

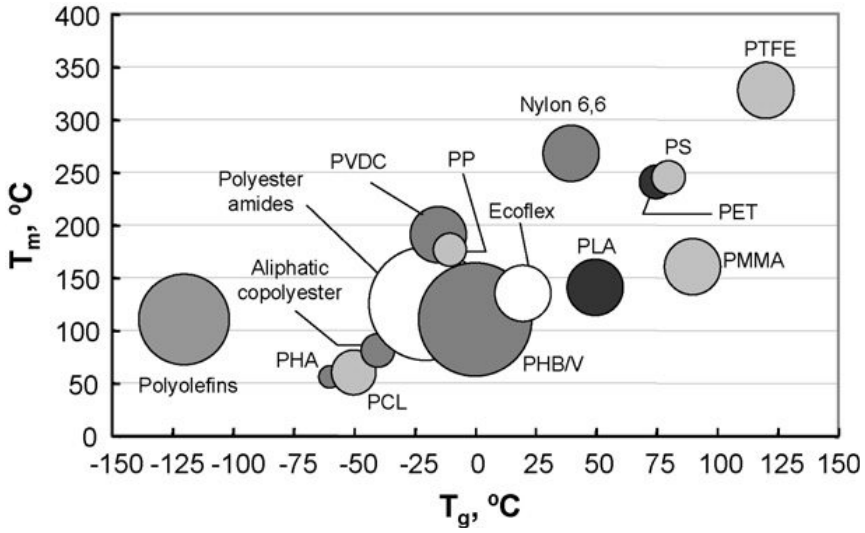

Figure 11 – Glass transition temperature and melting temperature of PLA and other thermoplastics.[38]

The properties of PLA such as thermal stability and impact resistance are inferior to those of conventional polymers used for thermoplastic applications.[38] The inherent brittleness of PLA has been a major bottleneck for its large-scale commercial applications.[39] Therefore, PLA is not ideally suited to compete against the conventional polymers.[38] Despite the good mechanical properties and processability as well as biocompatibility of PLA, to replace the polyolefins in packaging material and hygiene products, as diapers, and milk cartons, PLA film have to be flexible, because in the industrial production line of packaging material as well as diapers, there is no tolerance for the film cracking or tearing when folded or subject to force during manufacturing.[40] Since PLA is rigid and brittle with low ability to plastic deformation below glass transition temperature, numerous approaches such as plasticization, block copolymerization, blending with tough polymers, and rubber toughening have been adopted to improve the toughness of brittle polylactide bioplastic.[39] The major drawbacks of these methods are the substantial decreases in the strength and modulus of the toughened polylactide. So, a polylactide-based material having good stiffness-toughness balance along with high biobased polylactide content is still elusive.[39]

One of the most used methods to overcome the problem of the brittleness is plasticize the PLA in order to produce flexible films. Several types of chemicals have been tried to plasticize PLA such as citrate esters, poly(ethylene glycol) (PEG), glucose monoesters and partial fatty acid esters, resulting in materials with better deformation capacity and

resilience.[41] Also, blends of PLA with various non-biodegradable polymers, and with others aliphatic polyesters such as poly (ε–caprolactone), poly(butylene succinate) and poly(hydroxy butyrate) were also reported in the literature.[41] Various compounds are reported as efficient plasticizing for PLA including poly(3-methyl-1,4-dioxan-2-one), poly(ethylene oxide), citrate esters, triacetine, and poly(ethylene glycol)s (PEGs).[42] Some of these blends were found to be immiscible, resulting in fairly poor mechanical properties.[41]

The expansion of PLA´s application to the packaging industry passes essentially through the ability to tailor its gas barrier properties and flexural properties such as rigidity and brittleness, which are an expression of its low deformation at break. The choice of polymers or plasticizers to be used as modifiers for PLA is limited by the requirements of the application. For packaging and hygiene applications, only nontoxic substances approved for food contact and personal care can be considered as plasticizing agents.[40]

Antioxidants are widely used as food additives to improve the stability of lipids to oxidation and to prolong shelf-life of dried products and oxygen sensitive foods. They have also been incorporated in small concentrations in films to obtain additional stability (chemical, thermal) under processing conditions. [27–29,43–45]

In this context, antioxidant-active packaging is a promising approach to extend the shelf-life and improve safety and sensorial properties, while maintaining the food quality. Several antioxidants have already been incorporated into different polymeric film structures for the intentional purpose of migration into food to prevent its oxidation.[28,46–48] The impregnation of Food and Drug Administration (FDA) approved antioxidants, in polymeric films has also been subject of research. α-tocopherol (the component of Vitamin E which has the highest free radical scavenging activity) is a natural antioxidant that has already been studied as a polymer film stabilizer as well as an antioxidant. Recognized as safe and worldwide approved for use in food applications, α-tocopherol has been used to improve the biostability and biocompatibility of different materials.[43,49,50] Reno et al.[51] studied the effect of α-tocopherol added to poly((D,L)lactic acid) for medical applications and it was verified that it alters the surface wettability. Wessling et al.[29] observed that incorporation of high levels (3600 ppm) of α-tocopherol into LDPE films inhibits the oxidation of organic acids stored in contact with the film. More recently, Byun et. al[52] clearly showed the high antioxidant activity of α-tocopherol, by the incorporation of 1 %

of α-tocopherol PLA films, which increased the radical scavenging activity from 0.84 % to 90.43 %.[52] Manzanares-López *et al.*[53] added 2.58 wt% of α-tocopherol into PLA films and studied the films thermal and optical properties as well as effect of the release of the antioxidant on the oxidative stability of soybean oil. No significantly effect was observed on T_g and T_m. Ortiz-Vazquez *et al.*[54] studied the use of butylated hydroxytoluene (BHT), another antioxidant also approved by FDA, in PLA films for packaging of coconut oil and concluded that the addition of 0.79 wt.% of BHT to the PLA film had no effect on thermal, oxygen and water barrier properties of the PLA films.

Nevertheless, recent contradictory results show that the addition of 1 wt.% of synthetic phenolic antioxidants including BHT, butylated hydroxyanisole, tert-butylhydroquinone (TBHQ) and propyl gallate had no significant effect on the glass transition and melting temperature, water vapour and oxygen permeability of PLA films.[55] However, Hwang *et al*. [56] demonstrated that the combination effect of two natural antioxidants (α-tocopherol and resveratrol) with differing concentrations can play a critical role on the thermal and mechanical properties of PLLA films.

In conclusion, the available literature only addresses the incorporation of very small amounts of antioxidant and most studies only assess rates, effects and release mechanisms of the antioxidants. This chapter explores the incorporation of antioxidants into PLA films and their effect on thermal, surface and mechanical properties. For that purpose, three antioxidants were selected, one natural (α-tocopherol) and two synthetic (BHT and TBHQ). α-tocopherol, a lipid-soluble antioxidant that has already been intensively studied as a polymer film stabilizer, was chosen due to its highest free radical scavenging activity.[57] BHT and TBHQ are commonly used in food industry and were chosen because they have similar structures but different molar volumes.[55] The chemical structures of the antioxidants used in this work are shown in Figure 12.

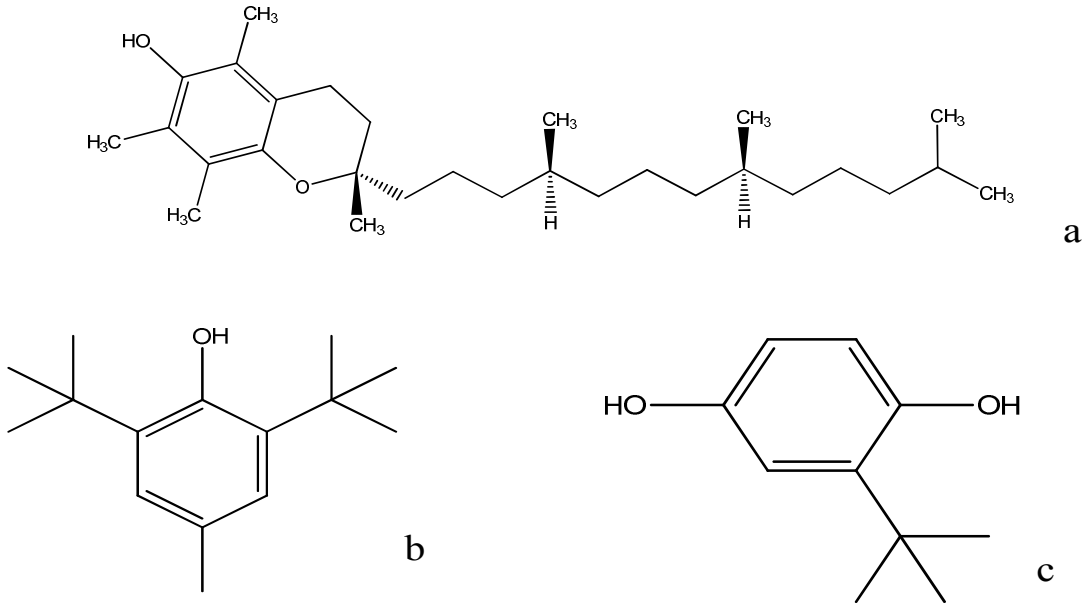

Figure 12 – Chemical structures of antioxidants used in this work. a)-α-tocopherol, b)- 2,6-bis(1,1-dimethylethyl)-4-methylphenol or (Butylated hydroxytoluene) BHT and c)- 2-(1,1-Dimethylethyl)-1,4-benzenediol or tert-Butylhydroquinone (TBHQ)).

BHT is a lipid-soluble antioxidant commonly used in the plastics, pharmaceutical and food industries. BHT terminates free-radical chain reactions by donating hydrogen atoms to free radicals producing more stable compounds. In the U.S.A., direct addition of BHT to some food emulsion is specifically regulated, but this antioxidant is generally recognized as safe for use in food when the total content of antioxidants is not over 0.02 % of the fat or oil content[54].

2.2. Experimental

2.2.1. Materials

Linear poly(lactic acid) (PLA) with (L:D) ratio of 98:2 with molecular weight of 87,131 Da and density of 1.26×10^{-3} kg/m^3 [13] was kindly provided by Cargill-Dow Polymers (USA) in the form of pellets. (±) α-tocopherol with assay ≥ 97 % and Tert-butylhydroquinone (TBHQ) with assay ≥ 98 % were supplied from Fluka (Sintra, Portugal). Butylated hydroxytoluene (BHT), 99 % purity, was obtained from SAFC Global (Lisboa, Portugal). Dichoromethane was supplied from Sigma-Aldrich (Sintra, Portugal) with analytical reagent grade. Solvents were used with no further purification.

2.2.2. Samples preparation

PLA films with and without antioxidants were prepared from solutions with 60 mg/ml of PLA in dichloromethane. Different amounts of AT, BHT and TBHQ to the PLA were added to obtain solutions with concentrations of 2 wt%, 4 wt %, 6 wt% and 10 wt% of each antioxidants to the polymer. All the solutions were magnetically stirred during at least 12 h for complete dissolution Thin films were prepared by casting each solution into Petri dishes and dichloromethane was left to evaporate at room temperature from 24 h in the dark place (cabinet) to avoid antioxidants degradation. Solvent evaporation took place slowly in order to obtain homogeneous films. Structural, mechanical, thermal and barrier properties were investigated.

2.2.3. Film Characterization

2.2.3.1. Infra-red spectroscopy

Attenuated Total Reflection Fourier Transform Infra-Red (ATR-FTIR) spectrophotometer, FT Bruker IFS 55, was used to obtain spectra of thin films co-adding 256 scans at a resolution of 8 cm^{-1}. Spectra were collected from 4000 to 400 cm^{-1}.

2.2.3.2. Optical microscopy

Microscope Olympus BX51 with polarized light was used to observe the effect of α-tocopherol on the growth and morphology of spherulites when a sample is subjected to thermal treatment by melting and subsequent annealing at temperature above Tg or quenched at temperature 0 ºC. The study of the crystallite growth was achieved using films which were melted at 200 ºC for 3 minutes, and then crystallized at the annealing temperature of 140 ºC for 60 minutes.

2.2.3.3. Dynamic mechanical analysis

Rectangular specimens of the films prepared were tested in a dynamic mechanical analyzer Tritec 2000 DMA, Triton Technology Ltd. Displacement and force amplitudes were adjusted according to samples for a single cantiliver bending deformation mode. The experiments were done at 1 Hz of frequency in temperature range from 30 ºC to 100 ºC with heating rate of 2 ºC/min. The storage modulus or Young's modulus and the dissipation factor, tan δ, with temperature were monitored.

2.2.3.4. Thermal properties

The dynamic degradation was carried using a thermogravimetric analyser Shimadzu TGA-50. The dynamic tests were run at a heating rate of 10 K/min from room temperature up to 773 K and in nitrogen environment (flow rate 20 mL/min) to guarantee the constancy of atmosphere during the whole test. Samples between 4 and 20 mg were used without any previous treatment.

A differential scanning calorimeter (DSC), Shimadzu DSC-50/DTA-50, was used to determine the antioxidant effects on the glass transition temperature (Tg), melting temperature (Tm) and degree of crystallinity (χ_c) of the PLA films. About 5 mg of each film sample was weighed in an aluminum pan, and were subjected to the following three DSC runs at 10 K/min: i) heating from 263 K to 523 K; ii) cooling from 523 K to 263 K, and finally iii) heating from 263 K to 523 K. The first scan is used to measure the crystallization percentage, considering 93.6 J/g for a 100 % crystalline L-PLA[58] and the second scan is used to calculate the glass transition temperature without polymer stress.

The experiments were carried out under constant nitrogen atmosphere. The transition temperature as well as the enthalpy of melting (ΔH_m) was calibrated using indium as the standard. The degree of crystallinity of the PLA films was calculated according to the following equation:

$$\chi_c(\%) = \frac{\Delta H_m - \Delta H_c}{\phi \Delta H_m^0} \times 100 \qquad \textbf{(1)}$$

where ΔH_m is the experimental enthalpy of melting, ΔH_c is the enthalpy of cold crystallization and ϕ is weight fraction of PLA in the film. ΔH_m^0 is the enthalpy of melting for 100 % crystalline PLA, 93.6 J/g. [15]

2.2.3.5. Scanning electron microscopy

The morphology of the resulting membranes was characterized by Ultra-high Resolution Analytical Scanning Electron Microscope HR-FESEM Hitachi SU-70 equipment operating at 15 kV. To increase the conductivity, a carbon coating was deposited on top of all film samples.

2.2.3.6. Atomic force microscopy AFM)

For atomic force microscopy (AFM) observation, a NanoScope III scanning microscope equipped with a hot-stage accessory (Digital Instruments) was used. All experiments were carried out in the tapping mode. AFM height, amplitude and phase images were recorded simultaneously. Resolutions of 256×256 data points per image were used to collect the images. Si tips (PPP-NCHR) with a resonance frequency of approximately 320 kHz and a spring constant of about 40 N/m were used. The scanning rate was 0.5 Hz.

2.2.3.7. X-ray diffraction (XRD)

A Philips X-ray diffractometer X'Pert model equipped with a (CuKα) source was used to study the crystallites growth in films subjected to different thermal treatments. The analysis was performed at 25 ºC with a 2θ range of 5º- 40º using a scan speed of 1 º/min.

2.2.3.8. Contact angle measurements

Contact angle (θ) measurements with water, formamide, ethylene glycol and diiodomethane were performed at room temperature using a surface energy evolution system coupled with a video camera and image analysis software commercialized by Brno

University (Brno, Czech Republic). Each θ value is the average of five independent determinations acquired immediately after the drop deposition. These values were used to calculate the polar and dispersive components of the surface energy of PLA films using the Owens-Wendt's approach. [59]

2.3. Results and discussion

Before beginning the characterization of the films by different techniques, it is important to describe the appearance of the films after enriched PLA with the different antioxidants. The PLA films had different appearance depending on the antioxidant used. PLA films containing α-tocopherol have become yellowish over time while the films with BHT were very similar to neat PLA, becaming opaque. The brittleness remained in films containing the two antioxidants. Finally, PLA blended with TBHQ films were the most interesting, because the membranes were transparent and significantly more flexible. From visual inspection we can conclude that PLA/TBHQ films should be less crystalline that the other antioxidants enriched films.

2.3.1. Infra-red spectroscopy

The infrared spectra of PLA and PLA enriched with various concentrations of antioxidants films were recorded in the spectral region of 3500 to 500 cm^{-1} and are presented in Figure 13 for α-tocopherol, Figure 14 for TBHQ and Figure 15 for BHT. In Figure 13, the increase in the intensity of the band at 3000 cm^{-1} with the increase in the amount of α-tocopherol in films confirms that the additivation procedure was successful. The control of PLA structure is done using the band at 1748 cm^{-1}, corresponding to C=O stretching.

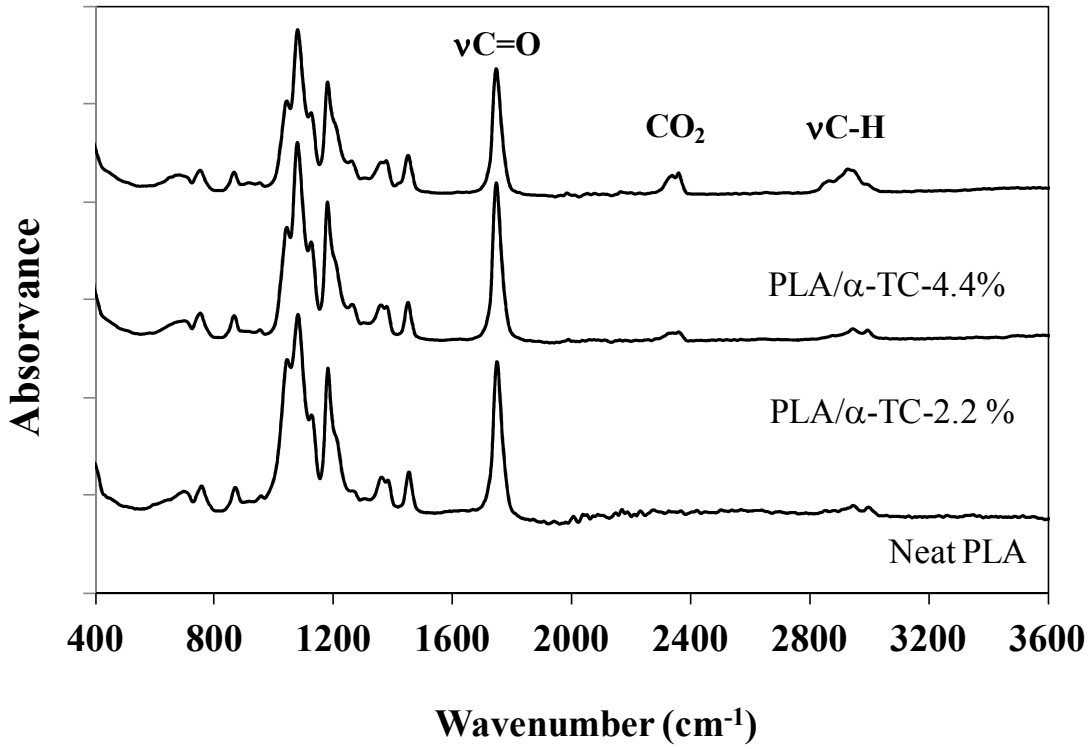

Figure 13 – ATR-FTIR spectra of PLA and enriched PLA with α-tocopherol films.

Figure 14 shows the spectra of TBHQ, neat PLA and PLA enriched with TBHQ (4,4 wt%). In the film of PLA/TBHQ spectrum, we can observe the appearance of the characteristic bands of TBHQ, thus confirming the presence of the antioxidant in the film. The broad band at 3508 cm^{-1} can be assigned to the –OH stretch of the phenol, which usually appears at 3445 and 3279 cm^{-1}, or –OH free from PLA which usually appears at 3571 cm^{-1}, or both. The bands from 2994 to 2874 cm^{-1} are assigned to the CH stretching region ($CH_{3(asym)}$, $CH_{3(sym)}$, and CH modes) of PLA and =C- (alkenes, aromatics) from TBHQ. The phenyl ring and –C-OH in plane are responsible for bands at 1590, 1490 and 1442 cm^{-1} in TBHQ.

Near these bands, the $\delta_{as}CH_3$ stretching of PLA appears at about 1452 cm^{-1}. The weak band at about 1500 cm^{-1} should be then assigned at phenyl ring and –C-OH in the plane bending. The increased intensity of the band at 1360 cm^{-1} and the band at 1310 cm^{-1} are assigned to the methyl bending vibration (δ_sCH_3 + δCH), found in both PLA and TBHQ. The bands at 810 and 775 cm^{-1} are assigned to –CH out of plan and ring torsion of the TBHQ.

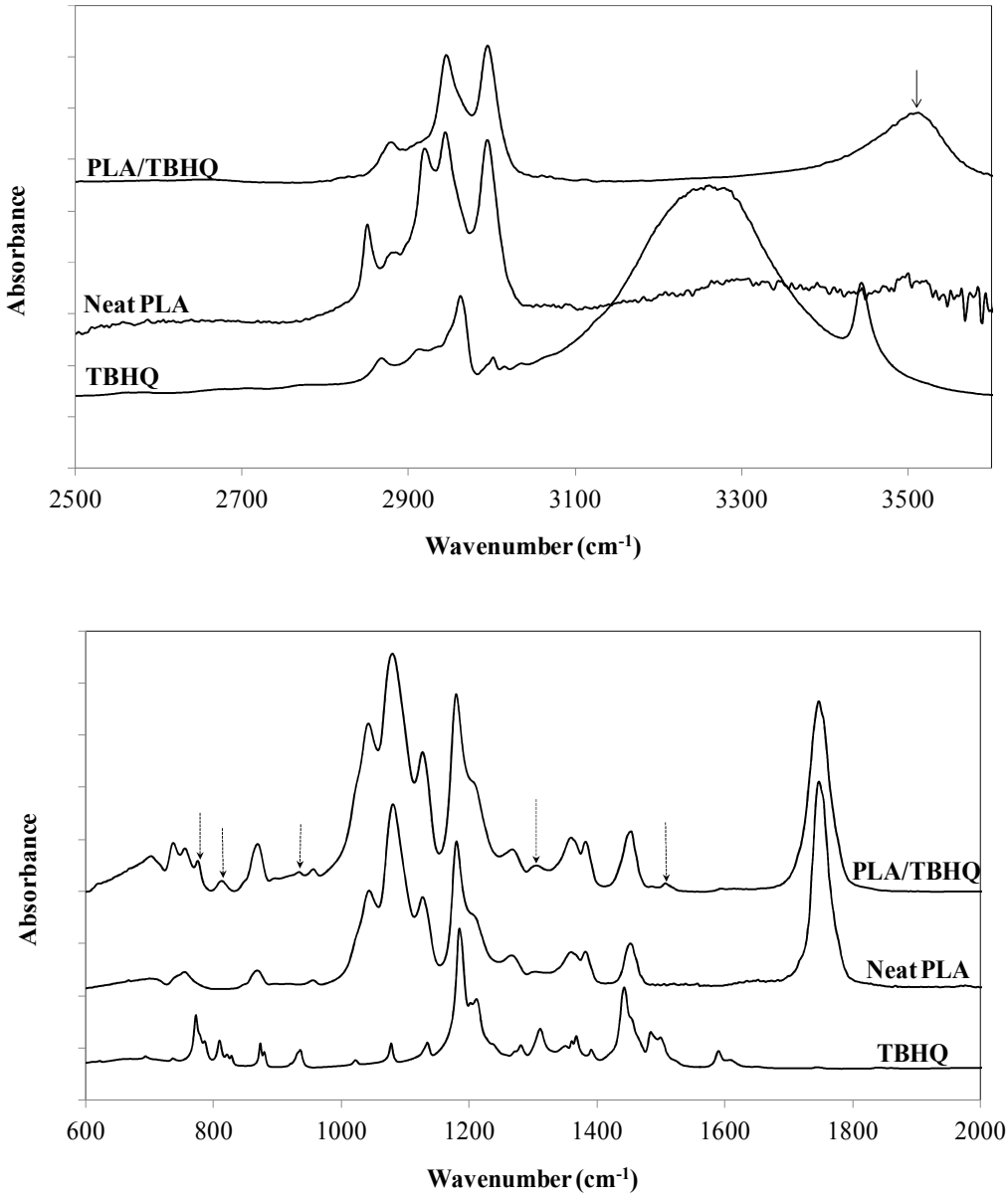

Figure 14 - ATR-FTIR spectra of PLA and enriched PLA with TBHQ films.

The bands that are assigned to BHT found in the additivated films, ensures presence of this compound in the films. The –OH stretching vibration at about 3630 cm^{-1} is the sharpest and the most commonly used analytical frequency for the evaluation de presence of BHT. In the spectrum of PLA/BHT, this band appears as a broad band. The broad band at about 3500 cm^{-1} may be assigned to the –OH stretch of the phenol, or –OH free from PLA. The increased band at 1360 cm^{-1}, and the band at 1306 cm^{-1} are assigned to methyl bending vibration ($\delta_s CH_3 + \delta CH$), and that at 920 cm^{-1} is assigned to ring torsion of the BHT.

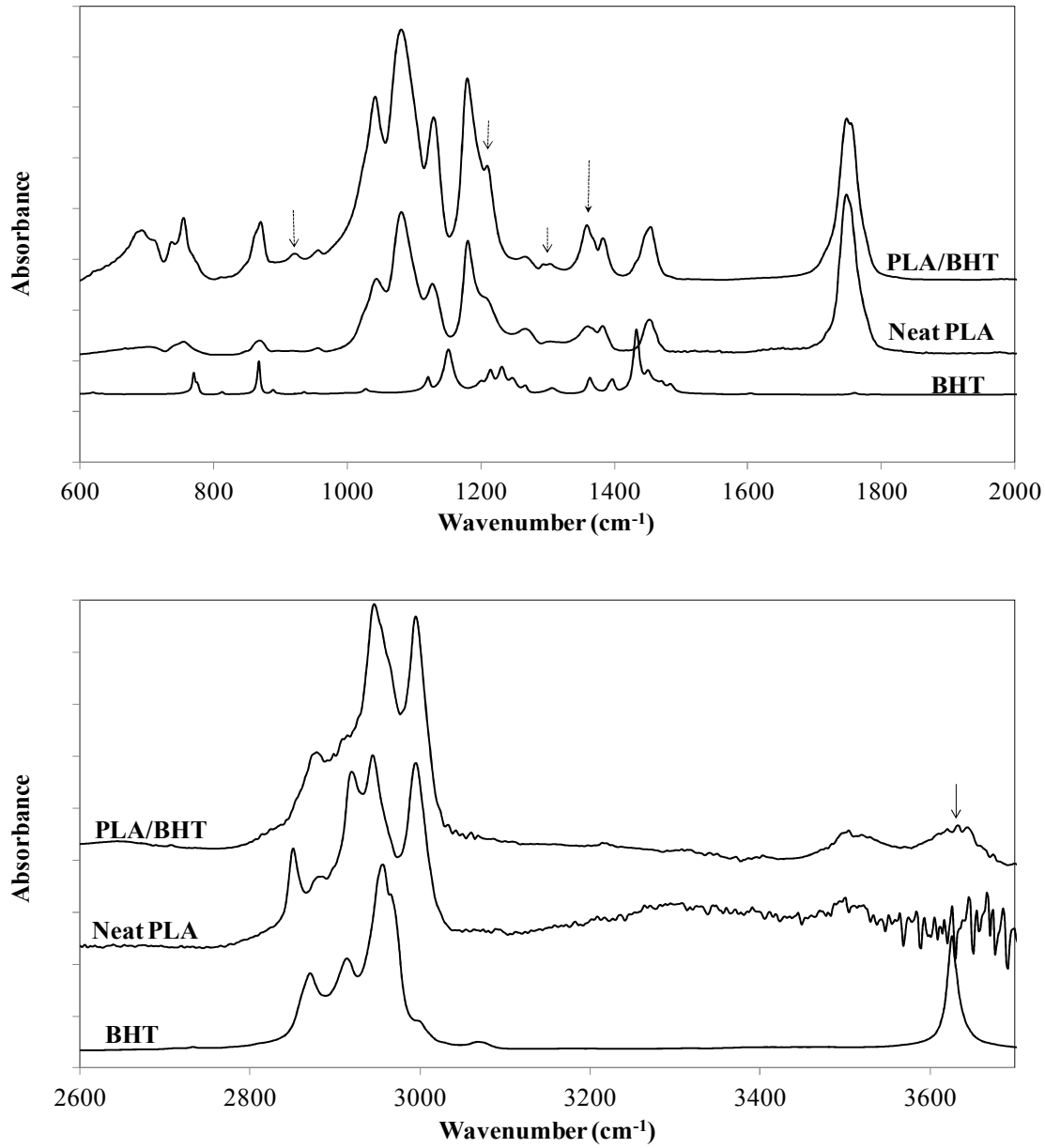

Figure 15 - ATR-FTIR spectra of PLA and enriched PLA with BHT films.

2.3.2. Optical microscopy

The enhancement of the thermal stability of PLA is a matter that has been receiving a large amount of attention, both from the processing and the application point of view. The effect of α-tocopherol in the density of spherulites when the films are melted followed by annealing at a crystallization temperature (T_c) above the Tg can be evaluated from the Figure 16. The polarizing optical micrographs show an increase in the number of spherulites with the increase of α-tocopherol content in the films. However, no spherulites are observed when the films are melted and quenched at 0 ºC. So, the overall crystallization of PLA enriched with α-tocopherol can be scrupulously selected and the final properties of films should be very well analyzed. As the crystallites can cause tortuosity, the present study on the effect of α-tocopherol on sorption of gases in additivated films will be performed using the last procedure to prepare our films, i.e., completely amorphous films.

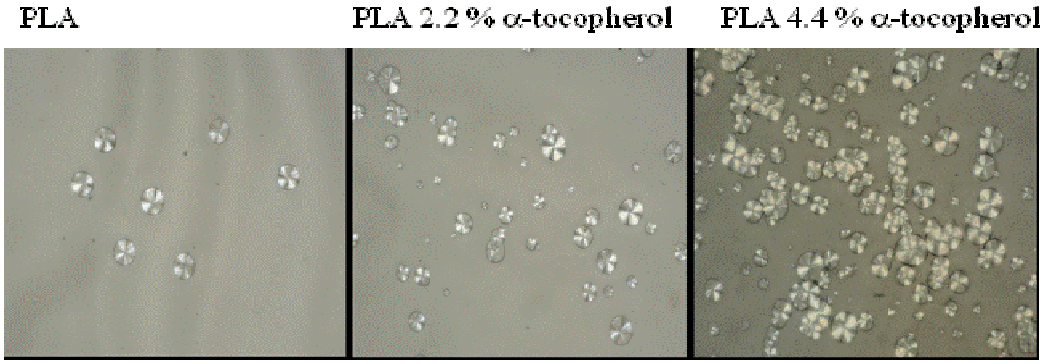

Figure 16 - Photomicrographs of the films annealed at 140 ºC from the melt for PLA enriched with 0 wt%, 2.2 wt% and 4.4 wt% of α-tocopherol.

2.3.3. Dynamic mechanical analysis

Dynamic mechanical spectra of samples, including PLA with 2.2 % and 4.4 % of α–tocopherol are shown in Figure 17. Polymeric properties are temperature-dependent. Plastics are hard and rigid at room temperature (20º C), but become softer at high temperature. This hardness or stiffness is measured as a modulus, a ratio of stress to strain at a certain stage of deformation. The decrease in Young's modulus (E') of samples is accompanied by a peak in the viscous dissipation, tan δ (Figure 18). Lower modulus values

are found in films with higher concentrations of α-tocopherol. A decrease of 37 % and 41 % for 2.2 % and 4.4 % were observed. This behaviour is similar to that found in plasticized films with glycerol, PEG or OLA by Martin *et al* [60] and suggests that the material became more flexible in the presence of α-tocopherol, i.e., lower storage modulus shows that the softness increases with addition of α-tocopherol content.

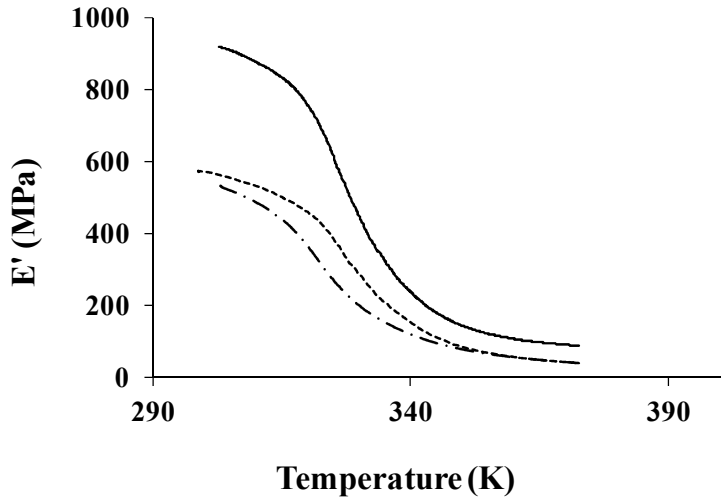

Figure 17 – Young's modulos of PLA and enriched α-tocopherol PLA (—) neat PLA, (- - -) PLA/α-tocopherol 2.2 wt%, (— . —) PLA/α-tocopherol 4.4 wt%.

Because the tan δ peaks related to glass transition of enriched films with α-tocopherol are very weak and broad, it was not possible the determination of Tg. Shibata *et al* [61] associated the broadening of the tan δ at a slight compatibility between two phases. In our case, and judging from the following SEM results, the broadening of the tan δ peak may be due a heterogeneous distribution of α-tocopherol into PLA.

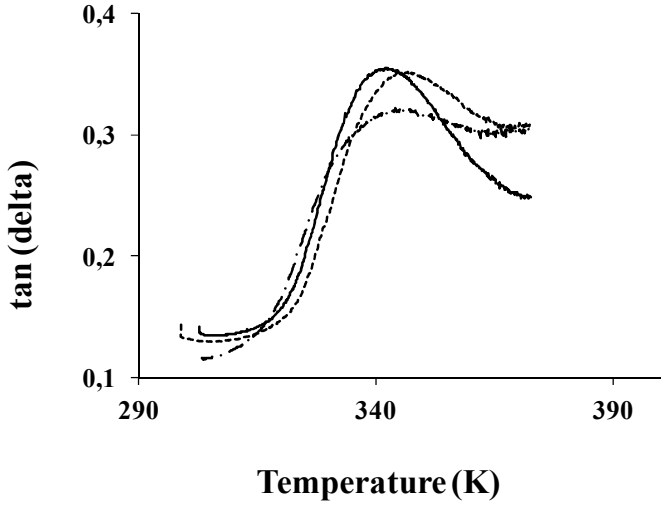

Figure 18 – Tan δ of PLA and enriched α-tocopherol PLA (—) neat PLA, (- - -) PLA/α-tocopherol 2.2 wt%, (— . —) PLA/α-tocopherol 4.4 wt%.

2.3.4. Thermal properties

The thermal stability of the films was monitored by themogravimetrical analysis. No significant differences were noticed in thermal degradation temperature, as can be seen from Figure 19 to Figure 21. All films exhibited similar degradations stages, characterized by only weight loss region. The degradation temperatures of the films containing different amounts of antioxidants were obtained by DTG curve analysis are shown in Table 3.

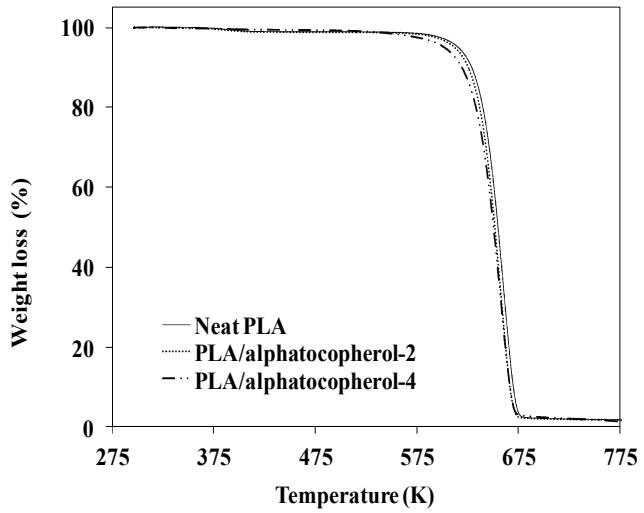

Figure 19 – TGA of PLA/α-tocopherol films (PLA/alphatocopherol-2 refers to 2 wt % of α-tocopherol content, and PLA/alphatocopherol-4 refers to 4 wt % of α-tocopherol into films.

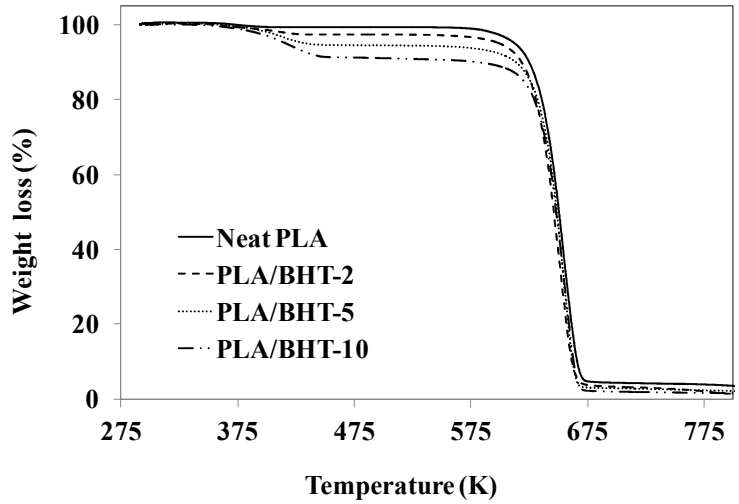

Figure 20 – TGA of PLA/BHT films (PLA/BHT-# refers to the BHT content in the films.

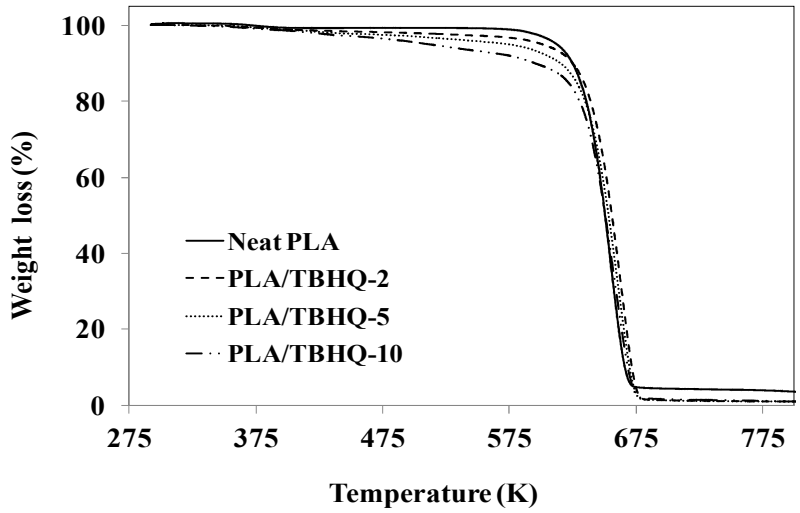

Figure 21 – TGA of PLA/TBHQ films (PLA/TBHQ-# refers to the TBHQ content in the films.

Table 3 – Weight loss and degradation temperature of PLA films.

Film	Weigh loss (%)	Degradation Temperature (K)
Neat PLA	95	660
PLA/α-tocopherol-2	95	658
PLA/α-tocopherol-4	94	658
PLA/BHT-2	92	655
PLA/BHT-5	90	656
PLA/BHT-10	87	656
PLA/TBHQ-2	95	662
PLA/TBHQ-5	94	660
PLA/TBHQ-10	88	658

For additivated films, the thermal stability decrease with the antioxidant content. Of the three antioxidants, TBHQ might act as a thermal stabilizer for the PLA/antioxidant films.

The DSC thermogram obtained during the first heating of the samples enriched with BHT 2 % wt and TBHQ 2 % wt are presented in Figure 22 and shows that the films enriched with TBHQ exhibits a broad crystallization in the range 350 K - 400 K, centered at about 378 K. This peak reflects the large amorphous component in the cooled PLA/TBHT film. When the polymer is heating, the molecules acquire thermal energy, and at glass transition temperature, the molecules have enough energy to overcome the intermolecular forces and they have more freedom of movement. The amorphous region becomes rubbery and the polymer become soft and flexible. With heat, the molecules in amorphous phase have mobility to arrange themselves into an ordered crystal. Crystallisation is an exothermic process, and a correspondent peak appears in the thermogram. During the first heating, this arranges crystalline appears in the same range of temperatures only for PLA enriched films with TBHQ and have a centered peak about 378 K to 2 wt% and 5 wt% of TBHQ and 374 K for PLA enriched with 10 wt% TBHQ, i.e., the T_C obtained from the first heating of the PLA/TBHQ films shift to lower temperatures (Figure 23). During the cooling, the amount of TBHQ decrease the enthalpy of crystallization, and causes a band broadening centered at about 369 K (Figure 24). PLA/BHT enriched films do not exhibit crystallization during the first heating. The Figure 23 and Figure 25 show that PLA films enriched with both antioxidants TBHQ and BHT exhibits a crystallisation peak in second heating. The rearrange that occurs in this heating should be of the crystals formed during the cooling after the first heating, are therefore of different nature from that appears in the first heat of PLA/TBHQ, ones formed from the solution and the other from the melted. The crystallization temperature shift to high temperature region for both BHT and TBHQ enriched films relatively at neat PLA. The results of DSC analysis are shown in Table 4 (firs heating) and Table 5 (second heating).

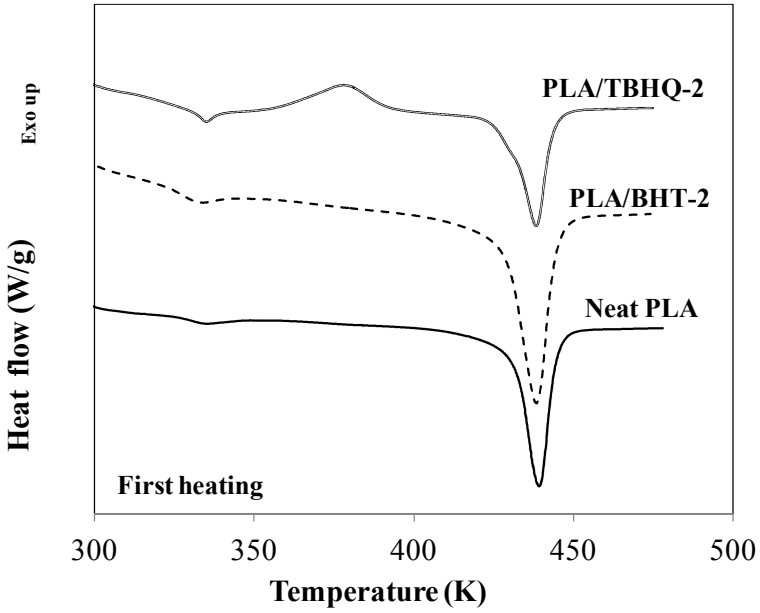

Figure 22 - DSC thermograph of first heating of neat PLA and PLA films containing 2 wt % of BHT and TBHQ.

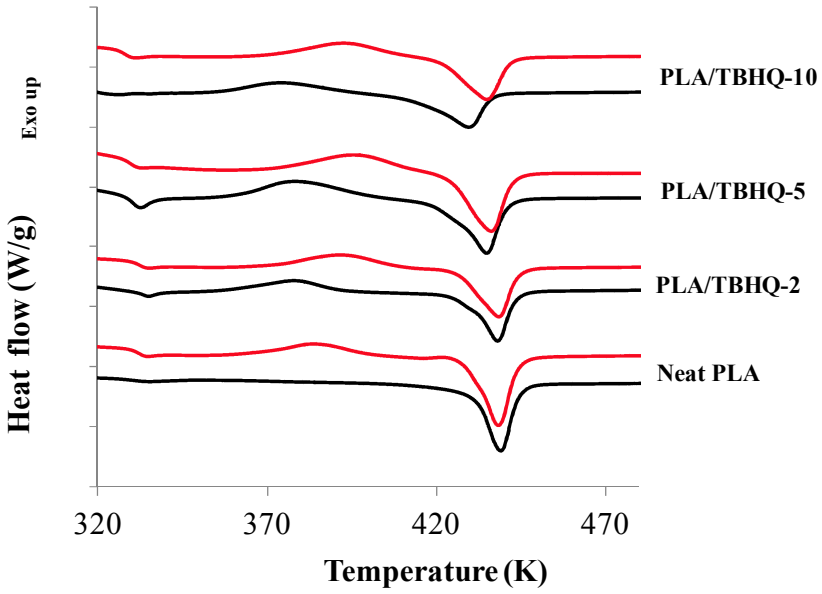

Figure 23 - DSC thermograph of PLA films containing 2 wt%, 5 wt% and 10 wt% of TBHQ. Black and red lines present the first and second heating runs, respectively.

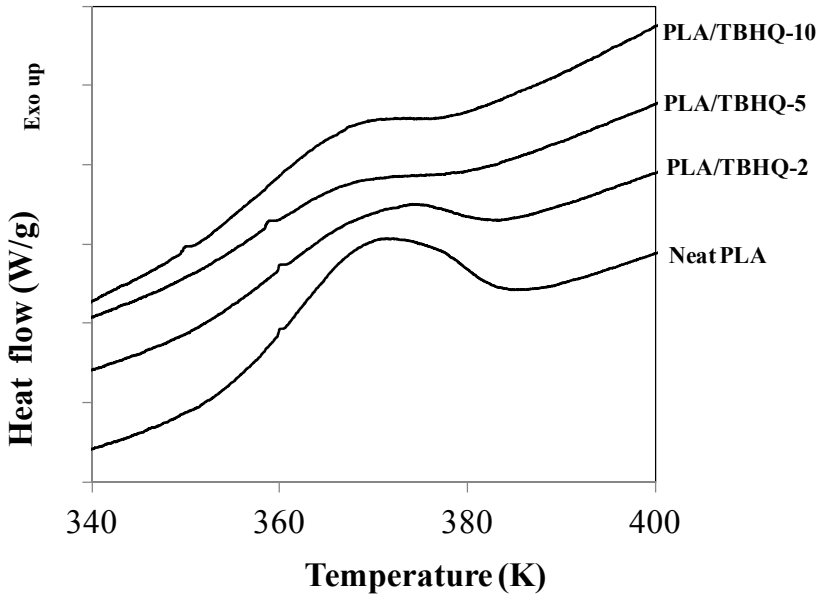

Figure 24 – First Cooling DSC thermograph of PLA films containing 2 wt%, 5 wt% and 10 wt% of TBHQ.

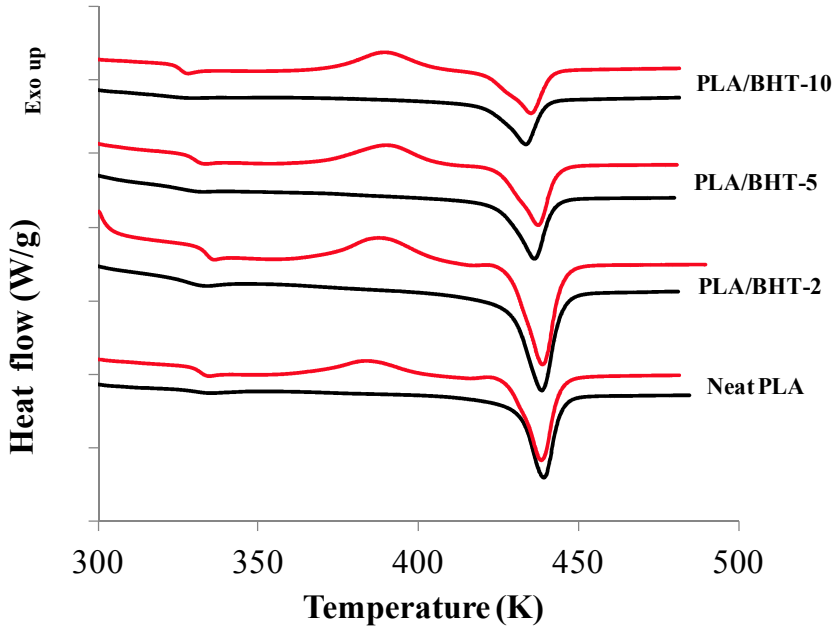

Figure 25 - DSC thermograph of PLA films containing 2 wt%, 5 wt% and 10 wt% of BHT. Black and red lines present the first and second heating runs, respectively.

Table 4 – Thermal properties of PLA films containing different percents of antioxidants (first heating).

Sample	T_C (K)	ΔH_C (J/g)	T_m (K)	ΔH_m (J/g)	χ(%)
Neat PLA	-	-	439	42.9	46
PLA/BHT-2	-	-	438	43.2	47
PLA/BHT-5	-	-	436	36.6	41
PLA/BHT-10	-	-	434	35.6	42
PLA/TBHQ-2	378	14.6	438	32.3	18
PLA/TBHQ-5	378	25.6	435	33.3	9
PLA/TBHQ-10	374	16.2	430	29.2	15

The addition of BHT and TBHQ increase the crystallization temperature of the melted samples formed during the cooling after first heating. The highest Tc = 396 K was obtained for PLA with 5 wt% of TBHQ, more 12 K than neat PLA. In the samples with thermal treatment by DSC, the crystallization occurred around 390 K for all samples, more 6 K than for neat PLA.

For films without thermal treatment by DSC, the crystallinity of PLA/TBHQ films seems to be independent of the antioxidant content and is about 61 % lower than neat PLA. The crystallinity increase 1 % relatively at neat PLA for 2 wt % of BHT and then decrease 11 % to 5 % and 10 wt % of BHT.

Neat PLA melted in DSC presents a crystallinity of 20 %, i.e., 56 % lower than without thermal treatment. The crystallinity of PLA/BHT melted films decrease with the amount of BHT into the film, from 16 % to 9 % to 2 wt % and 10 wt % of BHT, respectively. For enriched films with TBHQ, the crystallinity is almost constant ~12 % and independent of the amount of TBHQ in the film.

Melted pure PLA exhibited a T_g around 331 K and a melting temperature, around 438 K. The addition 2 wt % of BHT increase 3 K the T_g, and 10 wt % of BHT decrease 5 K. It is thought that the increase of Tg with small amounts of BHT disturb the mobility of amorphous PLA. The presence of strong interactions between the PLA and BHT seems to occur, despite the fact that the presence of aromatic rings in the backbone should have a more dramatic effect on T_g. Their presence seems to hinder the lateral polymer chains to moving, acting as a filler. At high concentrations of antioxidants, we can observe a small plasticizer effect, since the T_g decrease about 5 K relatively at neat PLA. Similar results

were found for PLA/TBHQ films. The Tg decrease with the amount of TBHQ into the film, decreasing only 6 K to 10 wt% of antioxidant. The melting temperature decrease 4 K for BHT and 3 K for TBHQ, both BHT and TBHQ 10 wt%.

What happens with α-tocopherol, a large molecule compared with BHT and TBHQ compounds? Figure 26 show the effect of the addition of α-tocopherol on T_g, T_C and T_m.

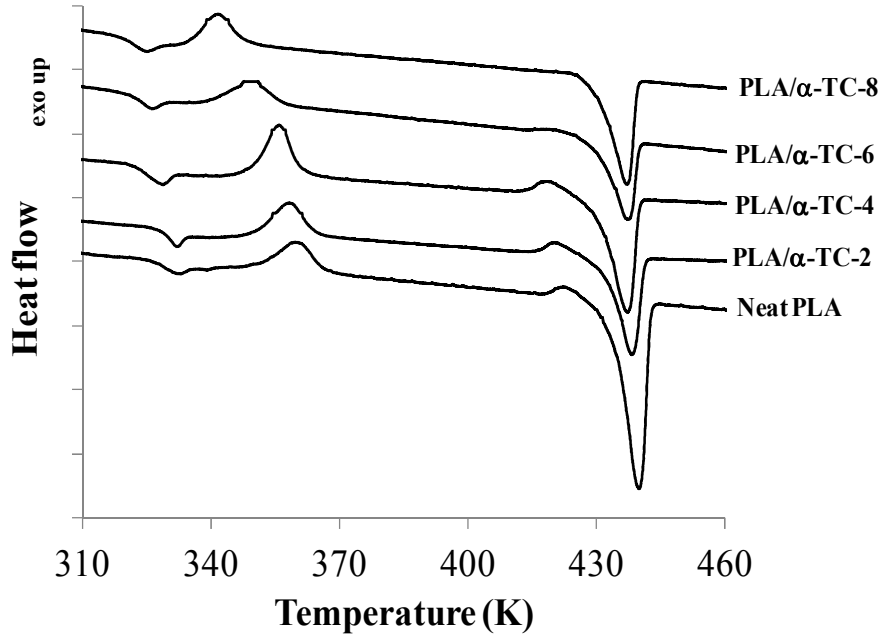

Figure 26 - DSC thermogram obtained during second heating of samples enriched with 2 wt%, 4 wt%, 6 wt% and 8 wt% of α-tocopherol.

The crystallization temperature for enriched films with α-tocopherol shift to a lower temperature and its enthalpy increases by incorporation of a small amount of α-tocopherol (2 wt %) but decrease with the increase of α-tocopherol in the film (Table 5). The α-tocopherol causes an opposite effect on Tc than the other antioxidants, while BHT and TBHQ shift the T_C to higher temperatures, α-tocopherol shift to lower temperature. Crystallization temperature decrease to 342 K with the incorporation of 8 wt % of α-tocopherol, a decrease of 42 K when compared to that of neat PLA.

Table 5 - Thermal properties of PLA films containing different percents of antioxidants (second heating).

Sample	T_g(K)	T_C (K)	ΔH_C (J/g)	T_m (K)	ΔH_m (J/g)	χ(%)
Neat PLA	331	384	16.0	438	36,9	20
PLA/BHT-2	334	388	21.5	439	36,6	16
PLA/BHT-5	330	390	20.4	436	33,5	15
PLA/BHT-10	326	389	25.6	434	33,4	9
PLA/TBHQ-2	330	392	19.4	438	31,8	13
PLA/TBHQ-5	327	396	22.8	436	33,5	12
PLA/TBHQ-10	325	393	20.2	435	30,6	12
PLA/α-tocopherol-2	330	358	25.6	438	39.9	16
PLA/α-tocopherol-4	325	356	22.4	437	35,4	14
PLA/α-tocopherol-6	321	349	22.1	438	35,9	16
PLA/α-tocopherol-8	320	342	20.3	437	41,3	25

The crystallinity does not change with the amount of α-tocopherol content in the film up to 6 % and then increases to about twice from 16 % to 25 % to 8 wt% of α-tocopherol. No significantly changes were observed for melting temperature. For 8 % of α-tocopherol, the Tg decrease 11 K, indicating that α–tocopherol behaves as a plasticizant, i.e. increasing the mobility of PLA chains in the amorphous regions, thus allowing more rearrangements of polymer chains and consequently higher crystallinity. Piorkowska *et al.*[62] have obtained a similar result when PLA was plasticized with poly(propylene glycol), PPG.

In what concerns the glass transition temperature, a decrease of 11 K for when to 8 wt % of α-tocopherol content into the film was observed. Overall, the antioxidants incorporation into PLA increases the free volume of the polymer matrix and consequently promotes the enhancement of polymer chain mobility. Therefore, these antioxidants possibly act as plasticizers in the PLA matrix. It is well known that the addition of low molecular weight compounds decreases PLA rigidity and brittleness by reducing its glass transition temperature.[59] The results obtained in this work for antioxidants concentrations above 2 wt % are in agreement with some works which demonstrate that PLA melting point shifts to lower temperatures with the addition of different plasticizers[59], however the incorporation of only 2 wt % of each antioxidant into PLA films did not affect the melting temperature. Manzanares-López *et al* [53] and Jamshidian *et al.*[55] found similar results

regarding the melting temperature after the incorporation of 2.58 wt% α-tocopherol and 1 wt% BHT, respectively, into PLA. However, the results here obtained contradict those of Jamshidian *et al.*[63], who showed that the melting point of PLA decreases about 8 K with the incorporation of only 2 wt% α-tocopherol. Table 6 presents a short summary of the effect of the antioxidants incorporation into PLA, by different processes. Films extruded are formed from the melted, whereas those formed by casting are from the solution. Then the results obtained from the first heating can be compared with the casting and the results obtained from the second heating can be compared with the extruded films.

Table 6 - Thermal properties of PLA films containing different percents of antioxidants from others works.

PLA	(wt %) compound	Method for Film preparation	Tg	Tm	Tc	χ (%)	Reference
94% L	0	Extruded	58.58	147.32	142.79	25	Manzanarez-López *et el*[53]
	(2.58) α-tocopherol + (0,75)BHT		57.19	146.35	141.15	5.6 – 5.7	
94 % L	0	Extruded	55.96	149.01		14.04	Hwang *et al*[56]
	α-TC-10 / RSV- 40		52.47	143.66		7.49	
	α-TC-20 / RSV- 30		51.81	144.75		5.37	
	α-TC-25 / RSV- 25		52.23	146.22		1.71	
	α-TC-30 / RSV- 20		51.05	145.75		1.84	
	α-TC-40 / RSV- 10		50.13	146.46		5.16	
94 % L	0	Extruded	57.8	151.6		0.3	Ortiz-Vazquez *et al*[54]
	(1.5) BHT		57.2	150.3		0.5	
? 4000 series	0	Extruded	66	166	127	-	Byun *et al*[52]
	(0.01)BHT/ (0.1)PEG		51	142/151	101	-	
	(1) α-Tc/ (0.01) BHT / (0.1)PEG		52	165	83	-	
21-30 %L	0	Casting	59.7	150.7	95.1	20.3	Jamshidian *et al*[63]
	(2) α-tocopherol		58,2	142.6	74.1	13.6	
	(1) ascorbil palmitate)		59.2	147.4	94.6	13.4	
21-30 %L	0	Casting	55.3	144.7	107.0	19.5	Jamshidian *et al*[55]
	(1) TBHQ		54.6	140.8	95.3	14.1	
	(1) PG		55.8	140.1	100.4	14.8	
	(1) BHT		55.1	143.3	97.6	14.3	
	(1) BAH		54.3	143.4	98.4	13.8	

2.3.5. Scanning electron microscope (SEM)

Enriched films with antioxidants were crio-fractured in order to examine the microstructure aspects. Photomicrographs of blended films of PLA with 2 % of α-tocopherol fracture revealed formation of voids, considerable ductile tearing and inhomogeneity. PLA/BHT 2 wt% revealed absence of ductile tearing as in neat PLA and an integrity at the surface. PLA/TBHQ 2% wt revealed considerable ductile tearing, rough surface and integrity at the surface. Some powder grains can also be observed (Figure 27). BHT enriched films maintain the brittle failure of the PLA.

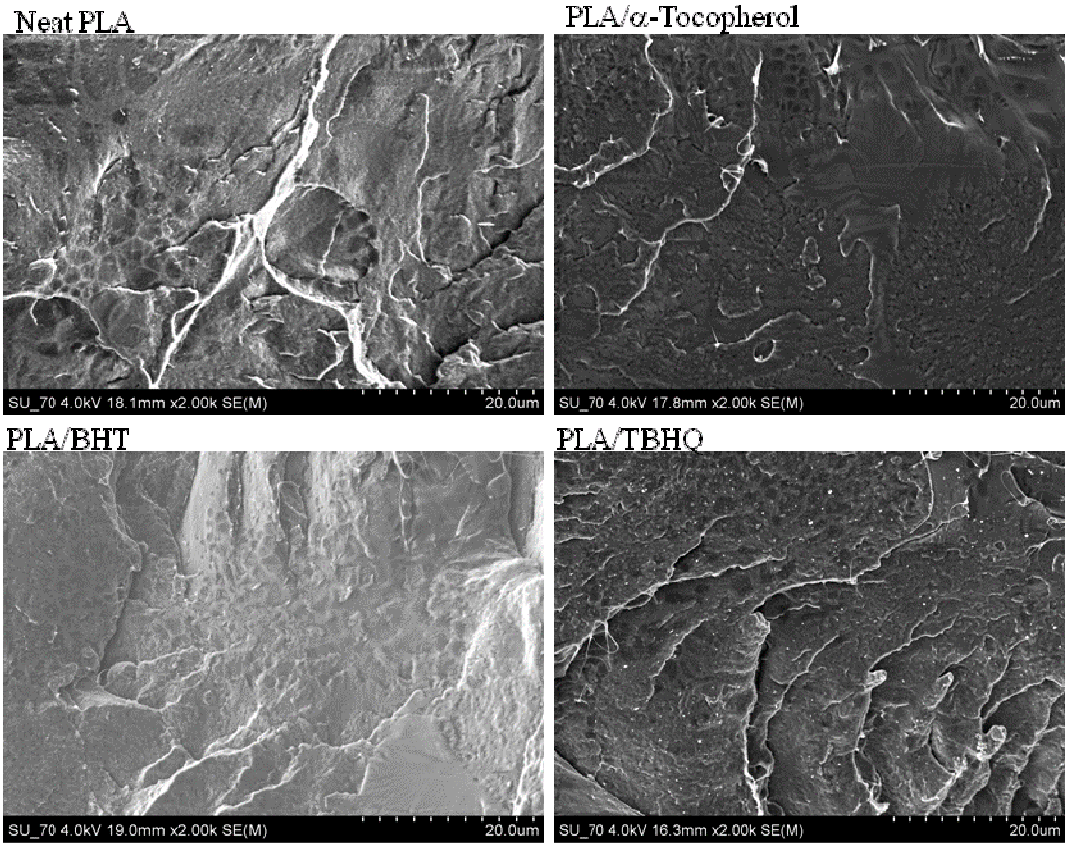

Figure 27 – SEM micrographs of fracture surfaces of blends with 2 % of each antioxidant.

The voids are present in the α-tocopherol film with 5 % α-tocopherol. However the film seems to be more homogeneous than a previous sample with 2 % of α-tocopherol (Figure 28). A dramatically difference appears in TBHQ 5 wt% film, that revealed homogeneity, increase of ductile tearing and a completely smooth surface. The increase of TBHQ seems

to improve the compatibility with PLA. Both films are less bright, which can be due the less crystallinity. Films of PLA/BHT 5wt% revealed brittle failure, and the presence of some powder grains (Figure 29).

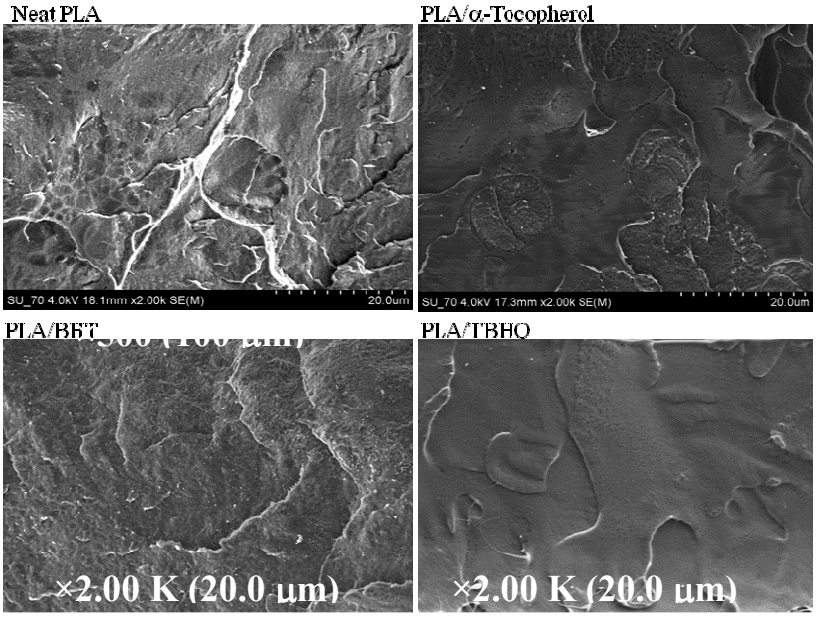

Figure 28 – SEM micrographs of fracture surfaces of blends with 5 % of each antioxidant.

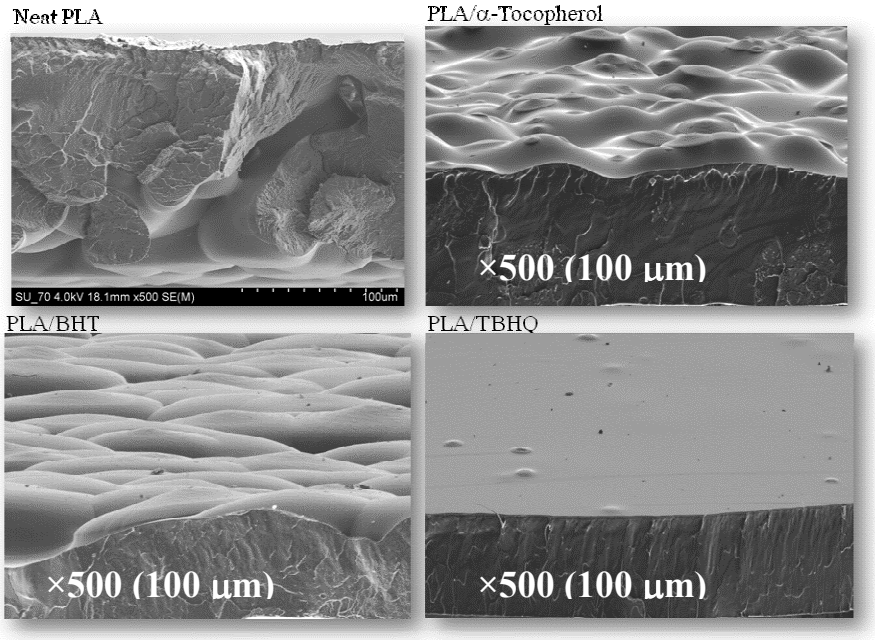

Figure 29 – SEM micrographs of fracture surfaces /surfaces of blends with 5 % of each antioxidant.

Finally, micrographs of PLA films enriched with 10 wt% of antioxidants are shown in Figure 30. The addition of large amounts of these antioxidants does not seem to improve the structural characteristics of the films, PLA/BHT seems now to be very homogeneous surface, indicating ductile tearing of the films. Films with 10 wt% of α-tocopherol revealed inhomogeneity, formation of voids and absence of ductile tearing. This is an indication of phase separation due to incompatibility of the antioxidant with the PLA, and brittle failure. Very smooth films were formed by addition of TBHQ.

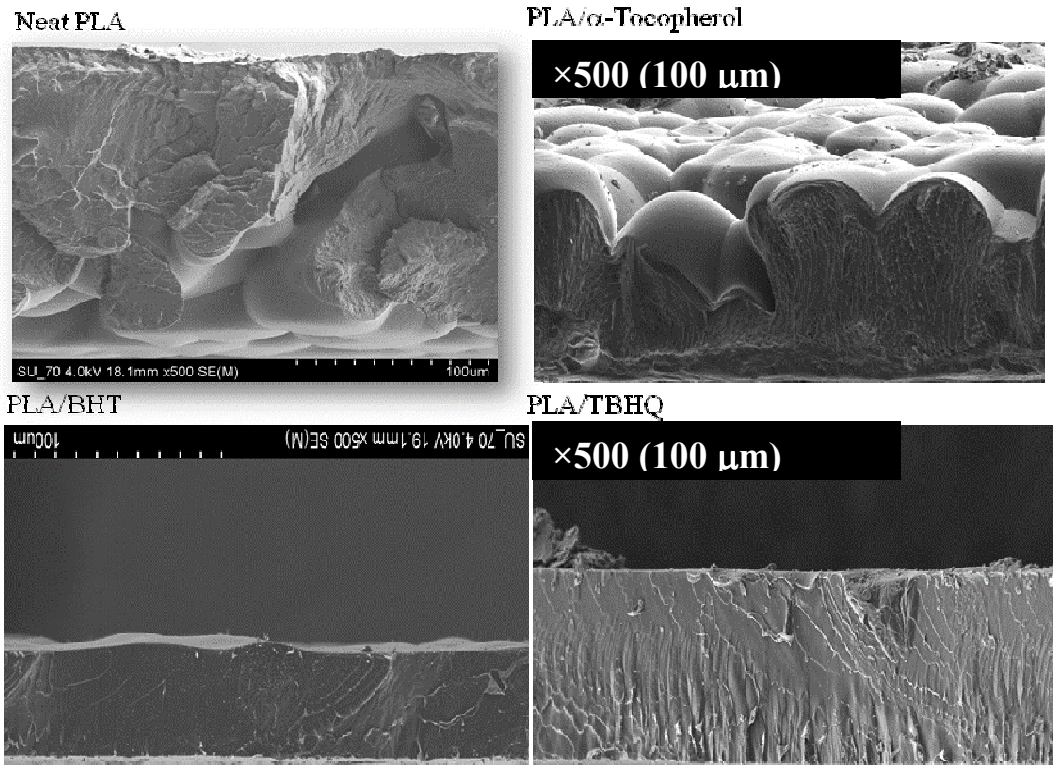

Figure 30 – SEM micrographs of fracture surfaces /surfaces of blends with 10 % of each antioxidant.

Figure 31 and Figure 32 show that at above a certain concentration an incompatibility, immiscibility, between the selected antioxidants occurs, due to the hydrophobic character of α-tocopherol and BHT conferred by their hydrocarbon chains. These incompatibilities cause morphological changes in the PLA film structure, which can be clearly seen in the SEM micrographs.

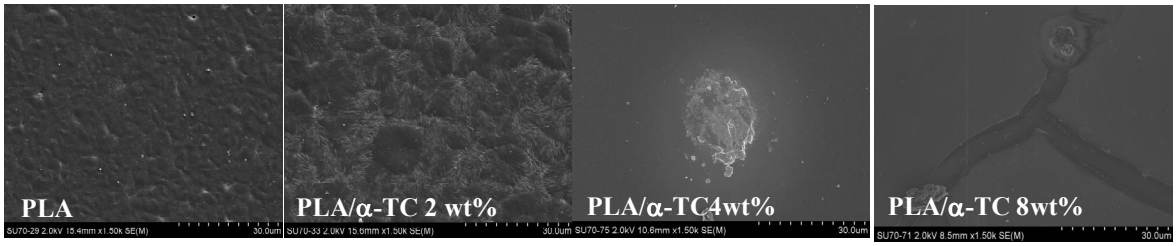

Figure 31 – SEM micrographs of surface of PLA with and without α-tocopherol (α-TC).

In conclusion, TBHQ has better compatibility with PLA and its addition provides a significant flexural enhancement of PLA. The increase of crystallinity for high concentrations of α-tocopherol should result from the phase separations, because the aggregates of α-tocopherol trap the PLA and improve the interaction, promoting the crystals formation.

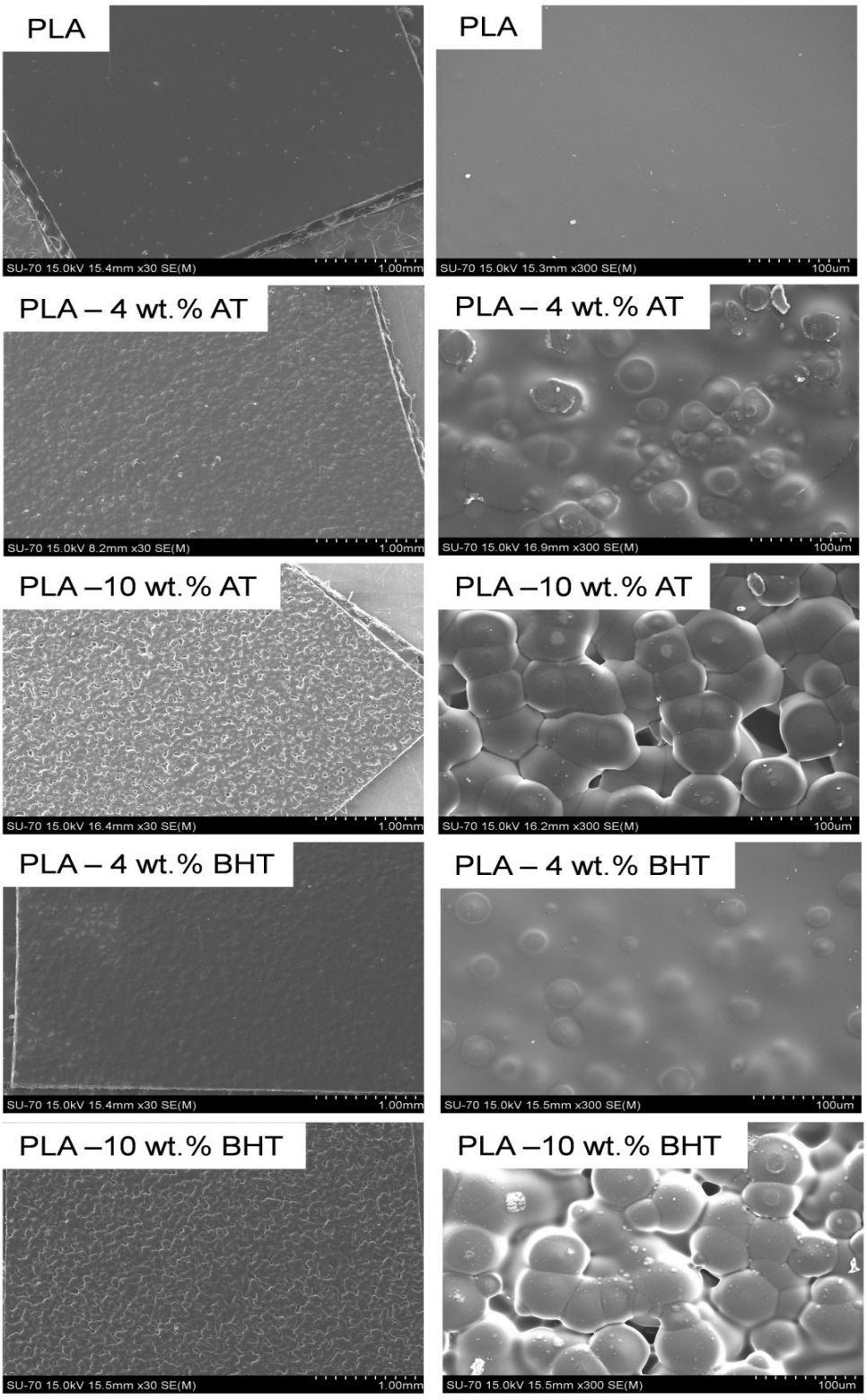

Figure 32 – SEM micrographs of the pure PLA films with 4 and 10 wt% of α-tocopherol or BHT incorporated.

2.3.6. X-ray and AFM

Figure 33 shows the X-ray diffraction data of neat PLA and enriched PLA with α-tocopherol. These films were not subject to a thermal treatment. Neat PLA exhibits a crystalline peak at 2θ about 12º, which agree with data previously published with characteristic peaks at 2θ about 12.5, 14.7, 16.6, 19.1 and 22.3 ºC.[64] This peak vanish with the addition of α-tocopherol, this seems to hinder the mobility of the chains of the polymer and consequently the formation of the crystals. The films containing α-tocopherol 2 and 6 wt % present a broad amorphous peak from PLA around 16º, confirming that PLA has an amorphous microstructure (Figure 34). From AFM observation, it can be concluded that the samples resultants of the addition of α-tocopherol have a smoother surface compared with the uneven rough surface of neat PLA (Figure 35 and Figure 36). Since X-ray give us only results from whole volume of sample, the AFM was used as complementary analysis, because showing only the surface image. The combination of both techniques allows to conclude where the ordered crystalline phase is, and in the case of neat PLA is placed deeper, i.e., into internal layers of films. The smoothness of the surface films containing antioxidant may be due to its plasticizer effect.

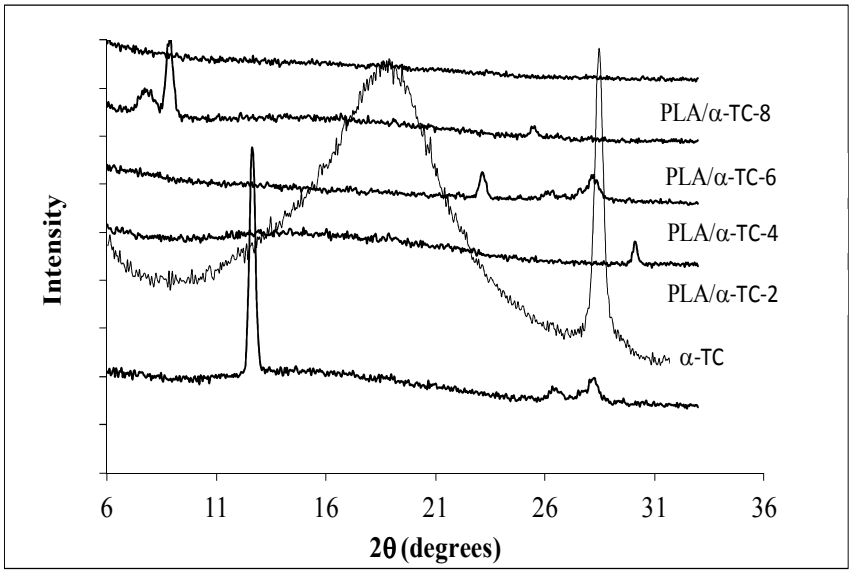

Figure 33 - X-ray diffraction data of neat PLA and enriched films with 2 wt%, 4 wt%, 6 wt% and 8 wt% of α-Tocopherol (α-TC).

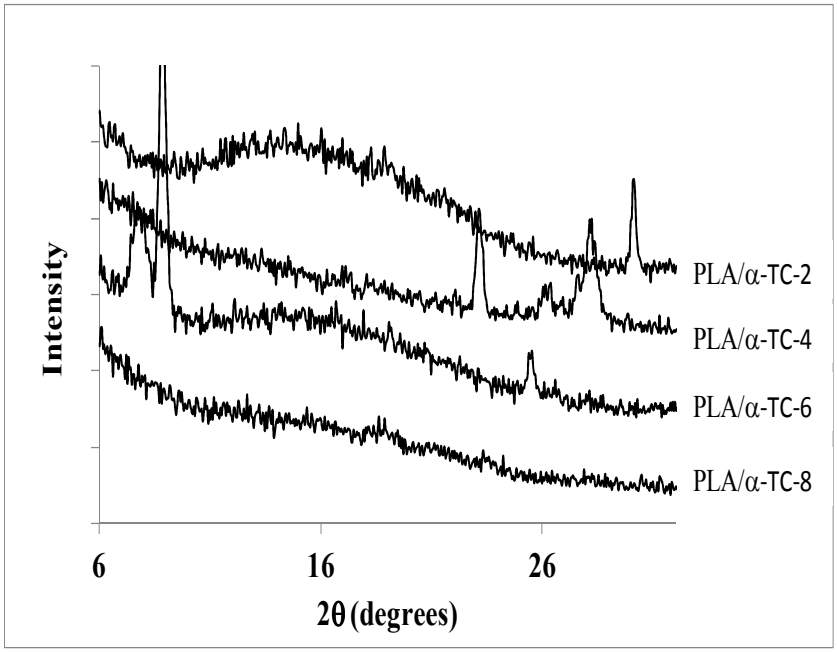

Figure 34 – X-ray diffraction data of enriched films with 2,4, 6 and 8 wt % of α-Tocopherol (α-TC).

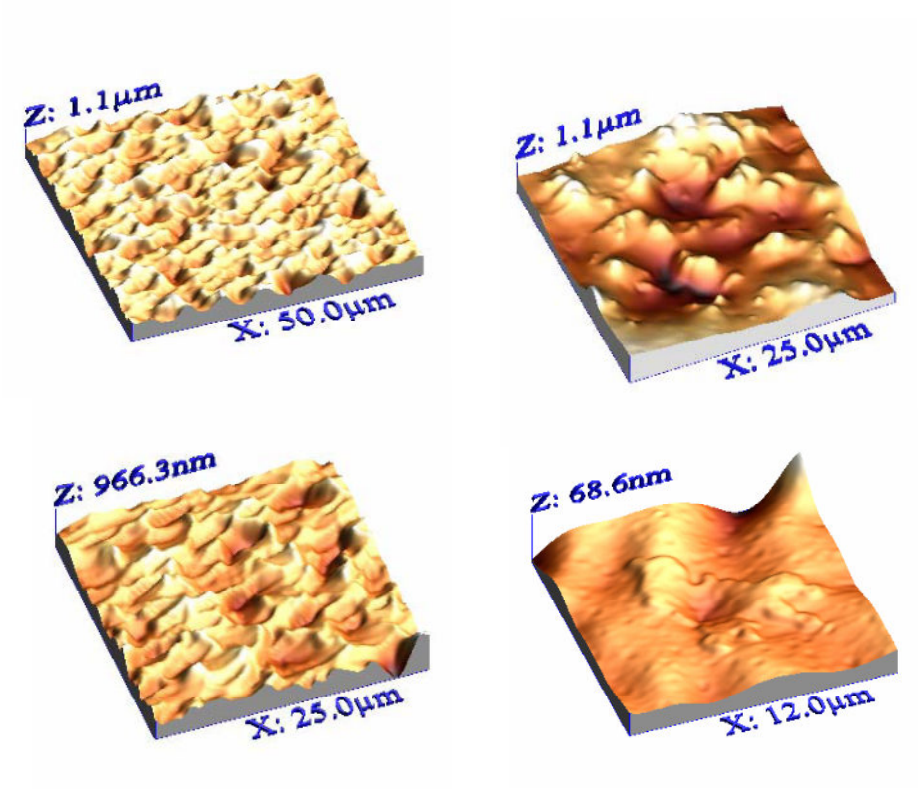

Figure 35 – AFM images of neat PLA (left) and PLA/α-tocopherol 2 wt % (right).

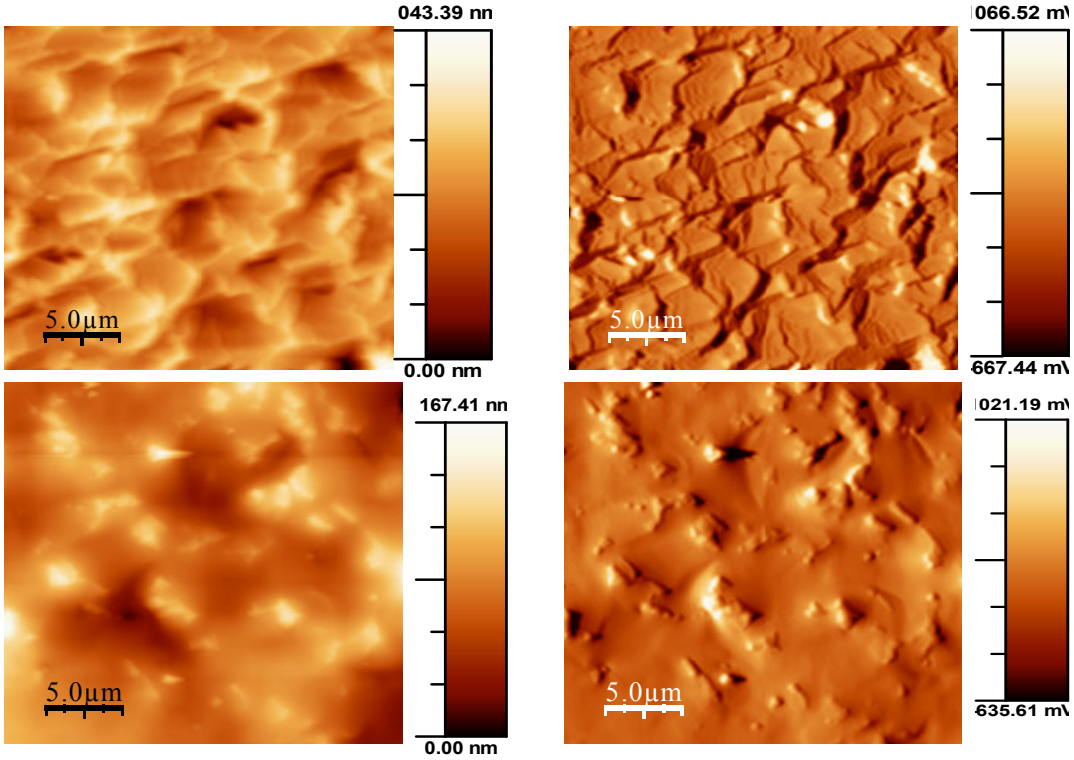

Figure 36 – AFM images of neat PLA (top) and PLA/α-tocopherol (bottom).

2.3.7. Contact angles and surface energy

The water contact angle value measured on the pure PLA film (65º) is in good agreement with the literature, which ranges from 69º to 87º.[59] The enhancement of the hydrophobic character of the PLA film surface with the antioxidants incorporation was clearly shown by the increase of water contact angles from 76.5º to the highest value 98.5º for PLA-10 wt% α-tocopherol. This increment can be attributed to the hydrophobic nature of each antioxidant and demonstrates the decreased wettability of PLA films by the antioxidants incorporation. Jamshidian *et al.* [55] observed exactly the same behaviour for PLA-BHT and PLA-TBHQ films, but with less pronounced effects since only 1 wt.% of antioxidant was added. Moreover, Hwang *et al.* [56] also concluded that the water contact angles of PLA films additivated with both AT and revesratrol slightly increase when compared to that of neat PLA films. Table 7 lists the average contact angle (θ) of water deposited onto PLA films surface.

Table 7 – Water contact angles (θ, degree), polar (γ_s^p) and dispersive (γ_s) components of surface energy (γ_s) of the PLA films.

Film sample	θ_{Water} (º)	γ_s^p (mJ/m^2)	γ_s^d (mJ/m^2)	γ_s (mJ/m^2)
PLA	76.5 ± 0.3	4.7	33.2	37.9
PLA - 2 wt.% AT	83.3 ± 0.7	2.6	31.8	34.4
PLA - 4 wt.% AT	89.1 ± 0.7	1.3	31.4	32.7
PLA - 10 wt.% AT	98.5 ± 0.7	0.1	32.5	32.6
PLA - 2 wt.% BHT	81.1 ± 0.7	2.5	36.5	39.0
PLA - 4 wt.% BHT	86.4 ± 0.4	1.4	35.6	37.0
PLA - 10 wt.% BHT	90.2 ± 0.7	0.7	36.4	37.1
PLA - 2 wt.% TBHQ	79.8 ± 0.7	3.2	35.3	38.5
PLA - 4 wt.% TBHQ	83.3 ± 0.3	2.1	36.0	38.1
PLA - 10 wt.% TBHQ	86.2 ± 0.9	1.2	37.3	38.5

Surface energy and its polar and dispersive components of PLA films were calculated from the contact angle values formed by liquids (water, formamide, ethylene glycol and diiodomethane).[59] As can be seen in Table 7, no significant changes were observed in the surface energy of PLA-BHT and PLA-TBHQ films when compared to pure PLA. On the other hand, the surface energy of the α-tocopherol/PLA films decreases with the α-tocopherol content essentially due to the reduction of the polar component, which can be linked to the non-polar aliphatic chain of this natural antioxidant.

2.4. Conclusion

Addition effects of α-tocopherol, BHT and TBHQ on physical, mechanical, structural and morphological properties of solvent-casted PLA films were studied. Enriched films with α-tocopherol became yellowish, which is not desirable in terms of consumer acceptability. SEM images of membranes enriched with BHT show that the miscibility of BHT and PLA was not good, and the powder agglomerates increase with the BHT content increase. PLA/BHT 2 wt% membranes revealed a cohesive structure with brittleness failure. The method used to produce enriched films with α-tocopherol needs to be improved since the membranes revealed inhomogeneity at lower concentration and for higher concentrations phase separation occurs. TBHQ seems to be the best antioxidant, because the films were transparent, smooth, with good flexibility (visible evaluation). However, this antioxidant decreases the crystallinity, and as we know, reduction of crystallinity is a negative point regarding mechanical and barrier properties. This was the only antioxidant that seems to improve the thermal stability, despite the reduction of the crystallinity. Membranes obtained with 2 wt% of TBHQ revealed some powder. However, for higher contents of TBHQ no powder is visible and the flexibility increases, while the crystallinity remains constant. These conclusions are valid for concentration up to 10 wt%.

3. Selectivity and barrier properties of poly(lactic acid) films using quartz crystal microbalance

3.1. Introduction

The piezoelectricity was first detected in 1880 by Pierre and Jacques Curie. This property feature of some materials is based on an electric potential produced when a material, such as a quartz crystal, is subjected to mechanical stress. Piezoelectric crystal sensors are passive solid-state electronic devices, which can respond to changes in temperature, pressure, and most importantly, to changes in physical properties at the interface between the device surface and a foreign fluid or solid. Such changes in physical properties include variation in interfacial mass density, elasticity, viscosity, and layer thickness.[65] The incorporation of various chemically sensitive layers has enabled the transition from the microbalance to the mass sensor and gave rise to an explosive growth of piezoelectric sensors in recent years. This type of sensor operates by observation of the propagation of an acoustic wave through the solid-state device. Sensing is achieved by correlating acoustic wave-propagation variations to the amount of analyte captured at the surface and then to the amount or concentration of analyte present in the sample exposed to the sensor, or to the changes of physical properties of interfacial thin films.[65] A selective sensor is obtained when a sensor surface is coated with a selectively interacting thin film.[65] This sensor principle employing bulk acoustic waves (BAW) was introduced by King[65] in 1964 with the construction of his piezoelectric sorption detector.[65] There are two types of piezoelectric crystal sensors: the AT-cut quartz crystal sensor using BAW, the other is based on surface waves (SAW) device (Figure 37). [65]

In 1959, Sauerbrey introduced a new method for mass measurements, using the change in the frequency of a quartz resonator to measure the mass of a film adherently deposited on the quartz resonator surface.[66] The Sauerbrey's mass measuring instrument was named quartz crystal microbalance, QCM.[66] QCM is a thickness-shear-mode acoustic wave sensor, generally used as a microgravimetric sensor. A thin mass layer deposited on the surface of the quartz crystal can be measured according to the decrease of the resonant frequency. The frequency is the most accurately quantity that can be measured, of the order of $\Delta f/f_0=10^{-7,}\ 10^{-8}$, which corresponds to a mass of the order of a nanogram in the case of standard QCMs of 9 MHz.[67] The decrease of the resonant frequency of a thickness shear

vibrating quartz crystal resonator, having AT or BT cut (AT or BT expressed the crystallographic orientations of the quartz resonator), is proportional to the added mass of the deposited film:[66]

$$\Delta f_r = -\frac{f_q^2 \Delta m_f}{N \rho_q A} = -2.3 \times 10^6 f_q^2 \frac{\Delta m_f}{A} \qquad \textbf{(2)}$$

where Δf is the resonant frequency shift due to layer (Hz), f_q is the resonant frequency of the quartz (MHz), N the frequency constant of the specific crystal cut (N_{AT}=1.67×10^5 Hz.cm; N_{BT}=2.5×10^5 Hz.cm), ρ_q=2.649 kg/dm^3 the quartz density, A the surface area of the deposited film (cm^2) and Δm_f (g) the mass. [66, 68]

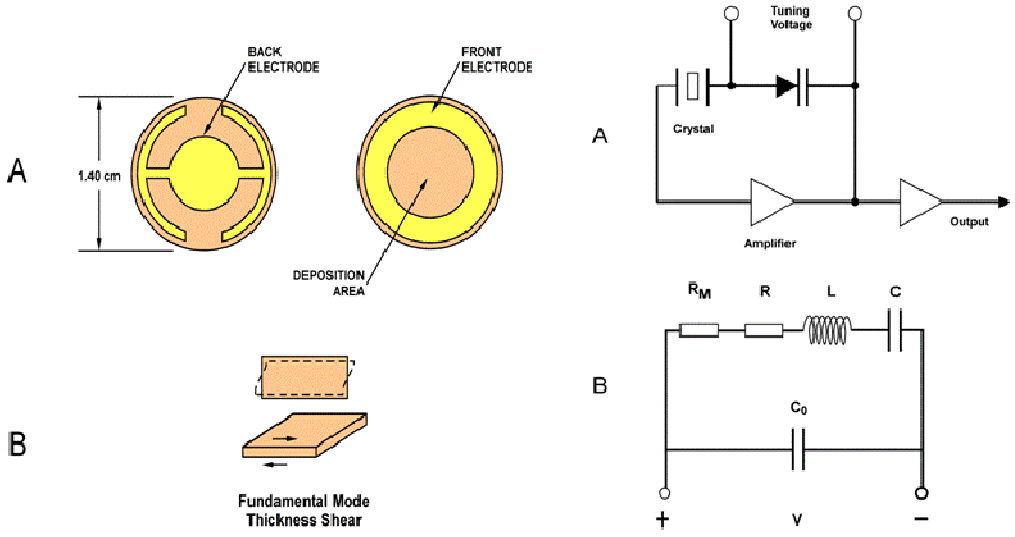

Figure 37 - A typical quartz crystal resonator used for mass measurements left picture: A-Schematic of typical quartz crystal microbalance; B-Illustration of transverse shear mode of oscillation; right picture: A-Simplified oscillating driving circuit schematic for a quartz crystal; B-Circuit equivalent diagram for a quartz crystal.[69]

This treatment is rigorously valid only for infinitesimally thin films that have an acoustic impedance (for shear waves) close to that of quartz, conditions that are valid for a fairly rigid, firmly attached thin films.[68]

Schrag *et al* [68], developed theoretical models to predict the mechanical response of a model quartz crystal microbalance to viscoelastic thin layer. Special care should be taken

so that the Sauerbray equation is valid, meaning that the added mass needs to be evenly distributed over the electrodes and is much smaller than the mass of the quartz disk, $\Delta f/f << 1$.[70]

These conditions are important since it is known that the moisture or vapors absorbed in the coating makes it less rigid, allowing for deviations from the well-known Sauerbrey expression. A critical term, $\beta_1 D$ (β is related to the shear wavelength λs and D the thickness of sample layer), can be used to determine deviations from ideal behaviour equations (3) and (4).[68]

$$\beta = \frac{2\pi}{\lambda_s} = \sqrt{\frac{\omega\rho}{\eta_M}} \cos\left[(\pi/4) - (\phi/2)\right] \quad \textbf{(3)}$$

$$\alpha = \sqrt{\frac{\omega\rho}{\eta_M}} \sin\left[(\pi/4) - (\phi/2)\right] \quad \textbf{(4)}$$

were ω is the radian frequency and ρ the density and α specifies the spatial attenuation of the wave. The angle ϕ of the complex viscosity is readily specified in terms of α and β. For a perfectly viscous medium ($\phi = 0º$), $\alpha = \beta$; for a perfectly elastic material ($\phi = 90º$), $\alpha=0$. For more typical applications of the QCM ($\beta_1 D \leq 1$, $\beta_1/\beta_2 \leq 0{,}001$), were β_1/β_2 corresponds to a case polymer layer/air or vapour.[68]

An application of the oscillating quartz crystal microbalance is the measurement of sorption of gases in polymers thin films: carbon dioxide in polymers[71]; nitrogen, oxygen, carbon dioxide and water in poly(lactic acid)[13]; carbon dioxide in conventional and plasma polymerized methyl methacrylate[72]; carbon dioxide, ethylene and water in PLA[73]; carbon dioxide in PLA at high pressures[74]; carbon dioxide in PS.[75].

3.2. Gas/Vapor Sorption Models

The sorption of a gas in a polymer film can display a variety of behaviours. There are three main types of vapour sorption isotherms in glassy polymers, as shown in Figure 38. The concentration of penetrant gas/vapour is represented in the *y-axis* and the activity of the gas in the *x-axis*.

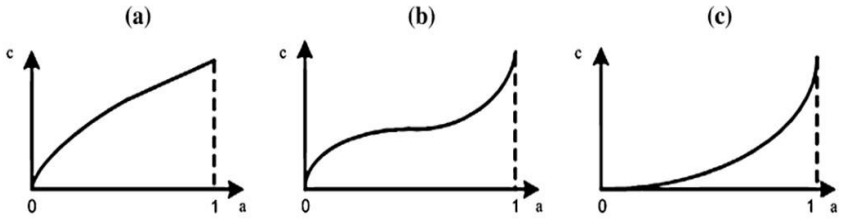

Figure 38 – vapour sorption isotherms in glassy polymers.[76]

Type 1 is concave towards the activity axis at low activities and almost linear at higher activities Figure 38a). Most of the vapour sorption isotherms in glassy polymers display Type 1 diagrams.[76] Type 2, usually referred to as BET type II, is a sigmoidal isotherm, which is concave towards the abscissa at low activities and convex at high activities, as illustrated in Figure 38b). There is an inflection point in the isotherm. Many vapour sorption isotherms in glassy polymers also display this behaviour.[76] Type 3 is always convex towards the activity axis, as shown in Figure 38c). Only a few of vapour sorption isotherms in glassy polymers belong to this type.[76]

Depending on the specific characteristics of the vapour-polymer system, different mathematical models have been proposed to describe and analyse the sorption results obtained. The interpretation of the sorption phenomena based on these models may lead to interesting conclusions since the model coefficients are usually linked to properties that have a role in the sorption mechanism. In particular, the dual-mode sorption model (DMSM) has been widely used to correlate the solubility of gases in glassy polymers films. This model assumes that sorption takes place by two distinct modes: one that follows the Henry's law and the other a Langmuir adsorption isotherm.[77] Analytically, these two contributions can be given by equation (5):

$$\mathrm{C} = C_D + C_H \qquad \textbf{(5)}$$

were C_D and C_H are the penetrant concentrations by Henry's law mode and Langmuir mode, respectively, represented by equations (6) and (7):

$$C_D = k_D p \qquad \textbf{(6)}$$

$$C_H = \frac{C'_H bp}{1 + bp} \quad \textbf{(7)}$$

Then, equation (8) express analytically the DMSM:

$$\mathrm{C} = k_D p + \frac{C'_H bp}{1 + bp} \quad \textbf{(8)}$$

were k_D is the Henry's law dissolution constant; b is the microvoid affinity constant; C'_H is the Langmuir saturation constant.

While DMSM has encountered an enormous success in the description of gas or vapour sorption isotherms concave towards the activity axis, only the engaged species induced clustering (ENSIC) model is able to describe isotherms convex towards the activity or pressure axis.[78] The model considers the probability of insertion of one non-polymeric solute molecule (e.g. gas, vapour or solvent) in a polymer/solvent matrix containing only two types of species (i.e. the polymer and the sorbed molecule), one (the polymer) being present only in the condensed phase.[78] The sorption process of a molecule in the vapour phase is governed by its intrinsic affinity for either a polymer segment (k_p) or an already sorbed solvent molecule (k_s) (Figure 39).

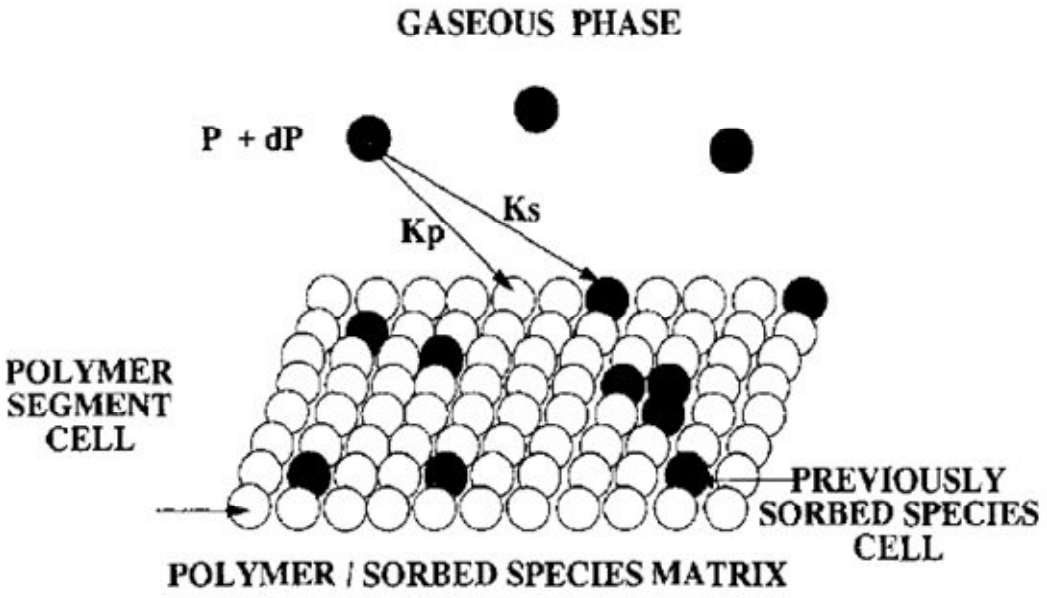

Figure 39 – Basic sorption mechanism according to the ENSIC model. Insertion of a solvent molecule (●) in the polymer (○) / solvent matrix is governed by the two elementary insertion probabilities k_s and k_p.[78]

Neither the DMSM nor the ENSIC models enable the prediction of the isotherm shape given in Figure 38b), because both models are unable in mathematically modelling sigmoidal curves.

To describe sigmoidal sorption isotherms, Feng, H.[76] reported the modelling of vapour sorption in glassy polymers using a new dual mode sorption model. Besides describing the two mechanisms previously referred, the new model can simultaneously describe sigmoidal isotherms which could only be addressed by Guggenheim-Anderson-de Boer (GAB) model.[76] The underlying sorption mechanism can be explained as a contribution of two sorption phenomena, one of which occurs in the matrix region and the other in the microvoids (Figure 40).

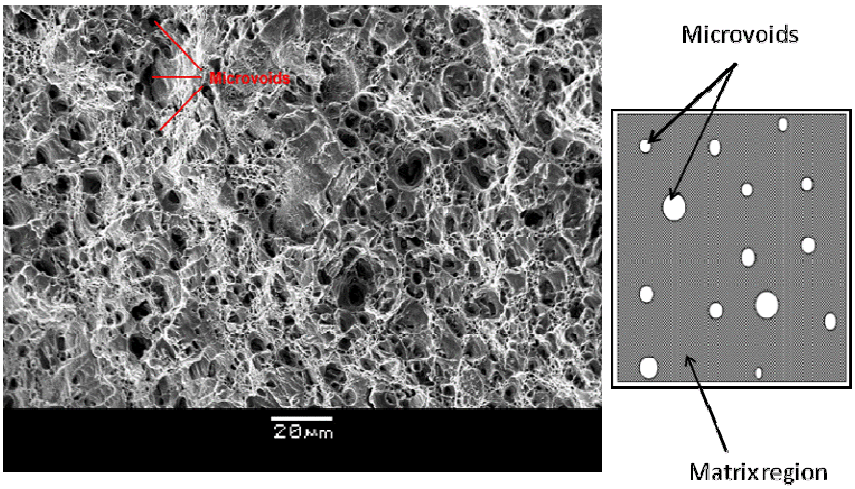

Figure 40 – Left picture: SEM image of the fracture surface of duralumin[79]; Right picture: scheme of the surface of a glassy polymer.[76]

The sorbate concentration in the polymer described through this new model is also a sum of both mechanisms given by equation (9):

$$c = \overline{C}_P \frac{k^{'} p}{1 - k^{'} p} + \overline{C}_p \frac{\left(A^{'} - 1\right) k^{'} p}{1 + \left(A' - 1\right) k' p} \qquad \textbf{(9)}$$

The new dual mode sorption has three parameters, $\overline{C}_p$, $k^{'}$ and $A^{'}$, as many as the conventional dual mode sorption. As shown in the Figure 41, the sorption occurs in two modes or distinct places of the film: i) in the matrix region of the glassy polymers, given by the first term in equation (9) described by a downward curve similar to that of sorption in rubbery polymers; ii) in the microvoids, give by the second term in equation (9), described by an upward curve.

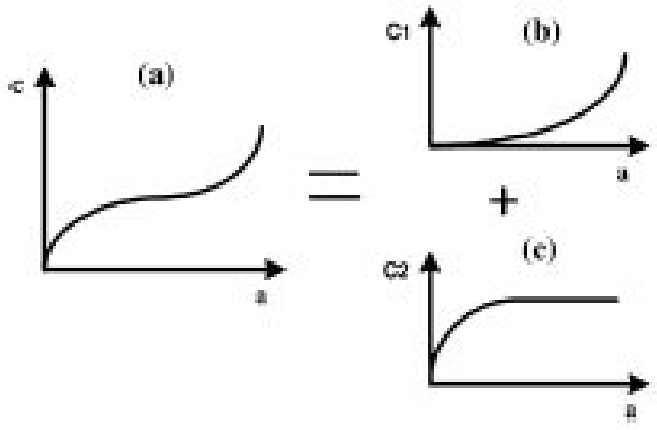

Figure 41 – Schematic representation of the new DMS model.[76]

The total amount of vapour molecules in the glassy polymers is equal to the sum of the two different sorption modes.[76] In both modes, $\overline{C}_p$ is the weight value of the sorption capacity of the polymer to the sorbate, gas or vapour and it mainly depends on the structure and physical state of the polymer and on the volume of the sorbate; k' is the difference between the interaction of vapour molecules among themselves and the interactions between the vapour molecules and the polymer molecule segment; large k' values indicate strong interactions between the sorbate and the polymer; A' is a measure of interactions between the sorbate molecule and the microvoid. $(A'-1)k'$ is a measure of the affinity between the vapour and the microvoid of the polymer.

Indeed, equation (8) is a special case of equation (9) when $k'<<1$.

3.3. Overview

In contrast to glass or metal packaging materials, packages made with plastic are permeable at different degrees to small molecules like gases, water vapor, and organic vapor and to other low molecular weight compounds like aromas, flavor, and additives present into food. As a consequence of the barrier properties of the material, the transfer of this molecules ranges from high to low.[80] Transport of gases, vapors and liquids through polymers is an important in some cases, controlling factor in several application such as

protective coatings, membrane separation processes and packaging of foods and beverages.[81] It is important to know if there is interaction between food and packaging and consequently to well understand the factors that can influence the transport mechanism through the material. The knowledge of the sorption/diffusion/permeation behaviors of these molecules through the polymer film has become more and more important in recent years, especially for polymers used in the food packaging field where contamination from external environment has to be avoided.[80] For the food industry a precise knowledge of O_2 and CO_2 sorption properties by the packaging is particularly important for product quality for the development of plastics and coatings for bottles. PLA films impregnated with antioxidants have been recently studied[52–55,63,82,83]

The effect of the antioxidants in the gas barrier properties of PLA, were not well investigated before, as well as the transport mechanisms. So, in this chapter we will present the sorption results of oxygen and carbon dioxide in PLA films enriched with α-tocopherol, BHT and TBHQ. Not less important than to establish the mechanisms and laws, relating solubility and transport in polymer membranes, of small molecules, is to study the influence of the size and shape of penetrant molecule in the sorption. While smaller permeants will have a greater diffusion coefficient, the polymer will be less plasticized, whereas the lower diffusion coefficient of the larger permeants will be compensated for the higher degree of sorption.[81] In the second part of this chapter, we will present the sorption results of flavors in PLA films with different thermal treatments, an area were few data are available. The main objective was to study the effect of the flavor size on sorption. Finally, we come back at the study of the solubility of ethylene in PLA films. Oliveira et al[73] reported the sorption of ethylene, in PLA films, regarding the ethylene as a gas can be released into the package from fruits, vegetables and flowers, which, if were sensitive to ethylene, when exposed to it, can ripen or mature quicker. Despite the nonpolar nature of the ethylene, we found that there is moderate interaction with PLA. At the time, has being developed membranes with group ester which had performance characteristics suitable for the separation of ethane/ethylene. We explore a little a new area that could use PLA membranes, where their poor properties barrier and their lack of flexibility could be useful.

3.4. Experimental

3.4.1. Materials

Oxygen with 99.995 % and carbon dioxide with 99.999% were from Air Liquid. Ethyl Acetate with 99.8% and butyl Acetate with 99.5 % of purity were purchased from Aldrich and were used with no further purification. Ethane with 99.99% and Ethylene with 99.5 % of purity were purchased from Aldrich. Solvent and gases were used with no further purification. PLA and antioxidants were previously described.

Quartz crystals of 9 MHz base frequency, with silver or gold electrodes were supplied by Euroquartz, Ltd.

3.4.2. Quartz crystal coating

The sorption of oxygen and carbon dioxide in PLA and PLA enriched with α-tocopherol, BHT and TBHQ films was measured using the QCM technique. Among the methods used to prepare thin film samples for the QCM, the drop coating method proved to be successful in our previous studies,[74] was used. The QCM apparatus used in this work to measure gas solubility in PLA films has been thoroughly described by Oliveira.[84] In this apparatus, the two 9 MHz quartz crystals used, with active area of 0.25 cm^2 were carefully cleaned with dichloromethane until the base frequency became constant (± 2 Hz). The measuring crystal was then coated with a thin polymer film, which was prepared by dropping a diluted solution on both sides of the quartz crystal electrode surface. The frequency change to the polymer layer after thermal treatment at 190 ºC during 10 minutes followed by fast cooling in a freezer (15 min) was 99.391 Hz for PLA; 70.404 Hz for PLA with 2.2 % α-tocopherol; 105.907 Hz for PLA with 4.4 % α-tocopherol; 83.313 Hz for PLA with 4.4 % TBHQ and 66.836 HZ for PLA with 4.4 % BHT. SEM images show that the thermal treatment is very important to improve the morphological structure. For example, dropping in a quartz crystal a solution with about 6 wt% of α-tocopherol in PLA, and carried out the thermal treatment for one of them, and the other was analyzed without any treatment, the results are shown in Figure 42. Thin films formed from the melted do

not have pores and are homogeneous. AFM images of a thin film of neat PLA is shown in Figure 43.

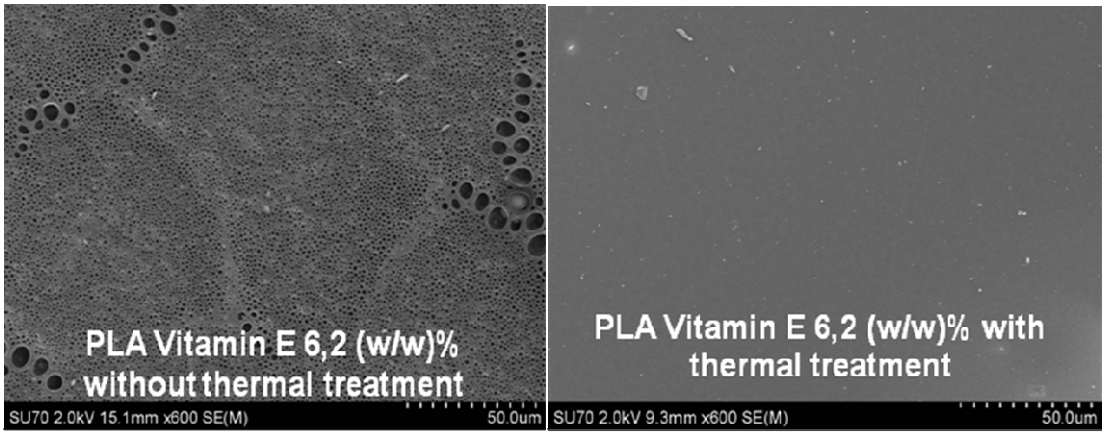

Figure 42 – SEM images of thin films trapped on quartz crystal.

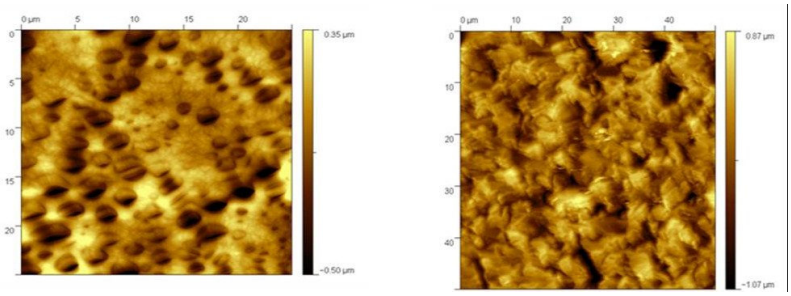

Figure 43- AFM topography of neat PLA thin films with and without thermal treatment.

Once again, it is clearly the existence of pores in membranes without thermal treatment. AFM images of melted thin films with 2 wt% and 4 wt% of α-tocopherol in PLA, revealed a roughness structure increase with the antioxidant amount present in the film. Large voids are present for PLA content 4 wt% of tocopherol. The voids that had appeared in membranes without thermal treatment vanished.

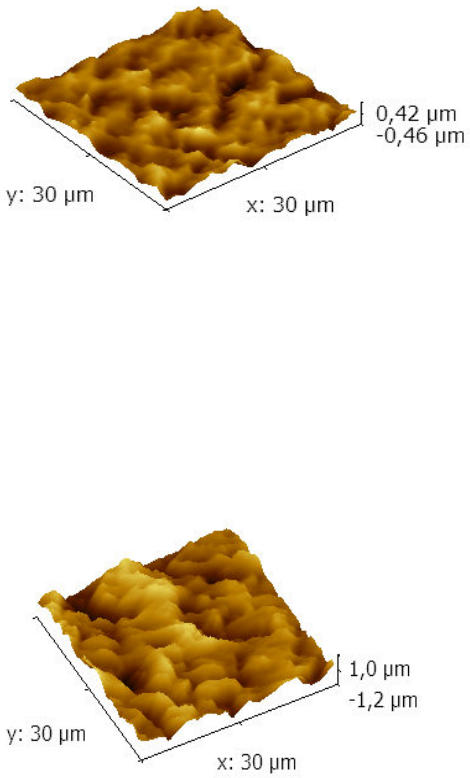

Figure 44 – AFM images of PLA films content 2 (top) and 4 (bottom) wt% of α-tocopherol.

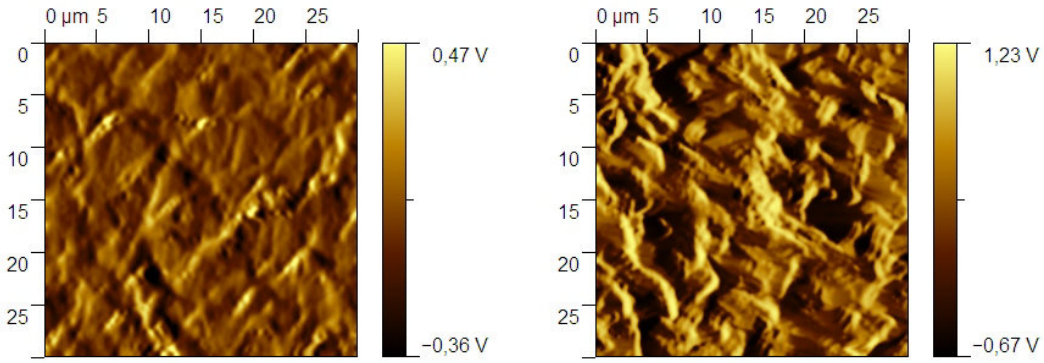

Figure 45 – AFM images of meted PLA films content 2 (left) and 4 (right) wt% of α-tocopherol.

3.4.3. Mass measurements using QCM

Two AT-cut Quartz crystals were use to perform the sorption measurements with a QCM apparatus: the measuring crystal coated with a thin layer of the polymer under study and the reference crystal, uncoated crystal, connected to an oscillator have been placed inside a solubility cell, which is placed inside a thermostatic water bath. The sorption measurements start by evacuating the apparatus until the frequency of both crystals are constant at a desired temperature. The gas or flavor, previously thermostatized is admitted into the solubility cell, promoting a change in the frequency of both crystals. The frequency change is monitored as a function of time until sorption equilibrium has been achieved, i.e. until a stable frequency is reached. Several pressures of the gas up to 1 bar have been studied and in the case of aromas, vapour pressures up to 10 % of saturated vapour pressure have been studied, using a heated Ceravac Transmiter, CTR 91 model, which have a measurement uncertainty of 0.2 % of reading ± temperature effect (0.01 of reading at span level and 0.005 of full scale at zero level).

If the polymer film is uniformly spread and vibrates synchronously with the quartz crystal, the frequency of the wave is a function of the coated mass, according to the equation (2). When gas, or solvent, is injected into the system, the frequencies of both crystals change. This frequency change is a sum of three independent terms: hydrostatic, impedance and sorption. The first two terms are measured together using the reference crystal. For each temperature and pressure, the frequencies of the coated and uncoated crystal were experimentally measured and their difference is proportional to the mass of the coating, polymer and gas, sorbed in it. Thus, the solubility of the gas in polymer, C, was calculated according to the following equation:

$$C = \frac{\Delta F_s \rho_{pol} V_m}{\Delta F_c M_{gas}} \qquad \textbf{(10)}$$

where $\rho_{pol.}$ is the polymer density, ΔF_C represents the total mass of polymer coated on the quartz crystal and is determined by the difference in the oscillation frequency measured before coating and after the thermal treatment of the crystal with the coating. ΔF_S is calculated from the frequency change due to gas sorption between the reference crystal

(uncoated) and the measuring crystal coated with polymer. *M* is the gas molecular weight and *Vm* is the gas molar volume at STP conditions (22414 cm^3mol^{-1}). This equation assumes that the gas obeys ideal gas behavior and that the volume of the film remains constant.

3.5. Oxygen and Carbon dioxide Sorption in antioxidants Poly(lactic acid) films

As mentioned before, the PLA has been intensively researched in an attempt to improve its barrier and mechanical properties which prevent its use in the food packaging industry and in the field of hygiene. In the last 5 years, the studies have been based on demand for non-toxic compounds which can be blended with PLA and its effect on thermal and mechanical properties of the final blended package. In Table 8 can be found a few studies were natural and synthetic antioxidants were impregnated in polymers used in food packaging and was adapted from Ref. 55 . As happened with others polymers also in PLA the main objective of the most studies were rates, effects, and mechanism of antioxidants' release.

Table 8 – Impregnation of antioxidants in polymers.

Object	Antioxidant(s)	Polymer	year	Reference
Migration to food simulants	BHT	HDPE	1982	Till, et al[85]
Migration to food simulants	BHT	PS	1987	Schwope et al[86]
Mobility in polymer in contact with fatty food simulants	α-Tocopherol, BHT	LDPE	1998	Wessling, et al[46]
Retention in polymer in contact with foodstuffs and food-simulating liquids	α-Tocopherol	LDPE, PP	1999	Wessling, et al[28]
Influence of antioxidant on the polymer properties	α-Tocopherol	LDPE	2000	Wessling, et al[29]
Stability of antioxidant in packaging film used for oatmeal	α-Tocopherol, BHT	LDPE	2001	Wessling, et al[27]
Migration of phenolic antioxidants from branch and linear polymer	Santonox, Irganox 1081, Low inox 22M46	PE	2006	Lundbäck, et al[87]
Antioxidant migration study of some polymers	BHA, BHT, AO 2246, Ethanox 330, Irganox 1010, Irganox 1076	LDPE, HDPE, PP, PVC, PET	2007	Dopico-Garcia et al[47]
Antioxidant migration into food simulants	Irgafos 168, Irganox 1076	LLDPE	2007	Jeon et al[88]
Release of antioxidants to dry milk products and food simulants liquids	α-Tocopherol, BHA, BHT	PLGA	2007	Van Aardt et al[89]
Release of antioxidant to asadero cheese and its effect on oxidation and odor stability	BHT	LDPE	2008	Soto-Cantú et al[90]
Improving antioxidant release by smart blending	α, β, and δ -Tocopherol	LLDPE:HDPE LLDPE:PP LLDPE: PS	2008	Schaich et al[91]
Migration to food stimulants (olive oil and waer)	carvacrol	HDPE	2009	Peltzer et al[92]
Release of antioxidant from polymer film to whole milk powder	α-Tocopherol, BHA, BHT	HDPE-EVA-LDPE (co-extruded)	2009	Granda-Restrepo et al[48]
Release of antioxidant from polymer film to distilled water	l-Ascorbic acid, l-tyrosine	CA	2010	Gemili, et al[93]
Influence of antioxidant on the polymer properties	α-tocopherol-BHT-polyethylene glycol	PLA	2010	Byun et al[52]
Influence of antioxidant on the polymer properties	α-tocopherol and Resveratrol	PLA	2011	Hwang et al[56]
Release of antioxidant from polymer to ethanol and soybean oil	α-tocopherol	PLA	2011	Manzanarez-López et al[53]
Release of antioxidant from polymer to water, ethanol and coconut oil	BHT	PLA	2011	Ortiz-Vazquez et al[54]
Influence of antioxidant on the polymer properties	BHA, BHT, PG, and TBHQ	PLA	2011	Jamshidian et al[55]
Influence of antioxidant on the polymer properties	Ascorbyl palmitate– α-tocopherol	PLA	2012	Jamshidian et al[63]
Release of antioxidant from polymer to ethanol	BHA, BHT, PG, TBHQ	PLA	2012	Jamshidian et al[83]
Release of antioxidant from polymer to water and oil	citrus extract	PET	2013	Contini et al[94]

3.5.1. Sorption Results

The oxygen and carbon dioxide sorption in PLA and enriched PLA films with α-tocopherol, were measured using the QCM. The sorption results obtained and their relative standard deviation are presented in Table 9 for oxygen and in Table 10 for carbon dioxide.

An example of the equilibrium sorption isotherms behaviour at 283 K is depicted in Figure 46. For both gases the sorption increases over the entire pressure range for all three films. The CO_2 sorption in the three films exhibits the dual mode sorption nature as typically observed for glassy polymers. The O_2 sorption follows a predominant Henry behaviour for the PLA, while the α-tocopherol enriched films present a convex behaviour towards the pressure axis, which is generally found for vapour sorption in polymers. [52-54]

Table 9 - Sorption of O_2 in PLA and PLA enriched with α-tocopherol.

PLA			PLA 2.2 (w/w)% α-tocopherol			PLA 4.4 (w/w)% α-tocopherol		
282.88 K								
P(bar)	$Cx10^2$ ($cm^3_{(STP)}/g$)	$\delta C/C$ (%)	P(bar)	$Cx10^2$ ($cm^3_{(STP)}/g$)	$\delta C/C$ (%)	P(bar)	$Cx10^2$ ($cm^3_{(STP)}/g$)	$\delta C/C$ (%)
0.280	2.89	0.49	0.435	5.37	0.37	0.168	1.59	0.83
0.419	4.58	0.31	0.594	7.26	0.27	0.283	3.17	0.42
0.570	6.34	0.22	0.629	8.46	0.24	0.379	5.49	0.24
0.723	8.25	0.17	0.739	9.65	0.21	0.475	6.42	0.21
0.894	10.3	0.14	0.763	10.5	0.19	0.534	8.07	0.16
0.990	11.5	0.12	0.872	11.6	0.17	0.618	9.85	0.13
			1.004	13.5	0.15	0.679	10.8	0.12
			1.016	14.0	0.14	0.828	13.7	0.10
						1.023	17.4	0.08
292.73 K								
0.234	1.62	0.87	0.203	1.79	1.11	0.392	4.83	0.27
0.396	3.88	0.36	0.331	3.68	0.54	0.523	6.28	0.21
0.529	5.36	0.26	0.493	5.77	0.34	0.684	8.73	0.15
0.644	6.06	0.23	0.682	8.06	0.25	0.814	10.4	0.13
0.699	7.61	0.19	0.867	10.4	0.19	0.996	14.1	0.09
0.883	9.87	0.14	1.013	12.0	0.17			
302.79 K								
0.243	1.69	0.83	0.385	2.69	0.74	0.167	1.16	1.14
0.441	3.17	0.44	0.533	4.18	0.48	0.330	3.17	0.42
0.611	4.58	0.31	0.560	4.88	0.41	0.431	4.56	0.29
0.824	6.55	0.22	0.674	6.37	0.31	0.573	6.96	0.13
1.051	8.32	0.17	0.830	8.85	0.22	0.643	8.07	0.16
			0.984	11.8	0.17	0.765	10.4	0.09
			1.019	12.1	0.16	0.954	13.4	0.10
312.72 K								
0.211	0.92	1.54	0.176	1.09	1.82	0.165	1.32	1.00
0.317	1.69	0.83	0.320	2.59	0.77	0.250	2.09	0.63
0.490	2.82	0.50	0.530	4.48	0.44	0.336	3.90	0.34
0.562	3.88	0.36	0.713	6.77	0.29	0.544	7.31	0.18
0.613	4.58	0.31	1.037	10.4	0.19	0.600	7.94	0.17
0.709	5.22	0.27				0.916	12.0	0.11
0.988	7.26	0.19						
1.030	8.32	0.17						

Table 10 - Sorption of CO_2 in PLA and PLA enriched with α-tocopherol.

PLA			PLA 2.2 (w/w)% α-tocopherol			PLA 4.4 (w/w)% α-tocopherol		
282.88 K								
P(bar)	C ($cm^3_{(STP)}/g$)	δ*C*/*C* (%)	P(bar)	C ($cm^3_{(STP)}/g$)	δ*C*/*C* (%)	P(bar)	C ($cm^3_{(STP)}/g$)	δ*C*/*C* (%)
0.123	0.76	0.005	0.128	0.99	0.015	0.275	1.48	0.007
0.278	1.51	0.003	0.381	1.66	0.009	0.442	2.17	0.005
0.402	2.01	0.002	0.512	2.08	0.008	0.589	2.70	0.004
0.472	2.31	0.002	0.682	2.57	0.006	0.731	3.17	0.004
0.628	2.89	0.002	0.833	2.97	0.006	0.889	3.66	0.003
0.735	3.18	0.001	1.103	3.62	0.005	1.047	4.11	0.003
0.921	3.84	0.001						
1.007	4.13	0.001						
1.047	4.14	0.001						
292.73 K								
0.130	0.55	0.007	0.175	0.62	0.023	0.131	0.53	0.018
0.280	1.09	0.004	0.335	1.08	0.014	0.274	1.03	0.009
0.487	1.74	0.002	0.494	1.48	0.010	0.401	1.43	0.007
0.681	1.28	0.002	0.652	1.86	0.008	0.577	1.94	0.005
0.922	2.91	0.002	0.835	2.26	0.007	0.721	2.32	0.005
1.065	3.27	0.001	1.063	2.71	0.007	0.871	2.70	0.004
						1.046	3.15	0.004
302.79 K								
0.136	0.38	0.010	0.157	0.34	0.038	0.159	0.41	0.024
0.283	0.76	0.005	0.332	0.75	0.020	0.252	0.64	0.002
0.468	1.20	0.003	0.480	1.03	0.014	0.325	0.80	0.012
0.638	1.58	0.003	0.628	1.33	0.011	0.534	1.27	0.008
0.814	1.95	0.002	0.834	1.66	0.009	0.671	1.56	0.006
1.098	2.51	0.002	1.064	2.02	0.008	0.828	1.85	0.006
						1.035	2.27	0.005
312.72 K								
0.145	0.28	0.014	0.189	0.32	0.046	0.112	0.22	0.044
0.297	0.56	0.007	0.193	0.33	0.044	0.267	0.53	0.018
0.459	0.85	0.005	0.339	0.55	0.027	0.316	0.60	0.016
0.631	1.15	0.003	0.342	0.55	0.026	0.433	0.83	0.012
0.798	1.43	0.003	0.472	0.75	0.020	0.540	1.02	0.010
1.082	1.89	0.002	0.630	0.97	0.015	0.571	1.10	0.009
			0.832	1.24	0.012	0.72	1.37	0.007
			1.047	1.51	0.010	0.844	1.58	0.006
			1.051	1.54	0.010	1.02	1.88	0.005

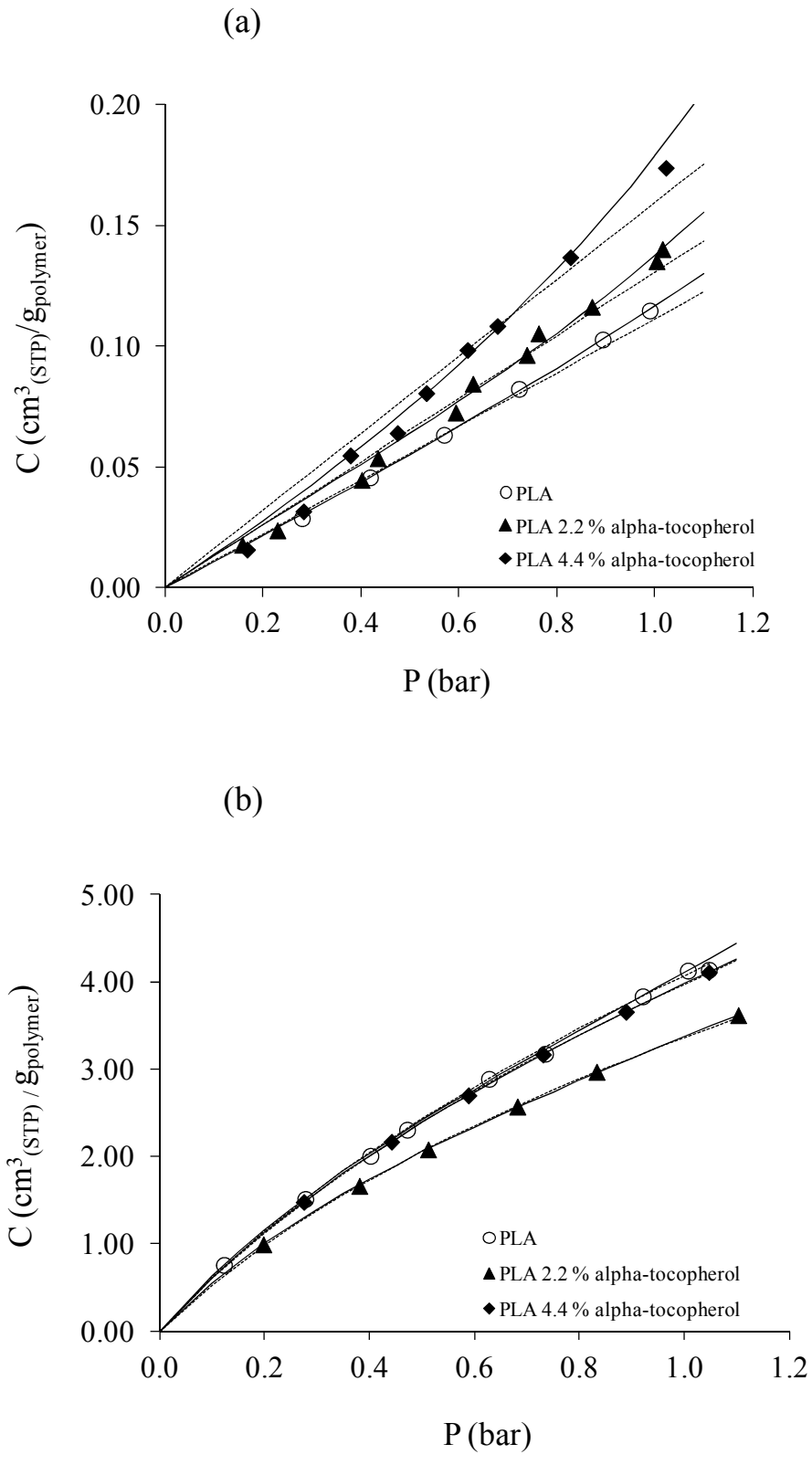

Figure 46 - Sorption isotherms at 283 K of (a) oxygen and (b) carbon dioxide in PLA and enriched α-tocopherol PLA. The solid lines and the dash lines are the new DMSM and DMSM equation, respectively.

This different behaviour has led to the choice of an alternative model to describe the sorption isotherms: the new DMSM, described by equation (9) was used to correlate the O_2 sorption results, while for the CO_2 isotherms the performance of both models, the classical DMSM represented by equation (8) and the new DMSM, was evaluated in terms of the average absolute deviation, AAD. The estimated model parameters are reported in Table 11 and Table 12 for oxygen and carbon dioxide, respectively.

Table 11 - Estimated values of the parameters of the New DMSM for oxygen in PLA and PLA enriched with α-tocopherol.

		New DMSM		
T (K)	C_p ($cm^3_{(STP)}$/g)	*k'*	A'	AAD(%)
		PLA		
282.88	0.299	0.266	1.220	2.76
292.73	0.306	0.256	1.138	2.72
302.79	0.486	0.128	1.120	1.41
312.72	0.583	0.102	1.121	8.64
		PLA 2.2 (w/w)% α-tocopherol		
282.88	0.249	0.283	1. 664	2.12
292.73	0.276	0.233	1.650	2.79
302.79	0.300	0.222	1.502	6.93
312.72	0.550	0.099	1.500	6.97
		PLA 4.4 (w/w)% α-tocopherol		
282.88	0.305	0.322	1.353	2.39
292.73	0.356	0.237	1.335	2.10
302.79	0.360	0.235	1.330	9.72
312.72	0.604	0.150	1.306	4.18

Although both models can provide an adequate representation of the CO_2 sorption data, the correct representation of the O_2 sorption isotherms can only be achieved when the new DMSM is used. As it was mentioned before, the model parameters can be used for interpretation of the sorption phenomena and provide relevant information about the system under study.

Table 12 - Estimated values of the parameters of the new DMSM and DMSM for carbon dioxide in PLA and PLA enriched with α-tocopherol.

New DMSM					*DMSM*			
T (K)	C_p ($cm^3_{(STP)}/g$)	*k'*	A'	AAD (%)	K_D	C'_H	b	AAD (%)
PLA								
282.88	4.29	0.28	5.80	0.26	1.90	4.02	1.16	0.75
292.73	5.48	0.14	5.67	0.69	1.41	3.79	0.80	0.71
302.79	5.76	0.11	4.79	0.33	1.27	2.89	0.57	0.26
312.72	6.66	0.08	3.63	0.21	1.09	2.78	0.32	0.19
PLA 2.2 (w/w)% α-tocopherol								
282.88	3.98	0.22	6.84	0.30	1.17	4.30	1.04	0.78
292.73	3.90	0.18	5.64	0.44	1.17	3.03	0.88	0.56
302.79	4.41	0.10	5.50	0.47	0.88	2.79	0.59	0.45
312.72	5.09	0.07	5.22	0.43	0.71	2.67	0.39	0.35
PLA 4.4 (w/w)% α-tocopherol								
282.88	5.42	0.19	6.46	0.03	1.61	4.64	1.04	0.21
292.73	5.46	0.13	5.85	0.49	1.15	4.44	0.70	0.53
302.79	5.89	0.10	4.44	0.22	1.000	4.40	0.38	0.22
312.72	6.40	0.10	3.08	0.89	0.999	4.01	0.17	0.81

The *A'* values are also 3-5 times higher for CO_2 revealing that this gas has higher affinity to the microvoids than O_2, and most probably the CO_2 sorption occurs to a large extent in microvoids. Surprisingly, the *k'* parameter has very similar values for the two gases, leading to the conclusion that the magnitude of the interaction polymer-sorbate is similar in both cases. Nevertheless, the convex behaviour of the oxygen isotherms indicates that there is a strong specific interaction between the molecules and the glassy PLA, fact that does not happen for CO_2.

Another form to evaluate the underlying sorption mechanism is through the use the infinite-dilution sorption, S_0, expressed by

$$S_0 = \lim_{P \to 0} \left(\frac{C}{P} \right) \quad \textbf{(11)}$$

S_0 gives an indication of whether a gas molecule prefers to dissolve in the polymer matrix or sorbs into microvoids and can help to understand the effect of α-tocopherol on the gas access to microvoids. In Figure 47 the weight of Langmuir capacity, $S_{H0} = Cp(A'-1)k'$, on total solubility for O_2 and CO_2 is reported. The most important conclusion is that the sorption mechanism of both gases in PLA is not affected by the presence of α-tocopherol: the sorption of CO_2 occurs essentially in microvoids while the O_2 solubilizes mostly in the polymer matrix. For CO_2 the Langmuir capacity is roughly the same (around 80 %) for the three films in the studied temperature interval. The O_2 sorption presents an almost constant Langmuir capacity of about 20 % for PLA and 4 % enriched PLA films in the all temperature range, while values around 40 % are observed for the 2 % enriched film.

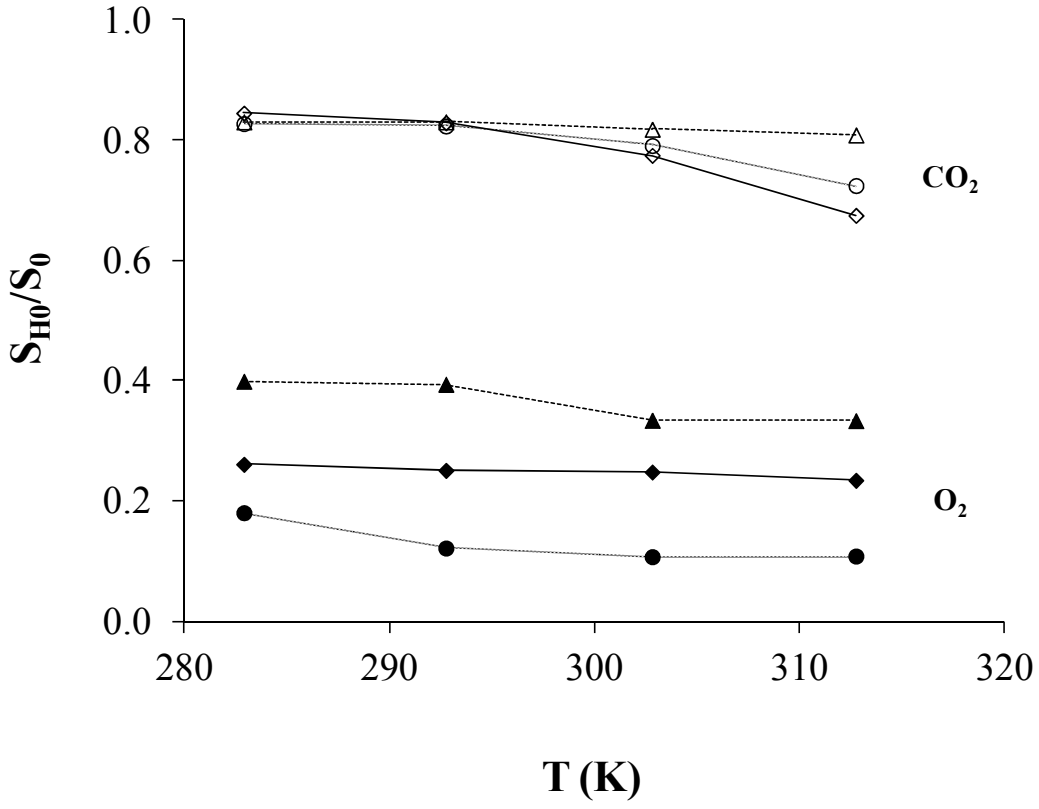

Figure 47 - Effect of α-tocopherol on Langmuir capacity of O_2 and CO_2 sorption in PLA (○) and enriched PLA 2.2 % (Δ) and 4.4 % (◊) of α-tocopherol.

The product *Cpk'* can also yield valuable information regarding the sorption mechanism since it is related to the sorption sites and the properties of the penetrant. This product is presented for each isotherm for both gases in Figure 48. The difference in

magnitude of *CpK'* between the two studied gases reflects the CO_2 higher polarity and condensability relatively to O_2. It is also interesting to observe the change in relative magnitude of *CpK'* for PLA and PLA 4.4 % enriched films below, at and above the CO_2 critical temperature (304.1 K) .[55] Note that this type of data does not allow us to infer about what happens at the molecular level about the role of α-tocopherol in the sorption of the two studied gases.

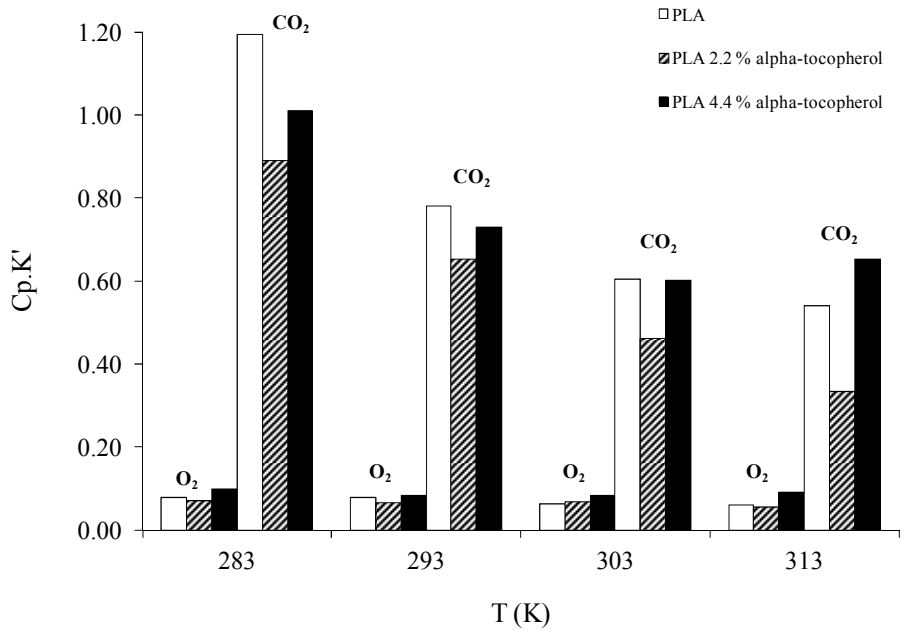

Figure 48 - CpK' results for O_2 and CO_2 to the PLA and enriched PLA.

For CO_2 the unexpected behaviour for the 2.2% (w/w) enriched films is captured by the model parameters, where *CpK'* is consistently lower than what would be expected from the values for the 4.4 % (w/w) enriched films for each gas. As shown previously in Figure 47, the presence of α-tocopherol in PLA films only influences the O_2 solubility which displays an increasing sorption with the α-tocopherol content. The CO_2 solubility in PLA and PLA enriched films with 4.4 % of α-tocopherol is roughly the same, while the CO_2 solubility in enriched films with 2.2 % of α-tocopherol is always lower. Since the sorption of CO_2 takes place predominantly in the microvoids, the α-tocopherol content seems to somehow affect their size and distribution in 2.2 % (w/w) enriched PLA film.

Finally, the enthalpy change due the sorption of the gas was analyzed. Figure 49 shows the sorption behaviour with temperature at 1 bar for both CO_2 and O_2. The enthalpy of sorption, ΔH_S, for both gases in PLA and enriched PLA films was obtained using the van't Hoff relationship. The error bars are the 95 % confidence interval of the mean obtained from at least three independent values of solubility. The *t* student was obtained to (n-1) degrees of freedom.[95] The sorption process is exothermic for both gases. The ΔH_S values obtained for CO_2 in PLA and PLA enriched films with 2.2 % and 4.4 % α-tocopherol are almost constant -24.1 (±0.1) kJ/mol, -23.2 (±0.1) kJ/mol and -21.9 (±0.2) kJ/mol respectively, indicating again that the presence of α-tocopherol does not affect the energetics of CO_2 sorption. Nevertheless, the ΔH_S values obtained for O_2 in PLA enriched films with 0 %, 2.2 % and 4.4 % α-tocopherol are -15.1 (±0.1) kJ/mol, -11.9 (±0.1) kJ/mol and -6.6 (±0.2) kJ/mol, respectively, show that the sorption of oxygen is clearly affected by the increasing concentration of α-tocopherol, in agreement with the sorption results, rendering a less exothermic processes.

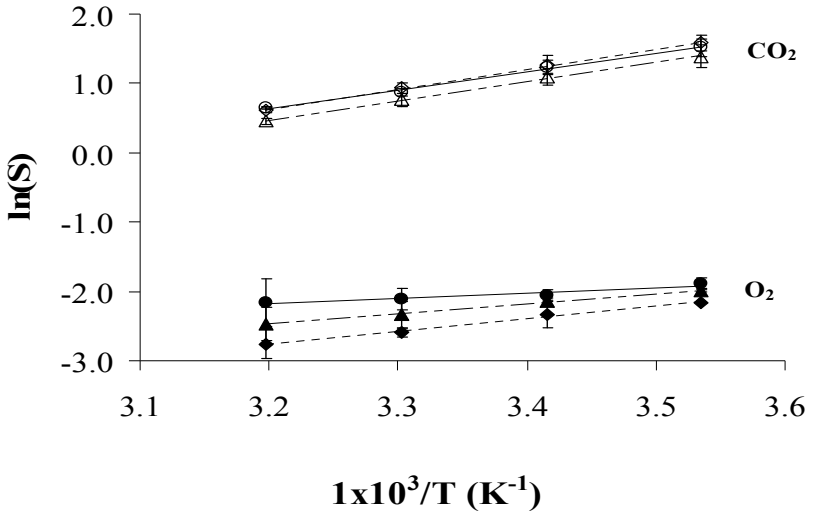

Figure 49 - van't Hoff relationship for O_2 and CO_2 to PLA (◊) and α-tocopherol enriched PLA 2.2% (Δ) and 4.4 % (○).

Sorption of melted PLA enriched with BHT and TBHQ 4.4 wt% were also studied, and an example of the equilibrium sorption isotherms of the oxygen behaviour, at 303 K, is shown in Figure 50. For all films the oxygen sorption increases over the entire pressure range.

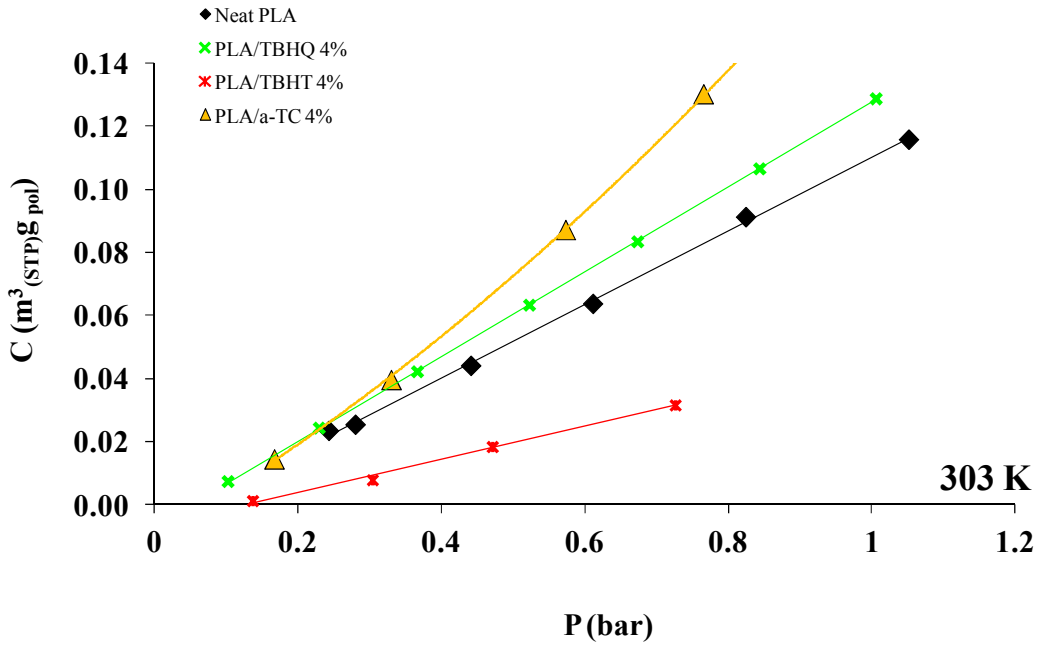

Figure 50 - Sorption isotherms at 303 K of oxygen in PLA and enriched PLA.

The sorption of oxygen in enriched films were determined and the result obtained are shown Figure 51. As expect from 283 K to 313 K the solubility decrease with the temperature, except enriched films with 4.4 wt% of α-tocopherol and 4.4 wt% of BHT which have a higher solubility at 313 K than 303 K. In spite of being very close to the Tg, as it is for TBHQ, and for this film we did not detect this anomalous behavior.

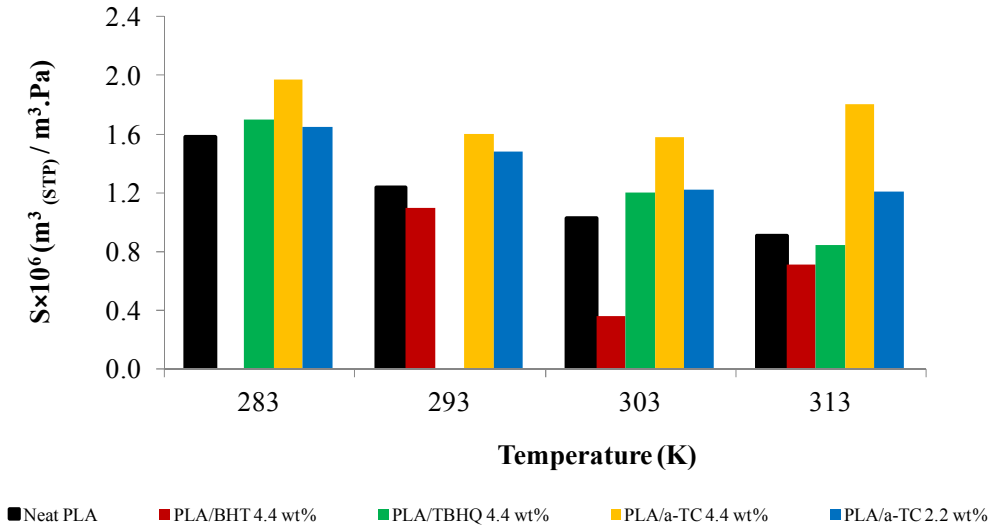

Figure 51 – Oxygen sorption of melted antioxidants PLA films. a-TC refers to α-tocopherol.

3.5.2. Conclusions

Sorption results of oxygen and carbon dioxide in melted PLA with and without α-tocopherol show that oxygen sorption increases with the α-tocopherol content and the convex shape of the isotherms indicates a strong interaction gas-polymer. The sorption mechanism for both gases remains unchanged with the addition of α-tocopherol: the sorption of oxygen occurs essentially in polymer matrix, whereas the carbon dioxide solubilises mostly in the microvoids. Enriched films with 4 wt% of TBHQ show a slight increase in the solubility of oxygen, but the same concentration of BHT decreases to about half the solubility value obtained for neat PLA at 303 K. As expected, the oxygen solubility of neat PLA and PLA/TBHQ films decrease with the temperature. An anomalous behaviour occurs for enriched membranes with 4 wt% of α-tocopherol and BHT, for which the solubility increases at the temperature of 313 K. This behaviour may be due to the proximity of the Tg, and the chain of the polymer acquire some mobility that promote rearranges, improve the free volume and consequently lead to oxygen solubility increase.

3.6. Ethyl Acetate and Butyl Acetate sorption in Poly(lactic acid) films

3.6.1. Introduction

Food packaging in recent years has experienced rapid advances and continuous growth due to consumer demand for conveniently packaged products. This has promoted a trend in packaging materials that has evolved from simple food wraps to sophisticated containers. Besides providing an adequate shelf life and product quality, it is desirable that the packaging material also participates in the overall flavor management of the packaged food, since flavor is an underlying factor in the consumer acceptability of all food products.[96] However, the sorption of food aromas, particularly by packaging materials, is usually perceived as a major factor contributing to the quality alteration of most foods during storage.[96] This causes changes in both the intensity and characteristics of the food flavors owing to their sorption by the packaging material, a phenomenon commonly referred to as "scalping". Flavor scalping is a term used in the packaging industry to describe the loss of quality of a packaged item due to either its volatile flavors being absorbed by the package or the food absorbing undesirable flavors from the packaging material.[96] The sorption of food constituents, especially aroma compounds, by polymeric packaging materials has received considerable attention during the past decade, and is generally considered to be a problem within the food packaging industry.[97]

There are innumerous publications about transport of small molecules as gases (O_2, CO_2) or water through flexible food packaging, including in PLA. However, the barrier properties of PLA against aroma compounds have been the subject of only a few studies.

Aroma compounds are very important among the volatile molecules that can interact with packaging materials, but these interactions are much more complex than the interactions between packaging and gases or water molecules.[34] Several factors can influence the transfer of aroma compounds through food packaging as, the package itself, the chemical structure of the aromatic compound, the environment and the food matrix.[34] Food packaging interactions, defined as an interplay between food, packaging, and the environment, can produce an adverse effect on the food and/or the package.[96]

Interactions between the plastic package and the flavor constituents can cause adsorption and absorption of flavor volatiles by the packaging material, permeation of the flavor volatiles through the plastic material, food- and flavor-induced changes in the physical properties of the plastic polymer, as well as interactions of low-molecular-weight compounds in the plastic such as solvent and plastifiers with the food flavor or the food itself, thereby resulting in an overall imbalance in the flavor profile of the food.[96] Figure 52 shows the possible interactions between foodstuff, polymer film, and the environment and their adverse consequences.[96] Flavor losses that result from interaction with the polymer package can be either losse occurring by permeation or migration through the package or those from sorption by the container.[96]

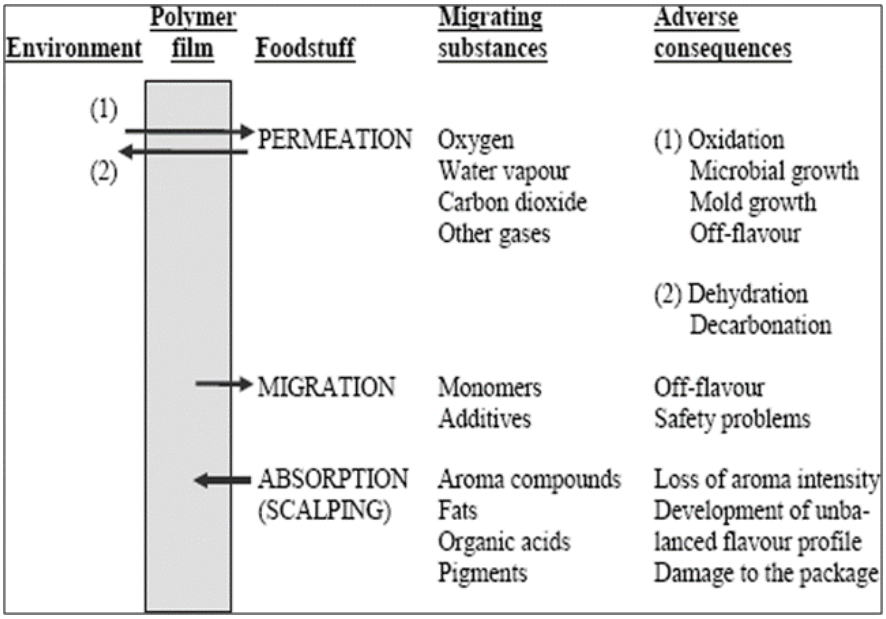

Figure 52 – Possible interactions between foodstuff, polymer film, and the environment and their adverse consequences.[96]

Among the parameters that may influence the mass transfer of aroma compounds, Tg of the polymer film can affect in a more important way the sorption by polymer than crystallinity. Indeed, flavor sorption in rubbery polymers (OPP or LDPE) can be several thousand times higher than in glassy polymers (PET, PC, PEN), even if the crystallinity percentage is the most important factor in rubbery polymers.[98] Nevertheless, among glassy polymers, flavor sorption is more important for the less crystalline polymer. In some cases, no effect of Tg could be seen on gas transfer. It is argued that perhaps the number of holes does not greatly change above Tg but mainly the size of the holes changes, i.e., the

amplitude of the segmental oscillations or rotations increases. If penetrant molecules are small enough, only minor changes would be displayed because the probability of a penetrant molecule encountering a hole would remain roughly the same. With larger penetrant molecules, the size becomes important and effect of the glass transition can be seen.[34]

The state of aroma compounds (liquid or vapor), as well as this physicochemical properties such as molecular weight, structure, hydrophobicity, and polarity, have an important effect on the affinity for the polymeric matrix (sorption) and also on the transfer kinetics (diffusion). For example, concerning the molecular weight of the aroma, its solubility increases with their boiling point of the a homologous series of ethyl esters (C_2 to C_6), whereas diffusivity decreases with molecular weight. The saturated vapor pressure of aroma compounds decreases with the increase in their boiling point, which is related to the increase in their molecular weight, thus making their sorption easier in the polymer film.[34] However, it is also reported that sorption of n-alkanes, n-aldehydes, n-alcohols, and aliphatic ethylesters (C_4 to C_{12}) in PE increases linearly up to ten carbon atoms.[34] For heavier sorbates (C_{12}), the solubility reaches a plateau. Concerning diffusion, as the molecular weight or molar volume of the aroma molecules increases, the steric hindrance in the polymeric matrix increases and the need for free volume as well. Short-chain esters (C_8 to C_{12}) diffuse much faster through a PVC film than the longer-chain ones (C_{14} to C_{18}) at 50°C.[34] Moreover, methyl esters diffuse faster than ethyl esters at the same conditions because the steric hindrance of the ethyl group is higher. Consequently, the depth of penetration of methyl esters into PVC decreases with their chain length.[34] Diffusion generally decreases linearly for aroma compounds up to about ten carbon atoms. For heavier molecules, diffusion behavior changes according to the chemical structure of the aroma compounds.[34]

Concerning the chemical structure of the aroma compound molecules, linear molecules sorb more easily in the polymeric matrix than cyclic molecules because their molar volume is smaller. The effect of the size and structure of the aroma molecules is more important for a polymeric matrix in the glassy state than in the rubbery state. Indeed, sorption of linear primary alcohol molecules (C_2 to C_4) in EVOH increases with sorbate molar volume below polymer Tg (glassy state) and decreases above polymer Tg (rubbery

state). The effect is even more important when the experimental temperature is far from the polymer Tg.[34]

The sorption behavior of aroma compounds in a polymeric matrix depends on a great extent on the relative polarity and hydrophobicity of the polymer-aroma system. The octanol-water partition coefficient (P) is the parameter usually taken to evaluate hydrophobicity, and is defined as the partition coefficient of the aroma compound between octanol and water usually expressed on a log scale (logP). Hydrophilic molecules have negative logP values (around −1.5 for diacetyl), while hydrophobic molecules have positive logP values (around 2.8 for ethyl hexanoate). Polarity is the distribution of electric charges in a molecule and is generally characterized by the dielectric constant (ε, adimensional). The dielectric constant of ethyl hexanoate is about 4, whereas a value of around 80 is obtained for water.[34] The chemical families of aroma compounds are usually classified regarding their decreasing polarity: acids, alcohols, esters, ethers, aldehydes, ketones, aromatic hydrocarbons, unsaturated aliphatic hydrocarbons, and saturated aliphatic hydrocarbons.[34] Aroma compounds are sorbed more easily in a polymeric matrix if polarity or dielectric constant of both the compound and the matrix are close.[34] It was observed while studying absorption of hexanal, decanal, carvone and limonene in OPP and PET after 14 days contact in solution at 40 °C, the more polar aroma molecules (aldehydes and carvone) are more sorbed into PET (moderately polar polymer) than in OPP (apolar polymer).[34] On the other hand, limonene, a more apolar and hydrophobic aroma compound is more easily sorbed in OPP than in PET. When the difference of dielectric constant between a polymer and an aroma compound decreases, vapor sorption of the aroma compound into the polymer increases. Limonene sorption (ε = 2.30) into polyethylene (ε = 2.26) is thus higher than hexanol sorption (ε = 13.30).[34] Table 13 shows the properties of PLA and others polymers commonly used for food packaging.[99] Polymers such as PET, PC, and PLA have a Tg above ambient temperature (67 ºC, 149 ºC and 60 ºC, respectively).[96]

Table 13 – Properties of PLA and other common plastics used in packaging industry.[99]

Polymer	Glass transition temperature, Tg(ºC)	Melting point (ºC)	Tensile elongation, EL, (%)	Tensile strength, TS, (MPa)	Dielectric dissipation factor tanδ (%)	Dielectric constant, ε	Resistivity, ρ (Ω.cm)
PLA	60	170	4	59	0,01	3.1	4.3×10^{17}
LDPE	-120	110	600-700	15-20	0,01	2.3	$>10^{16}$
HDPE	-120	130	650	12	0,01	2.3	$>10^{16}$
PP	5	165	800	38	0,05	2.2	$>10^{16}$

The aim of this section was to measure PLA sorption for two organic compounds: ethyl acetate and butyl acetate (Figure 53), with dielectric constant of 6.0 and 5.0 at 303 K, respectively.[100] Nevertheless, since aroma compounds are mainly hydrophobic molecules, PLA seems to be a promising material with efficient aroma barrier properties comparable to PET.[101] However, some small hydrophilic molecules can also be used in the food industry. Ethyl acetate is a natural compound and is environmentally safe and acceptable for food applications, such as booster and enhancer for fruit aroma. Ethyl acetate is the most hydrophilic aroma compound in the homologous series of the ethyl esters, and it was chosen here in order to test the performance of PLA in a rather unfavourable case. Butyl acetate is used in food industry as a component in synthetic flavours and also as a diluents for dyes in inks for marking vegetables and fruits. Butyl acetate is found in many types of fruits, where along with other chemicals it imparts characteristic flavors and has a sweet smell of banana or apple. It is used as a synthetic fruit flavoring candy, ice cream, cheeses, and baked goods. This compounds was chosen to evaluate the effect of incrementing the ethyl acetate molecule by two carbon atoms.

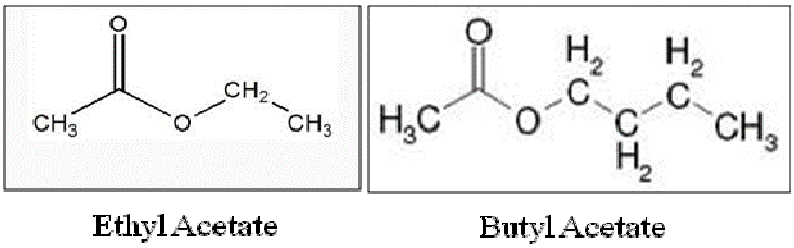

Figure 53 – Chemical structures of the flavours used in this work.

Auras *et al* [102] showed that PLA has a very good barrier to d-limonene, a hydrophobic aroma compound found in orange juice. However, the sorption of ethyl acetate in PLA is approximately twice than in PET, PP and LDPE.

3.6.2. Sorption Results and Discussion

The flavour sorption was carried out in quartz crystals coated with the neat PLA film which were submitted to two distinct thermal treatments: the melting and the annealing treatment. The first, consists in heating the coated crystal from ambient temperature up to 523 K, at 2 K/min, and cool it down to ambient temperature at 10 K/min. In the annealing treatment, the crystal is introduced into an oven at 336 K, slightly above the glassy transition temperature, for two days, cooled to room temperature for one day and introduced again into the oven at 336 K for one day more. The total mass of polymer coated on the quartz crystal is determined by difference in the oscillation frequency measured before coating and after the thermal treatment.

Figure 54 shows the frequency change, ΔF, when both crystals, uncoated and coated with melted PLA, were subject at an ethyl acetate vapour pressure at 283 K, 293 K and 403 K. It is important to have a linear relationship between mass and frequency change in range of pressures studied, so that the Sauerbrey equation can be confidently used.

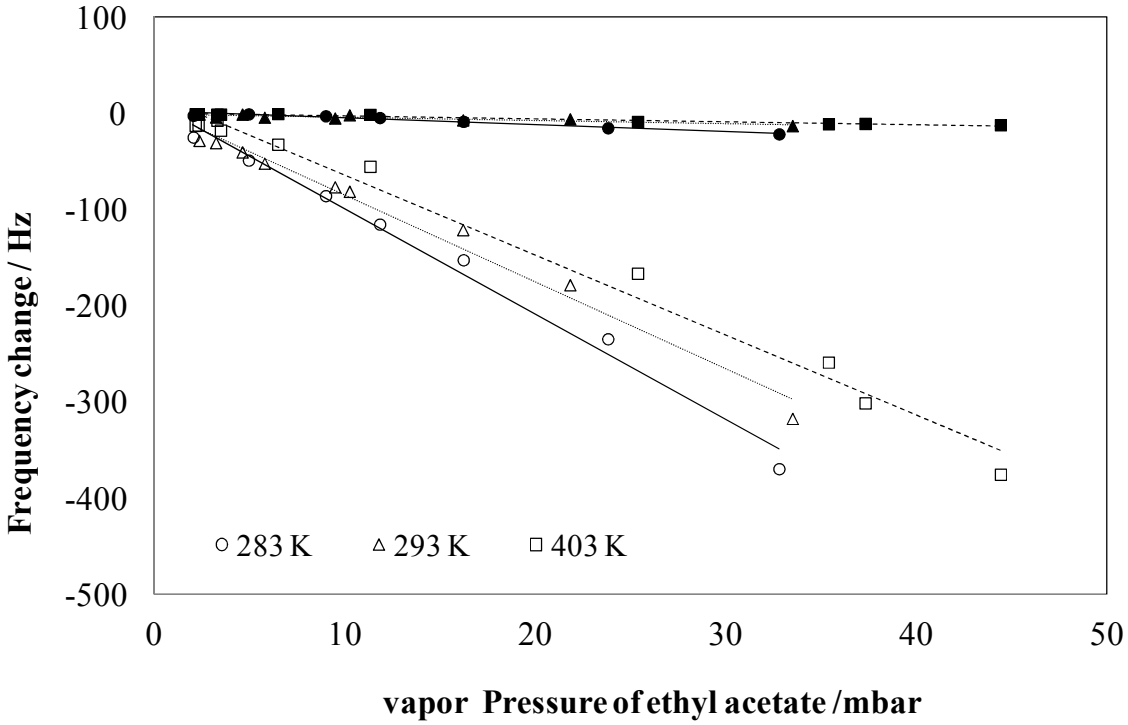

Figure 54 - Response of uncoated (fill symbols) and PLA melted coated crystals (open symbols) as a function of the ethyl acetate vapour pressure.

Using Sauerbrey's equation the weight fraction of solvent, $\omega_{1,}$ sorbed by the polymer can be calculated using

$$\omega_1 = \frac{m_1}{m_1 + m_p} = \frac{\Delta F_1}{\Delta F_1 + \Delta F_P} \qquad \textbf{(12)}$$

were ΔF_1 is the frequency change due to mass of solvent, m_1, absorbed by the polymer coating and ΔF_P is the frequency change due to the polymer coating of mass, m_p. The volume fraction of solvent, $\varphi_{1,}$ can be calculated from:

$$\varphi_1 = \frac{\Delta F_1 / \rho_1}{\Delta F_1 / \rho_1 + \Delta F_P / \rho_P} \qquad \textbf{(13)}$$

were ρ_1 is the density of the aroma and ρ_P that of the polymer.

Figure 55 gives sorption isotherms of ethyl acetate in annealed and melted PLA 98:02 over the studied range of temperatures. The data are reported on an amorphous basis. The lines represent the best-fit of new-dual mode sorption model.

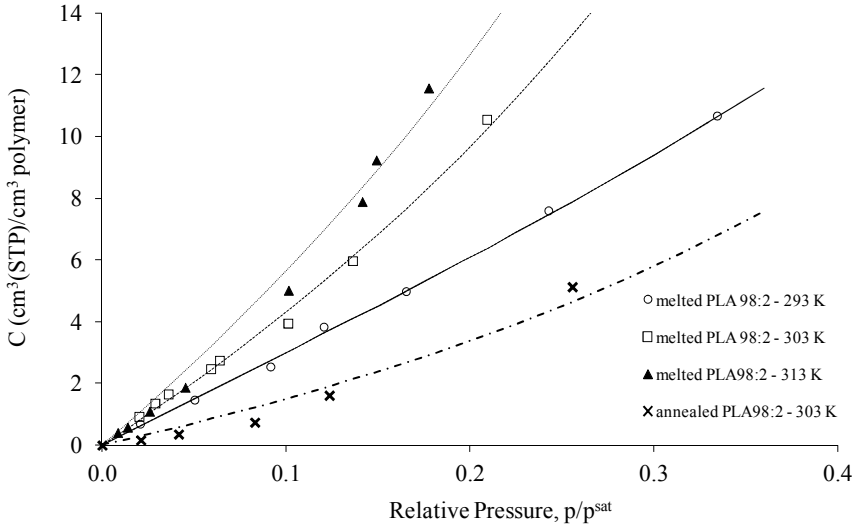

Figure 55 – Ethyl acetate sorption isotherms for temperatures between 293-303 K for ethyl acetate en PLA. The lines represent the new dual mode sorption model.

At 293 K the sorption isotherm of ethyl acetate in PLA is linear up to a relative pressure of 0.4. At 303 K and 313 K the sorption isotherms are convex towards the relative vapour pressure axis, at higher vapour activities. At high penetrant activities, the convex form is usually described for semi-crystalline polymers in their rubbery state, such as hydrophobic polymers in contact with organic compounds, and have been described predominantly using the Flory-Huggins or the engaged species induced clustering (ENSIC) model.[101] The formation of ethyl acetate clusters in the polymer film may be the reason why the sorption of ethyl acetate greatly increase for high activities of the aroma.

Table 14 and Table 15 list the estimated values of the parameters and the fitting efficiencies of the new DMS and DMSM models, respectively. The sum of squares due to error (SSE) and R^2 are utilized to estimate the goodness of the fit statistics for parametric models. SSE measure the total deviation of the predicted, $\hat{y}_i$, values from experiment values, y_i,$(=\sum_{i=1}^{n}(y_i-\hat{y}_i))$.

It is shown that the new DMS model agrees better with the experimental sorption data than the DMSM model. As mentioned before, the new DMS model for vapour sorption in glassy polymers assumes that two types of sorption contribute to the penetrant concentration in glassy polymers: one taking place in the matrix region of the glassy polymer responsible for the downward curve similar to that observed for rubbery polymers; the other occurring in the microvoids responsible for an upward curve.

Table 14 – Estimated values of the parameters of the new DMS and CDMS models for ethyl acetate vapour sorption in PLA subjected to the two different temperature protocols over the studied range of temperatures.

Melted PLA 98:2					
	New DMS model			CDMS model	
Temperature (K)	***k'***	***A'***	***Cp (volume fraction)***	$C'_H.b$	K_D
293	0.784	2.036	18.692	1.06×10^{-3}	31.4
303	0.998	1.00	38.799	1.66×10^{-5}	46.8
313	0.998	1.00	50.759	1.89×10^{-3}	59.6
annealed PLA 98:2					
303	0.998	1.00	15.311	3.48×10^{-5}	0.034

Table 15 - – Comparison of the fitting efficiencies of the two models for ethyl acetate vapour sorption in PLA.

Melted PLA 98:2				
	New DMS model		CDMS model	
Temperature (K)	**SSE**	**R^2**	**SSE**	**R^2**
293	0.12	0.9816	0.19	0.9564
303	0.40	0.9969	1.49	0.8861
313	1.58	0.9055	3.38	0.8493
annealed PLA 98:2				
303	0.62	0.7269	29.7	0.7612

Figure 56 and Figure 57 show the behaviour of $\overline{C}_p$, as well the *k'* and *A'* obtained for the sorption of ethyl acetate in PLA.

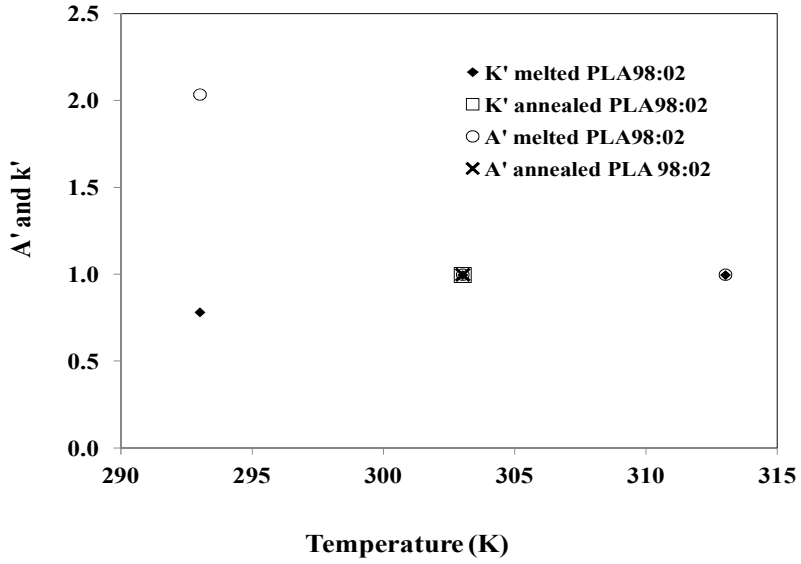

Figure 56 - *A'* and *k'* fitting parameters of the new DMS model as a function of temperature.

The $\overline{C}_p$ is the weighted mean value of the sorption capacity of the polymer to the vapour and it mainly depends on the structure and the state of the polymer. We can observe that this factor increases sharply with temperature. Therefore, the melted PLA sorption capacity for ethyl acetate increases with temperature. Along with this behaviour for $\overline{C}_p$, the decrease of *A'* with temperature, from values greater than 1 at 293 K to approximately 1 at 303 K, can be observed. Meanwhile, *k*' slightly increases in the temperature interval from 293 to 303 K, and remains constant at higher temperatures. At 303 K, the $\overline{C}_p$ value obtained for the annealed PLA is lower than that of melted PLA. Interestingly, *k'* and *A'* are close to 1 for both films from 303 K onwards.

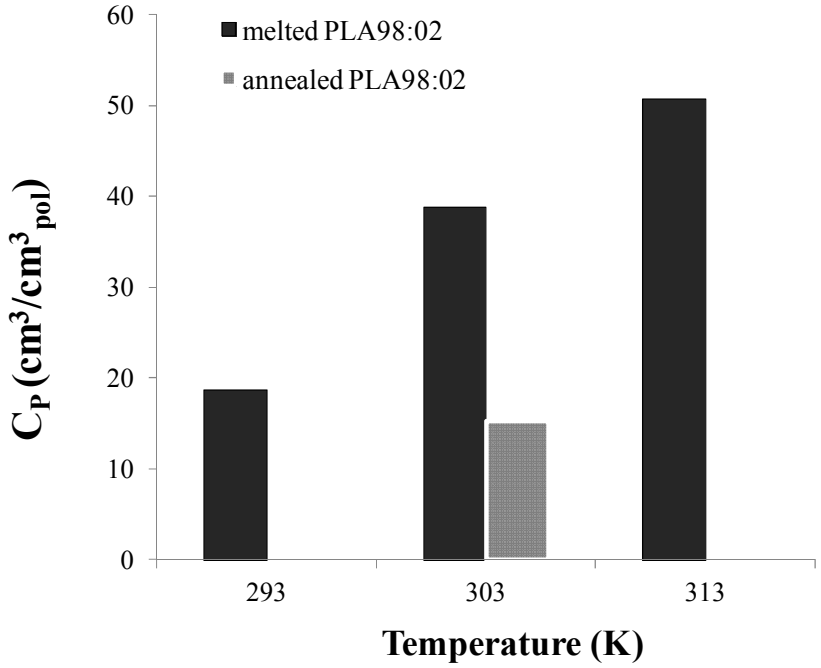

Figure 57 – $\overline{C}_p$ fitting parameter of the new DMS model as a function of temperature.

The *k*' parameter is related to the interactions between the vapour molecules and the polymer segment. A large *k'* indicates stronger interaction between the vapour and polymer, i.e., a large amount of sorbed vapour molecules in the polymer. The results obtained in this work show that ethyl acetate sorbes strongly in the PLA, regardless of the state of the polymer, melted or annealed. Moreover, the interactions established are not temperature dependent, since only a slight deviation from linearity is observed for this parameter in the studied temperature range. Since *A'* is a measure of the interaction of the vapor molecule and the microvoids, it can be concluded that only at 293 K there is affinity between the vapor and the microvoids of the polymer. At higher temperatures A' is equal to the unity, indicating that the polymer should be in its rubbery state. Since the Tg of melted PLA is 326 K, it should be in its glassy state at 293 K, 303 K and 313 K. Indeed, the melted PLA seems to be in the rubbery state at 303 K and 313 K, due to the shape of the sorption isotherms. This rubbery state is due to sorbed ethyl acetate, which acts as an effective PLA plasticizer, thus depressing the Tg of the polymer. Colomines *et al* [9] also reported that the sorption of ethyl acetate in PLA films can decrease the glass transition

temperature well below room temperature, to approximately 273 K. Due to the difficulties in controlling all the variables of the sorption apparatus, it was not possible to measure the sorption at 293 K and 313 K for annealed PLA. However, the study carried out at 303 K shows that this film is already in the rubbery state, as in the case of the melted PLA. For the same temperature, $\overline{C}_p$ is higher in the melted than annealed PLA, and the *A'* values indicate that both polymers are in rubbery state. Then, why this difference? Initially, the melted PLA film has 10 % crystallinity, whereas the annealed PLA film has 20%. If microvoids are changed during/after of the sorption of ethyl acetate, the sorption capacity of the polymer films is altered. Indeed, solvent-induced phenomenon can increase the sample dimensions after the sorption of solvent due to swelling of the polymer, causing the release of internal stress bringing about more mobility of the polymer chains and enabling crystallization at low temperature.[9] The chains of the melted polymer might have an additional facility to accommodate ethyl acetate molecules than annealed PLA. Another possible scenario is that the solvent-induced phenomenon can generate the appearance of crystallites in higher percentage for annealed PLA than melted PLA. This solvent induced crystallites has been described for the semi-crystalline polyester PET.[9] Unfortunately it was not possible to measure the crystallinity before and after the film have been exposed to ethyl acetate, however, SEM images (Figure 58) show that there was breakage film after exposure to this flavor. Both these aspects can explain the higher capacity of the melted PLA film to sorb acetate molecules, as shown in Figure 59.

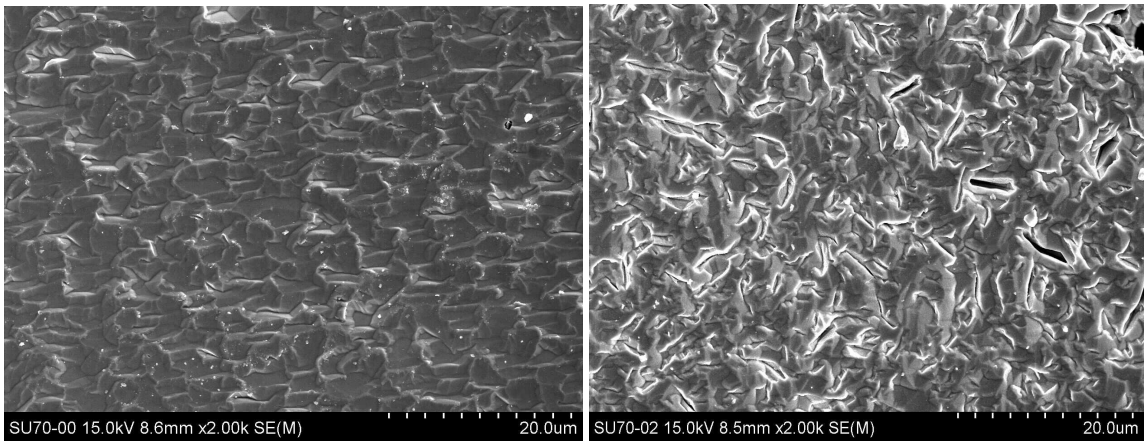

Figure 58 - SEM images of the surfaces of PLA films before and after exposure at ethyl acetate.

Since the size of the vapor molecule also has some influence on the sorption capacity of the polymer, and given the fact that smaller molecules have more sites available to sorb than larger molecules, it is expect that the capacity of sorption of butyl acetate is smaller than for the ethyl acetate. Figure 60 shows that the solubility of butyl acetate is about 20 times smaller than that of ethyl acetate in melted PLA, and 5 times smaller than that of ethyl acetate in annealed PLA. Although the dielectric constant of the butyl acetate is slightly lower than of ethyl acetate, the large size of butyl acetate hinders its access to small sorption sites, which are still available for the ethyl acetate molecules.

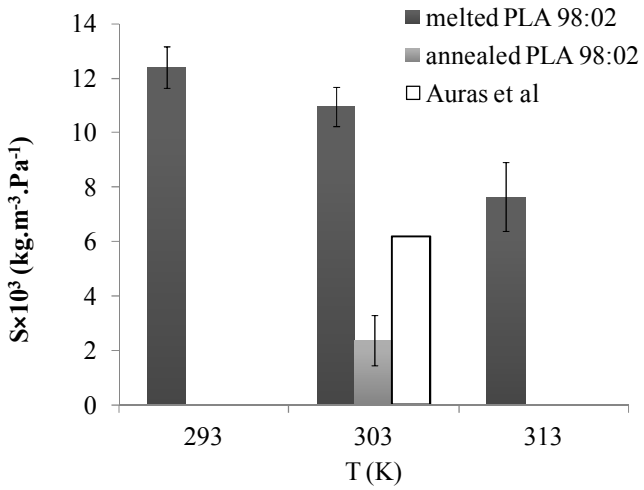

Figure 59 – Ethyl acetate solubility in melted and annealed PLA 98:2 over a range of temperatures (this work) and PLA 98:2 (Auras *et al*).[102]

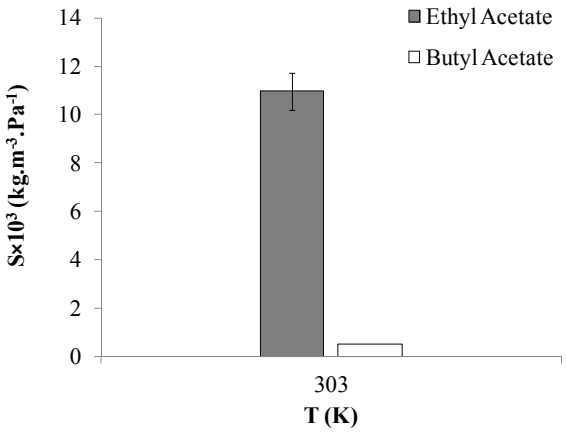

Figure 60 – Solubility data of ethyl acetate and butyl acetate in melted PLA 98:2, at 303 K.

The melted PLA has a higher sorption coefficient for ethyl acetate value and annealed PLA has lower values than that obtained by Auras *et al*[102]. Surprisingly in annealed PLA the values obtained for the sorption coefficient of ethyl acetate are very close to those of ethyl acetate in PP, LDPE and PET, which are hydrophobic polymers.[102] Butyl acetate has a much lower solubility that ethyl acetate, but higher than that of limonene in PLA.[102]

3.6.3. Conclusions

Sorption isotherms of ethyl acetate and butyl acetate in PLA films, with different thermal treatments protocols, were measured using QCM. The sorption isotherms of ethyl acetate in PLA films submitted to different temperature protocols show that swelling/plasticizing effect of matrix of the polymer occurred caused by the flavour. The transition of glassy state to rubbery state due to exposure to the flavour, was disclosed through the *A*' coefficient value obtained from the fitting of the data to the new DMS model. The obtained results show that the solubility of the ethyl acetate in PLA is similar to that of polymers commonly used in the food packaging.

3.7. Ethane/ethylene sorption in Poly(lactic acid) films

In recent years, the separation of olefin and paraffin gases has received increased attention. The usual method using cryogenic distillation is very expensive and thus a large demand for alternative energy saving processes that respect the enforced environmental regulations has been verified. Among a number of alternative processes, membrane separation technologies would be the best option if it wasn't for their low selectivity in terms of olefins relatively to parent paraffins.[103] Separation using facilitated transport membranes, which are composed of a polar polymer containing oxygen atoms with physically dissolved ion metals such as Cu^{+} or Ag^{+}, has been the subject of intensive research since high separation performances were obtained.[104, 105, 106] Recently, Kim H. *et al*[107] developed membranes based on zwitterionic compounds with an ester group that presented high performances for application in separation olefin-paraffin mixtures.

However, this technique still has some problems to be overcome, being the most important the poor chemical stability due to carrier poisoning.[108] The olefin/paraffin separation through the use of polymeric membranes without carriers has also been studied in the literature. In particular, poly(imides) showed a higher permselectivity for propylene/propane when compared to other polymers.[109–111]

In the present work, the solubility selectivity of PLA, a poly(ester) membrane, towards ethane/ethylene is investigated. Polyesters are polar polymers with oxygen atoms and their applicability in gas separation has not yet been studied. Nevertheless, interesting results of solubility of condensable gases, namely ethylene, carbon dioxide and water vapour in PLA films with various L:D ratios and thermal treatments were reported in earlier works. [13, 73,112] Gas sorption in polymers depends not only on the condensability of permeant gas but also on the polymer-penetrant gas interactions. In the present case of the ethane/ethylene separation, the carbon-carbon double bond in ethylene is responsible for the higher density of negative charge in the region of the π bond, susceptible to electron-seeking, and can interact favourably with the ester group of the polymer, that has hydrolytically labile aliphatic ester linkages in its backbone[112,113], thus promoting an increase in its solubility when compared to that of ethane. Despite its high condensability, the weak interaction between ethane and PLA results in lower solubility relatively to ethylene.

The polymer crystallization is also another parameter that has to be taken into account, since it determines the final properties of many technologically relevant systems based on semicrystalline polymers. The change of solubility, diffusivity and permeability coefficients with temperature and pressure can be explained in part by the "impermeability" of crystalline region. The effect of thermal treatment in the gas solubility of PLA films is well documented[73,112] and has proved to be a valuable tool in tailoring polymer films to obtained specific values for sorption, diffusivity and permeability. If the presence of crystallites can reduce the available volume for penetrant sorption, they can also increase the microcavities or Langmuir sites and thus the second mode of sorption (Langmuir type) can play a more important role than Henry's sites.[114]

The improvement of permeability and permselectivity of new membranes for gas separation has been object of study by many authors.[103,115–118] The first step in this type of work is to evaluate the solubility of the gas or gas mixture in the polymer film in order to

evaluate the possible interactions between them. The second step would be to address the transport properties that are necessary for this purpose. In this work we only explore the first aspect. The study of the influence of the structure of the polymer PLA film on the sorption and consequently on the sorption selectivity of ethane and ethylene was performed using the QCM technique, which has already been successfully used for that purpose.

3.7.1. Sorption Results and Discussion

In Table 16 the experimental sorption results obtained in this work for C_2H_6 in the three PLA films (annealed PLA 80:20, annealed PLA 98:2 and melted PLA 98:2) and for C_2H_4 in annealed PLA 80:20, between 283 K and 313 K and up to the atmospheric pressure are presented. The results were corrected for 100% amorphous polymer, taking into account that the crystalline regions do not accommodate any solute:

$$C_a = \frac{C}{\theta_a} \quad \textbf{(14)}$$

where C_a is the solubility in amorphous phase, C is the experimental solubility of semi-crystalline polymer and θ_a is the amorphous volume fraction of the polymer.[73]

Table 16 - Experimental results of sorption of ethane in PLA using QCM in the temperature range between 283 K up to 313K.

PLA 80:20 annealed		PLA 98:2 annealed		PLA 98:2 melted	
P/bar	$C_a/cm^3(STP)cm^{-3}$	P/bar	$C_a/cm^3(STP)cm^{-3}$	P/bar	$C_a/cm^3(STP)cm^{-3}$
283.1 K		**283.1 K**		**283.0 K**	
0.170	0.38	0.218	0.59	0.167	0.42
0.326	0.61	0.387	0.99	0.331	0.74
0.501	0.83	0.422	1.06	0.501	0.98
0.652	1.01	0.624	1.44	0.636	1.14
0.847	1.20	0.821	1.79	0.794	1.33
1.020	1.37	1.028	2.12	1.009	1.56
293.1 K		**293.0 K**		**293.1 K**	
0.167	0.20	0.166	0.32	0.171	0.27
0.325	0.42	0.322	0.62	0.325	0.48
0.497	0.65	0.489	0.91	0.469	0.64
0.665	0.79	0.676	1.23	0.717	0.89
0.868	0.99	0.874	1.48	0.867	1.03
1.014	1.08	1.027	1.68	1.030	1.14
303.1 K		**303.1 K**		**303.0 K**	
0.139	0.14	0.157	0.22	0.136	0.14
0.315	0.32	0.310	0.41	0.295	0.30
0.469	0.47	0.467	0.63	0.443	0.42
0.639	0.60	0.705	0.94	0.741	0.64
0.817	0.72	0.865	1.15	0.885	0.75
1.017	0.87	1.041	1.35	1.026	0.83
313.1 K		**313.1 K**		**313.0 K**	
0.145	0.11	0.158	0.19	0.153	0.11
0.332	0.25	0.318	0.37	0.301	0.21
0.437	0.35	0.471	0.53	0.459	0.31
0.614	0.47	0.623	0.69	0.613	0.40
0.810	0.60	0.770	0.84	0.895	0.57
1.015	0.73	1.003	1.07	1.037	0.65

The sorption results of ethane and ethylene are compared in Figure 61 and Figure 62 for 283 K and 313 K respectively.

The lines represent the correlation with de DMSM. The sorption results have a precision of ± 0.02 cm^3 (STP) of gas/vapour per cm^3 of polymer.

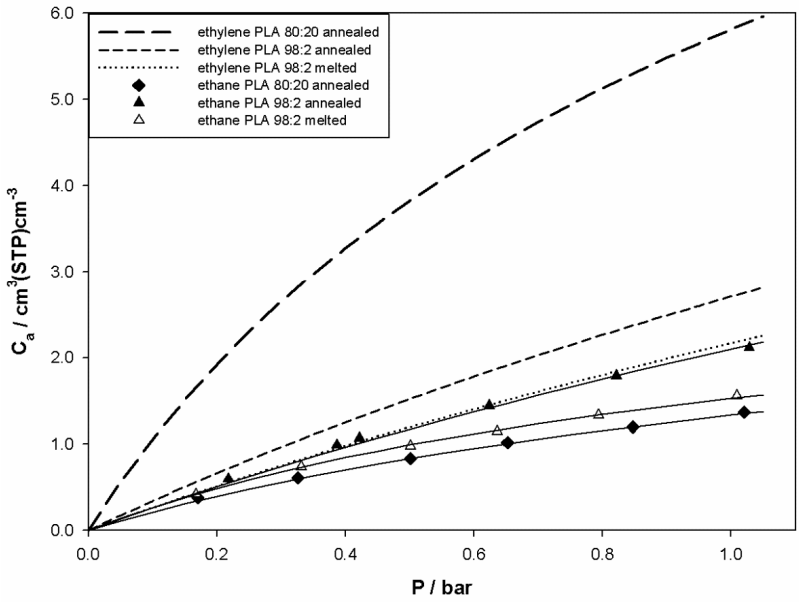

Figure 61 - Sorption isotherms of ethane (solid lines), present work, and ethylene (dashed lines), previous work[73] at 283 K. The lines represent, in both cases, the correlation with dual-mode sorption model.

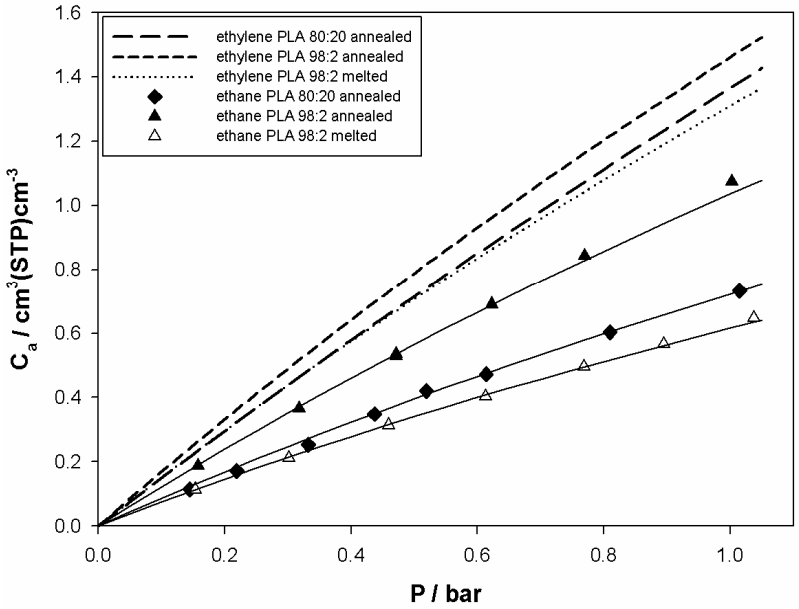

Figure 62 - Sorption isotherms of ethane (solid lines), present work, and ethylene (dashed lines), previous work[73] at 313 K. The lines represent, in both cases, the correlation with dual-mode sorption model.

The first conclusion that can be drawn from these Figures is that the solubility of ethylene is always larger than the solubility of ethane, for the same experimental

conditions. Unlike what is commonly observed the solubility of these gases does not follow their condensability order (T^c ethane = 305.3 K; T^c ethylene = 282.5 K).[119] The higher solubility of ethylene relatively to ethane can be explained by the strong interaction between this gas and the polymer. PLA is a poly (α-hydroxy acid) and, as all poly (α-esters) with hydrolytically labile aliphatic ester linkages in its backbone, can interact with the weak hydrogen bond basicity of alkenes, such as ethylene. On the other hand, ethane has no such capacity. For the studied systems, the polymer–penetrant interaction plays a more important role than the condensability of gas. Also as the temperature increases, the difference in condensability between the two gases decreases and thus the solubility of ethane and ethylene should become similar, which is not observed confirming that the polymer-penetrant interaction of ethylene is the driving force in the solubility of this gas in PLA.

Analyzing the sorption results in terms of the thermal treatments of the PLA films, the ethylene sorption presents an opposite behavior to that observed for ethane. The sorption of ethylene in the annealed films (either PLA 80:20 or 98:2) is higher than in the melted PLA 98:2 films. When the films are submitted to temperatures higher than the Tg, the polymeric chain mobility is enhanced. The re-organization of linkages can promote a different positioning of the hydroxyl groups to the outer side of the chain and thus the interaction of theses linkages with the double bond of ethylene becomes more favorable. The lower solubility of PLA 98:2 annealed relatively at PLA 80:20 annealed films should be due the presence of crystalline domains that difficult the molecular orientation and inhibit the interaction. Note also that the annealing process was performed on films which already contained many micro-crystallites, while in the melted PLA 98:2 film they are formed from the molten polymer. This means that the crystallites present in these two films are naturally different from each other and thus can influence in different ways the gas solubility.

At lower temperatures the results show yet a larger difference in solubility between the PLA 80:20 and PLA 98:2 for both thermal treatments. This difference decreases with increasing temperature and at 313 K they are similar. This behavior can be explained by a decrease of the condensability of gases with the temperature. Ethane has a same behavior on overall range of temperature. The sorption is higher in PLA 98:2 annealed than in the

other two films. The parameters of the dual mode sorption model for the studied systems are summarized in Table 17.

Table 17 - Dual-Mode Sorption Model parameters for ethane and ethylene in the studied films and respective average absolute deviation in percentage (AAD %).

		T	K_D	C'_H	b	AAD (%)
C_2H_6	Annealed PLA 80:20	283.1	0.29	2.20	0.90	0.9
		293.1	0.26	2.16	0.61	2.0
		303.1	0.25	2.00	0.44	2.8
		313.1	0.24	1.90	0.34	2.0
	Annealed PLA 98:2	283.1	0.36	7.18	0.32	3.9
		293.0	0.24	5.97	0.31	1.2
		303.1	0.19	5.34	0.25	4.0
		313.1	0.12	4.90	0.23	1.4
	Melted PLA 98:2	283.0	0.16	2.78	0.97	1.0
		293.1	0.14	2.45	0.67	0.7
		303.0	0.12	2.28	0.44	0.6
		313.0	0.11	2.19	0.30	1.0
C_2H_4	Annealed PLA 80:20	283.06	0.90	9.00	1.20	4.6
		293.04	0.74	8.01	0.64	3.0
		303.31	0.62	7.60	0.30	6.4
		313.23	0.47	6.49	0.16	3.3
	Annealed PLA 98:2	283.4	0.66	7.30	0.39	1.9
		292.7	0.58	6.20	0.34	3.4
		302.6	0.55	5.20	0.30	2.2
		312.1	0.52	4.30	0.28	1.3
	Melted PLA 98:2	283.0	0.39	7.90	0.29	3.1
		294.3	0.35	7.15	0.25	3.7
		303.2	0.32	5.85	0.24	2.6
		313.1	0.30	5.40	0.23	2.4

In Figure 63 and Figure 64, the parameters related to the first (Henry) and second (Langmuir) sorption modes for ethane are depicted. For all the films the Henry's solubility constant decreases as the temperature increases. The semi-crystalline polymers present

higher values for the Langmuir concentration, $C'_H.b$ when compared with the PLA 80:20 (100% amorphous). This behaviour shows that there is a strong correlation between the crystallinity and the microcavities, meaning that the crystallites might act as virtual cross-linkers enhancing the available free volume and thus the Langmuir sites.

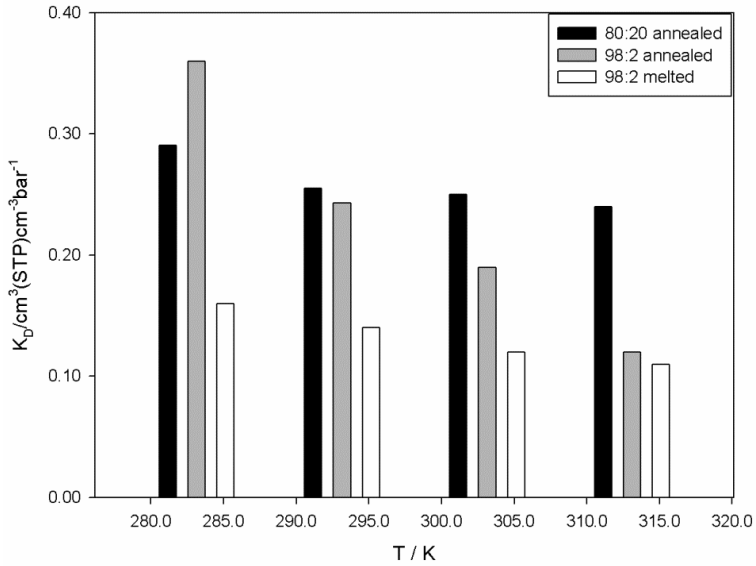

Figure 63 - Henry's law coefficient for ethane in annealed PLA 80:20 and 98:2 and in melted PLA 98:2 from 283 K to 313 K.

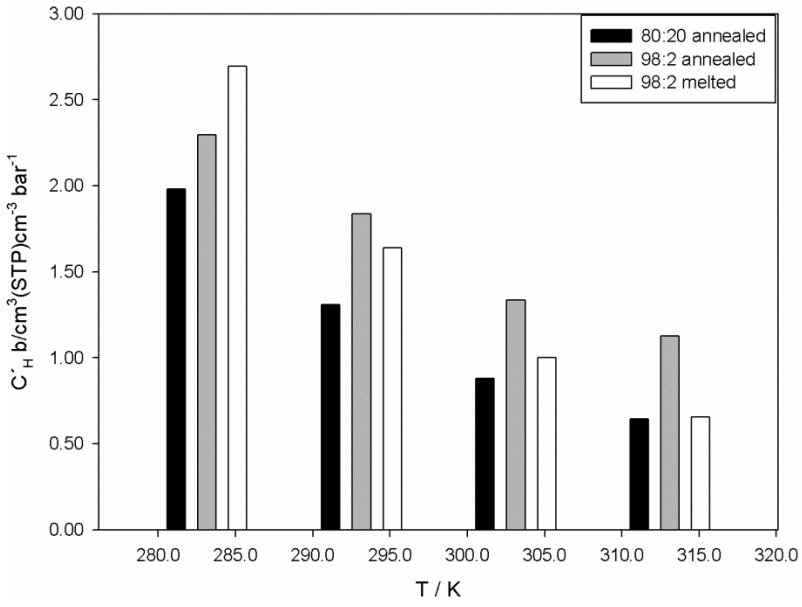

Figure 64 - Langmuir concentration for ethane and affinity parameter between ethane and annealed PLA 80:20 and 98:2 and in melted PLA 98:2 from 283 K to 313 K.

The DMSM correlates very well the sorption results obtained for both ethane and ethylene in the three polymer films in the temperature range from 293 K to 313 K with overall average absolute deviation (AAD) smaller than 3% for ethane and 5% for ethylene.

Semi-crystalline polymers have an important role at industrial level due to the fact that their properties can be manipulated to desired values, through the promotion of crystallites formation, as it can be seen in Figure 65. The change in the overall solubility coefficient in PLA 98:2 with temperature and thermal treatment performed is shown in Figure 65. As the temperature increases, the solubility coefficient decreases for all the studied systems. On the other hand, for the same temperature the solubility coefficient increases with the increase of crystallinity in the film for both gases.

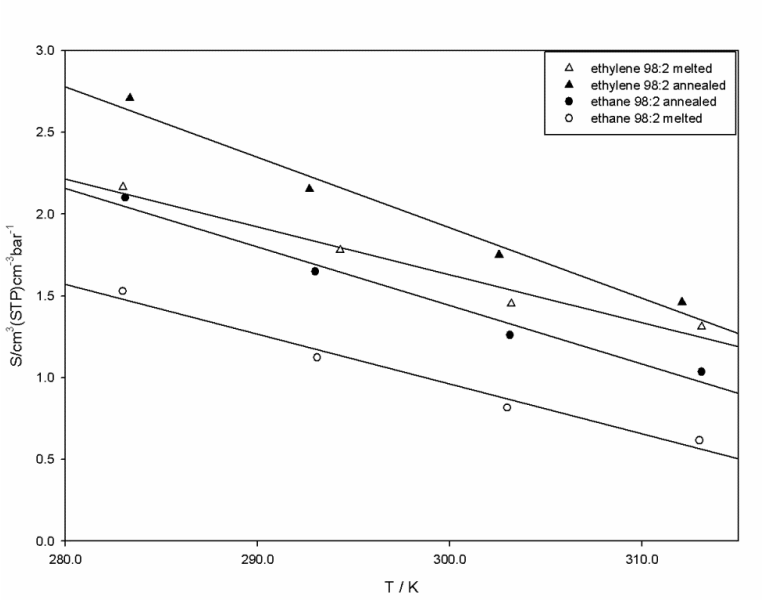

Figure 65 - Temperature dependence of the solubility coefficients of ethane and ethylene for PLA 98:2.

Finally, the solubility selectivity of ethylene over ethane was calculated for the different PLA films is presented in Figure 66.

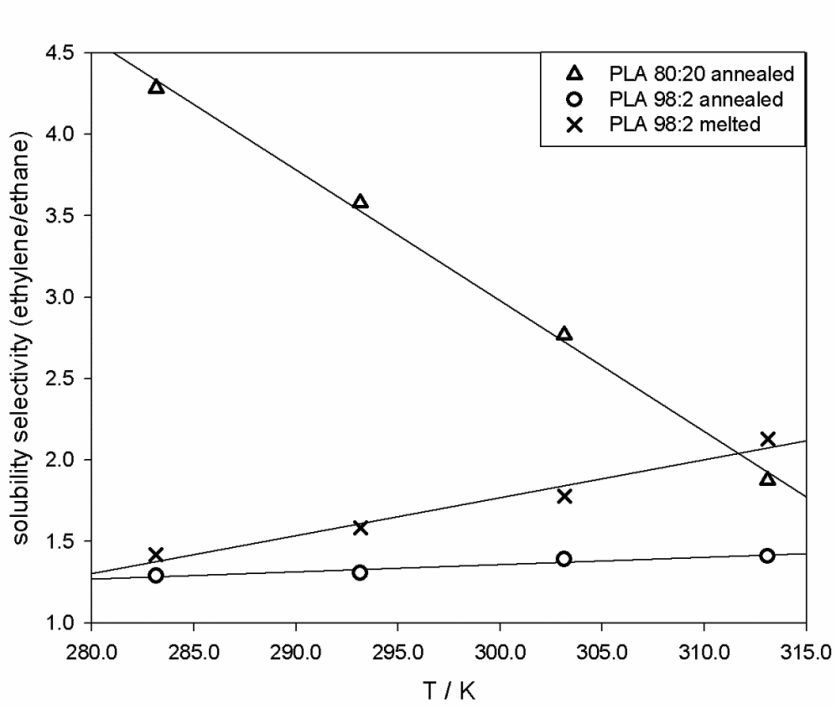

Figure 66 - Temperature dependence of the solubility selectivity of ethylene over ethane for the three different PLA films.

Surprisingly, three different behaviours are observed: for the annealed PLA 80:20 film the solubility selectivity decreases with temperature; for the melted PLA 98:2 film the solubility selectivity remains constant and for the annealed PLA 98:2 film the solubility selectivity increases with the temperature. These differences can be explained by the differences in solubility dependence with the temperature.

From the results presented so far it is obvious that the control of polymer structure is very important in the production of a PLA films with an adequate selectivity for the studied gases The difference in the interactions between ethane and polymer film and ethylene and the polymer film are due to a specific interaction of the latter with the polymer chains but this interaction is also due to the control of the polymer structure through the crystallinity, which results in different mechanisms of sorption. For the PLA 80:20, where no crystallinity was observed, the solubility selectivity can be enhanced by lowering the working temperature. As for the other two semi crystalline films, it is interesting to observe that while for the melted film (10% crystallinity) the temperature does not have any effect on the solubility selectivity, for the annealed film (20% crystallinity) this parameter can be improved by increasing the temperature. Moreover, if the working temperature of separation is higher than 310 K, better solubility selectivity is obtained if PLA 98:2 annealed films are used. Generally, among the membranes studied,

the PLA 80:20 presents the best performance, followed by the melted PLA 98:2 and the annealed PLA 98:2.

3.8. Conclusions

The use of PLA membranes for light olefin/paraffin separation was here studied for the first time. The QCM technique was successfully used to measure the solubility of C_2H_6 and C_2H_4 in PLA with 80:20 and 98:2 (L:D) content, within the temperature range from 283 to 313 K and pressures up to 1 bar. The differences in sorption between ethane and ethylene can be attributed to a specific interaction between ethylene and the polymer chains. A difference in sorption behaviour between membranes with different thermal treatments was explained by the creation of extra free volume due to the presence of different percentage of crystallites. The performance of these membranes decreases with the increase of their crystallinity.

4. Barrier Properties study using Time-lag Technique

4.1. Introduction

Gas transport through polymers is of fundamental importance as it impacts our lives in many different ways, from the tires on our cars and automobiles to the bags used in packaging food, to the membrane modules used in gas separation - the list goes on indefinitely.[120] Therefore, understanding gas transport and its dependence on the characteristics of the polymer is undoubtedly a corner stone that enables us to control and improve the properties of numerous products. In the field of polymer science, three parameters describe the gas transport through a given material; these parameters are gas sorption, diffusion, and permeability.[120]

The first observation of the permeation phenomenon goes back to 1829 when Graham[121] noticed the inflation of a rubber structure in the presence of carbon dioxide.

Permeability is the transfer of small molecules called "permeants" or "penetrants" through a membrane, and permeability also defines how easily the permeants transport through a membrane is achieved.[15] Large permeability values are attributed to poor barrier membranes, and small permeability values to good barrier membranes. Plastic materials provide a broad range of permeabilities to small molecules such as gases, water vapour, organic vapours, and liquids, and thus can range from being "excellent" to "poor" barriers.[15] The preservation of a food product packaged in a plastic film mainly depends on the maintenance of its original quality by protecting it against external deteriorative influences.[122] If on the one hand the loss of water may lead to undesirable drying, detrimental to both the texture of the product and is economically deleterious to the manufacturer, on the other hand an increase in the water concentration to an increase on the water activity (A_w) risking to approach the region of microbial spoilage above A_w = 0.8. More harmful than moisture is oxygen for foods from plant or animal origin due lipid oxidation reactions that can occur causing rancidity, especially when the package allows light transmittance.[122] The other requirements for the preservation of the qualities (physical, chemical, sanitary, organoleptic) of the food are prevention of changes in taste, colour and odour.[122]

The permeation through dense, non-porous polymers is usually described by a "*sorption-diffusion mechanism*"[123] and involves three steps: 1) sorption of the species at the membrane surface; 2) diffusion of the sorbed compounds through the membrane; and 3)

desorption of the compounds on the other side of the membrane, at the downstream face of the polymer. Steps 1 and 3 are very fast relative to step 2, therefore, diffusion through the polymer is rate-limiting step in mass transport across a membrane.[124] In other words, the permeation processes take place through a membrane that separates two fluid phases (gas, vapour, or liquid) containing low molecular weight species with differing chemical potential. The molecules at the side of higher chemical potential tend to diffuse through the membrane and equilibrate the chemical potential on both sides. The permeation process in continuous polymeric materials is accomplished by molecular diffusion within the polymer matrix.[15,125] Figure 67 shows a sketch of a diffusion process through a membrane.[15] Diffusion is a phenomenon controlled by temperature. Therefore, above the glass transition temperature, Tg, of a polymer, the molecules (Phase I) are first sorbed into the polymer and then diffuse through the polymer by an activated process of random movement induced by the Brownian motion of the polymer chains.[15] Below Tg, the permeant dwelled in a cavity of the polymer for a while and then performs a quick jump into an adjacent cavity.[15] The diffusing molecules move through the amorphous regions of a polymer within the free volume between the polymeric molecules.[15] Upon diffusion through the membrane, the molecules are desorbed from the membrane to the low chemical potential side (Phase II).[15] Various factors affect the permeability, sorption and diffusion in PLA as showed in Figure 68.

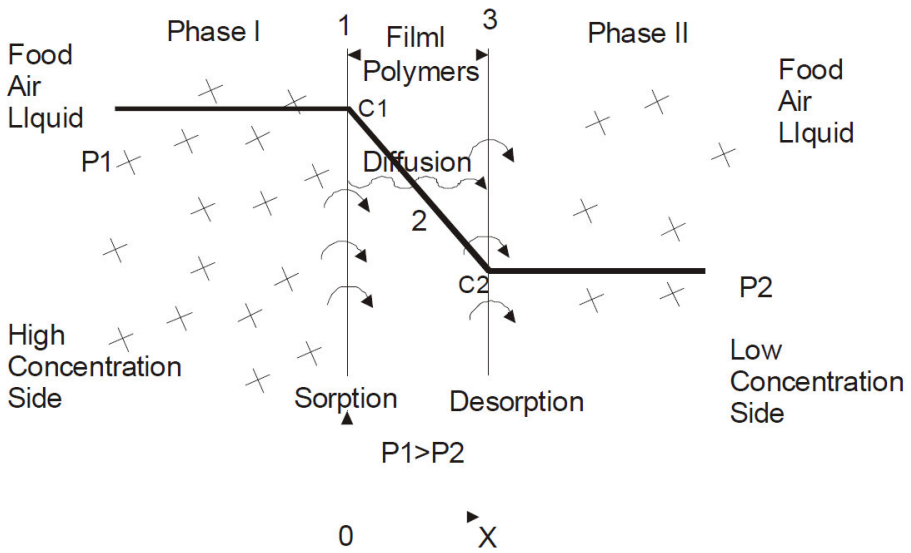

Figure 67 – Sketch of the diffusion process through a film.[125]

The diffusion processes which occur in steady state take place at a constant rate, that is, once the process starts the number of molecules crossing a given interface (the flux) is constant with time, i.e., the flux, *J*, of gas in a polymer matrix can be defined as the quantity of diffusing, *Q*, which crosses the membrane with area *A*, and thickness *l* during the time t:

$$J = \frac{Q}{At} \tag{15}$$

The Fick's First law describes the process, in which the flux through the membrane, *J*, is proportional to the existing concentration gradient and may be expressed by the following equation:

$$J = -D\frac{\partial C}{\partial x} \tag{16}$$

where *D* denotes the diffusion coefficient and *C* the concentration of the species inside the membrane, and *x* is the membrane spatial coordinate.[126] The negative sign in this relationship indicates that the particle flow occurs in a "down" gradient direction, i.e. from regions of higher to regions of lower concentration. Diffusion processes for membrane-gas pair under steady state follow the Fick's first law and the sorption isotherm is linear.[127] On the other hand, if diffusion occurs under non-steady state, the rate of compositional change is proportional to the "rate of change" of the concentration gradient rather than to the concentration gradient itself:

$$\frac{\partial C}{\partial t} = -\frac{\partial J}{\partial x} \tag{17}$$

Combining the equation (16) and (17) and assuming that D is constant in the membrane leads to Fick's second law:

$$\frac{\partial C}{\partial t} - \frac{\partial}{\partial x}\left(D\frac{\partial C}{\partial x}\right) = 0 \Leftrightarrow \frac{\partial C}{\partial t} = D\frac{\partial^2 C}{\partial x^2} \tag{18}$$

When a polymer membrane, of thickness *l*, is exposed to a gas and when the diffusion coefficient is constant, the integration of equation (16) gives:

$$J\int_0^l dx = -D\int_{C_1}^{C_2} dC \tag{19}$$

Then,

$$J = \frac{D(C_1 - C_2)}{l} \tag{20}$$

where C_1 and C_2 are the gas concentration in the membrane near both faces of the sample. The combination of equation (20), where *C* is related with the partial pressures by Henry's law, (equation (6)), gives the permeation equation:

$$J = \frac{DS(p_1 - p_2)}{l} \tag{21}$$

The product *DS* is called the permeability coefficient *P,* so that

$$P = D \times S \tag{22}$$

The temperature dependence of P, D, and S in equation (22) can be described by the van't Hoff-Arrhenius equation: [15]

$$S(T) = S_0 e^{\frac{-\Delta H_s}{RT}} \tag{23}$$

$$D(T) = D_0 e^{\frac{-E_D}{RT}} \tag{24}$$

$$P(T) = P_0 e^{\frac{-E_P}{RT}} \tag{25}$$

were ΔH_S is the molar heat of sorption, E_D is the activation energy of diffusion, and E_P is the apparent activation energy of permeation.[15]

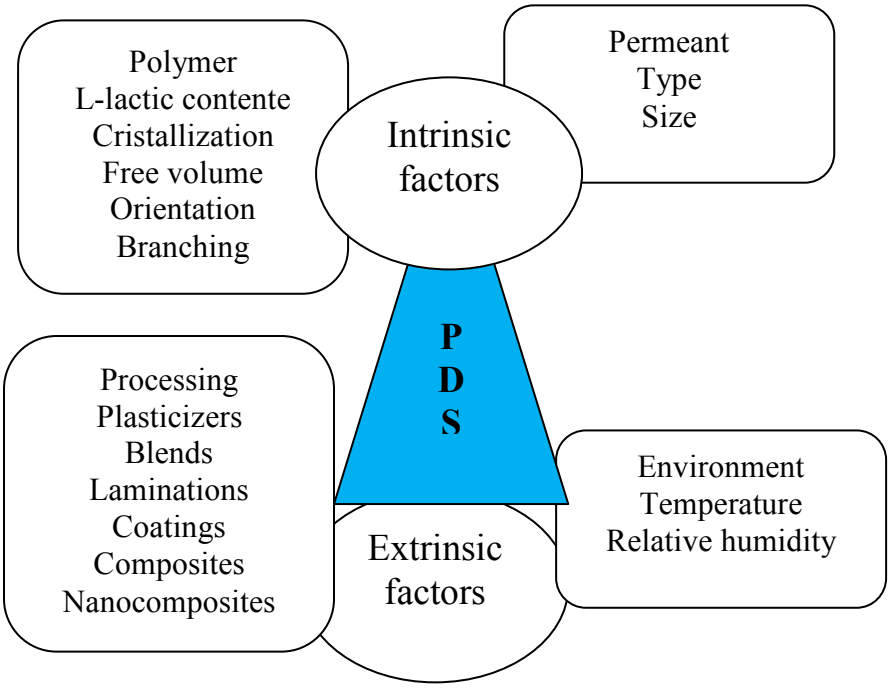

Figure 68 – Examples of extrinsic and intrinsic factors affecting P, D and S in polymers such as PLA. (adapted from ref. [15]).

The permeability, diffusivity and solubility of PLA films towards carbon dioxide and oxygen have been reported, and more recently, for PLA containing antioxidants films was also studied.

Several methods allow the measurement of one or more of these parameters and their description can be found in the literature.[121,127,128] Two methods have been commonly used to measure the permeation of pure gases through dense polymer membranes: the differential and integral methods.[127] Despite their advantages and disadvantages, the integral method, known as the time-lag method, is undoubtedly more frequently used since it allows for the simultaneous determination of permeability and diffusivity.[127] In this method a quasi-constant pressure difference is applied to both sides of the membrane and the accumulation of gas on the permeate side is measured using an accurate pressure sensor. [127] As the permeate side is initially at zero pressure, the partial pressure of gas subsequently is the absolute pressure in this compartment, which has a fixed volume, V^P, therefore, the number of moles is:

$$n = \frac{PV^{P}}{RT} \qquad \textbf{(26)}$$

where T is the absolute temperature and R the gas constant.

Then,

$$Q = \frac{n}{At} = \frac{\Delta P V^P}{ART}\frac{1}{t} \quad \textbf{(27)}$$

In many systems, the pressures p_1 and p_2 on each membrane face are known. As the p_1 is much larger than p_2 ($p_1 >> p_2 \sim 0$), the combination of the equation (21) with equation (27) gives the permeability coefficient, which may be written as

$$P = \frac{Ql}{At}\frac{1}{p_1} \quad \textbf{(28)}$$

In the time-lag method, when a gas pressure is applied at the feed membrane surface, before reaching the steady state, the flux and the concentration vary with time in every point inside the membrane. When t tends towards the very long times, the steady state is reached (Figure 69), and the time-lag, t_L, can be obtained graphically from the interception of the abscissa coordinate place at the initial permeate pressure with the linear extrapolation of the permeate pressure history at pseudo steady-state.[126] The time-lag parameter relates with the effective diffusion coefficient according with the following equation:

$$t_L = \frac{l^2}{6D} \quad \textbf{(29)}$$

Applying a best-fit straight line to the observed values for the permeate pressure as a function of time after steady-state is established, one obtains a slope, m and an intercept, b, which allow to determine the permeability coefficient and the time-lag.

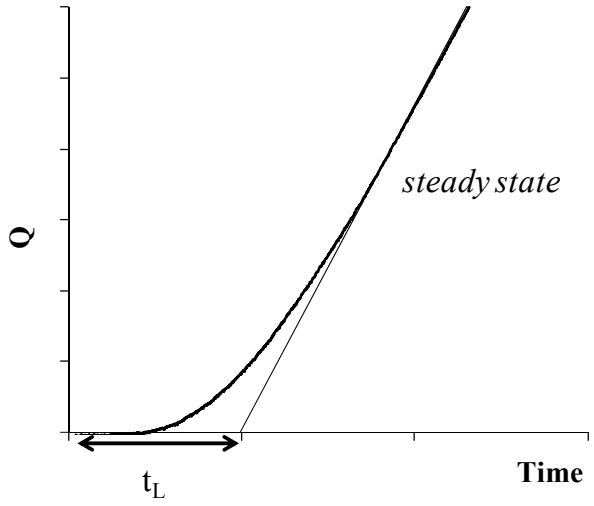

Figure 69 – Typical permeation and time-lag curve.

In this work, two time-lag units were used to measure the permeability of carbon dioxide and oxygen in PLA membranes, being one of them assembled in the framework of this thesis and other was used in Laboratory for Process Engineering, Environment, Biotechnology and Energy (LEPAE) at Faculty of Engineering of University of Porto in the research group headed by Professor Adélio Mendes and that served as traceability and validation unit for the new unit built at the University of Aveiro. The membranes performance obtained in our work were firstly studied in the time-lag apparatus in LEPAE, and then used in our apparatus to validate our equipment, i.e, the permeability of gases in PLA membranes in the UA unit could reproduce the results obtained in the time-lag apparatus from LEPAE, which had been previously calibrated and validated. The permeability, diffusivity and solubility of carbon dioxide and oxygen in PLA with and without antioxidants were measured.

4.2. Experimental

4.2.1. Time-lag apparatus

A diagram of the time-lag apparatus build is shown in Figure 70. It is composed of two stainless steel tanks, one of them with 5 dm^3 (feed) and the other with (34.2 ± 0.2) cm^3 (permeate). Both reservoirs are connected to the permeation cell, which has 13.9 cm^2 of effective area. This cell is composed of a sintered disk to support the membrane and a viton O-ring to seal the cell. Two sensors record the pressure, one at feed tank (S-10 WIKA, 600 KPa, ± 0.05 % FS, P1) and in the permeate tank there was a high precision absolute pressure sensor (MKS e-Baratron, ref. 628 C, 13.33 KPa, 0.001 % FS, P2) for measuring pressure variations. The time-lag unit was placed inside a thermostatic cabinet with a precision of ± 0.05 K. A rotatory high vacuum pump (BOC Edwards, RV3) guaranteed vacuum conditions. The temperature was measured with a Pt-100 placed very close to the time-lag cell and connected to a data acquisition switch unit (Agilent, model 34970 with 6 ½ digit digital multimeter using Agilent BenchLink data logger software). The vacuum was obtained with valves V_2, V_3, V_4 and V_5 that are manipulated from the outside of the cabinet in order to avoid temperature changes.

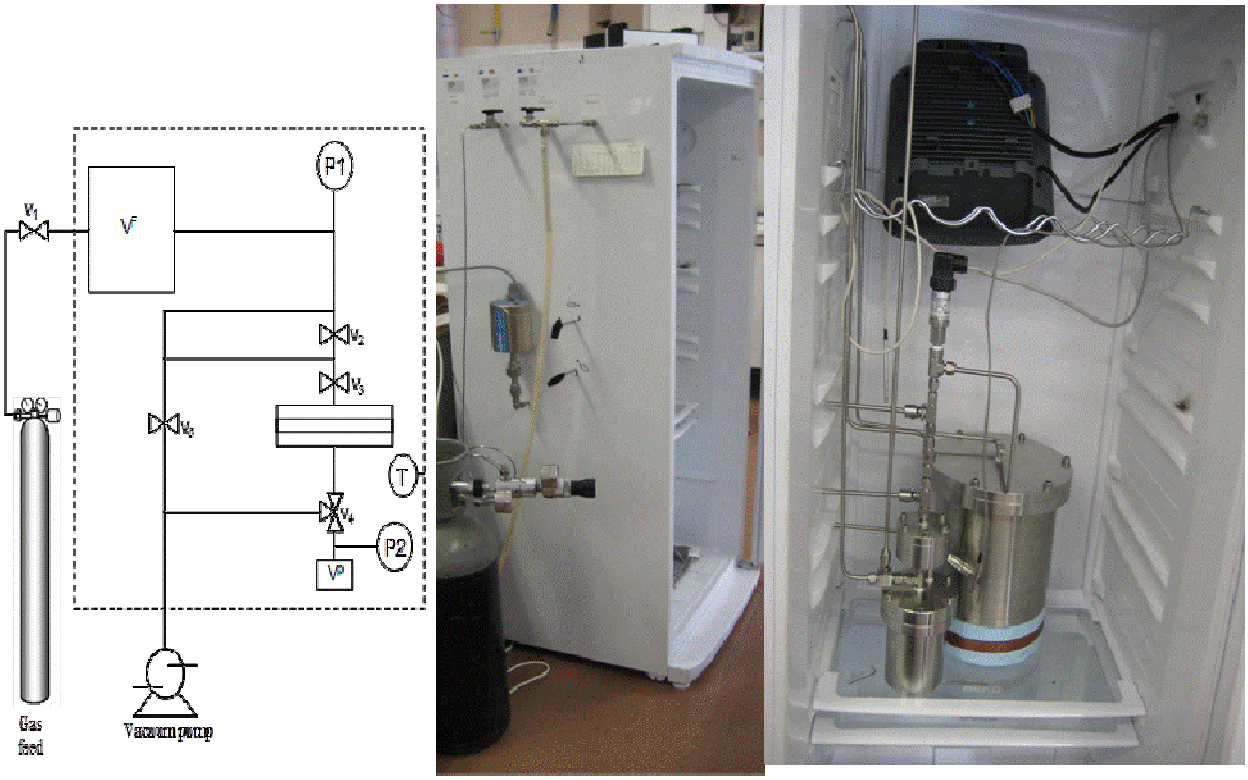

Figure 70 -Time-lag apparatus. P represents the pressure sensors, V the manual valves, V^F the feed tank, Vp the permeate tank and T a thermostatic air bath.

Before the measurements, the temperature thermocouple was calibrated as well the permeate volume (Appendix A).

4.2.2. Materials

4.2.2.1. Membranes performance

In this work, many attempts to produce thin membranes using the casting method were made. Initially we started by spreading a PLA solution on a flat surface and then smoothing it with a knife and allowing it to evaporate. The membranes obtained were very thin and fragile and no measurements could be achieved with them since the gas instantly passed through them. SEM images of these membranes show that these were porous membranes (Figure 71).

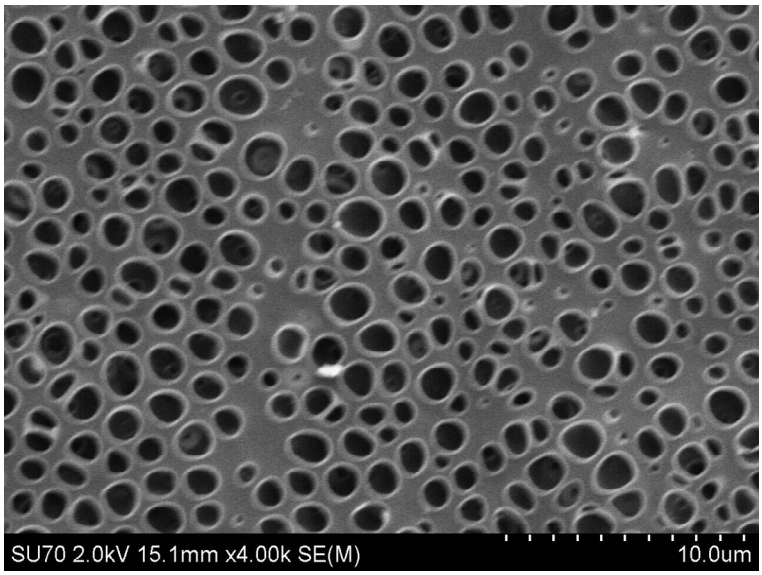

Figure 71 – SEM image of the membrane obtained by scattering method.

This method was further improved and extra care was taken especially with the evaporation rate of the solvent. The membranes with and without antioxidants were previously described in chapter 2, and were there characterized. Before testing, the thickness of the films was measured using a digital micrometer (model MDC-25S, Mitutoya Corp., Tokyo, Japan). Mean thickness was calculated from six measurements taken at different locations in each sample. At least, three samples of each film type were measured.

4.3. Results

4.3.1. Gas permeation properties

The barrier properties of PLA films are very important in the technological and functional aspects of packaging materials. In order to understand the effect of structurally different antioxidants incorporation on the barrier properties of PLA films, single gas permeation measurements using CO_2 and O_2 were performed at three temperatures (284 K, 293 K and 303 K) for all the PLA films. For 313 K, only PLA membranes were studied, because the membranes with α-tocopherol and BHT, exhibit an abnormal behavior at this temperature, perhaps because this temperature is close to Tg, and the chains can move and rearrange themselves in response to the stress imposed by the gas pressure.

4.3.2. Carbon dioxide permeation

Typical pressure history data for CO_2 permeation in PLA films in the temperature interval between 284 K and 303 K are shown in Figure 72. As the temperature increases, the time-lag becomes smaller, meaning that the diffusivity increases with temperature.

In Table 18 are presented the results obtained by time-lag technique for PLA based films. Also, for neat PLA, comparison with data found in other works with PLA membranes containing a percentage of L-lactid near the PLA used in this work was performed. The results for neat PLA films towards CO_2 at 303 K are in good agreement with that reported by Auras *et al*. [129] and Bao *et al*.[130]

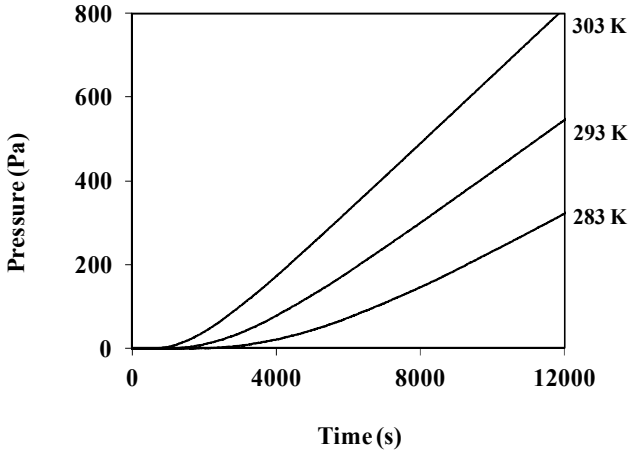

Figure 72 - Typical pressure history for CO_2 permeation in the neat PLA film at different temperatures.

Table 18 – Experimental data obtained from time-lag technique for carbon dioxide in PLA films with and without antioxidants. Each result is an average of least three measurements.

T (K)	P_i (Pa)	P_f(Pa)	P_{feed} (Pa)	t_L (s)	Slope	Intercept	$P \times 10^{17}$ (m^3. m/m^2.s.Pa)	$D \times 10^{13}$ (m^2/s)	$S \times 10^5$ ($m^3_{(STP)}.m^{-3}.Pa^{-1}$)
PLA (67.5 µm)									
284	123	576	91440	4956	0.0459	-227	0.80	1.5	5.2
293	123	541	94810	2991	0.0602	-180	0,97	2.5	3.8
303	131	647	96990	1924	0.0807	-155	1.2 (0.8) [a] (1.8) [b]	4.0 (4.4) [a]	3.1 (1.9) [a]
314	417	1603	99460	1066	0.108	-115	1.6	7.1	2.2
PLA/BHT-2% (60.6 µm)									
282	323	701	100130	8433	0.0302	-255	0.43	0.73	5.9
292	388	787	100063	4124	0,0574	-226	0.58	1.0	5.6
303	236	1071	101467	2924	0,0526	-154	0.67	2.1	3.2
PLA/TBHQ-2% (50.0 µm)									
283	399	769	98597	6323	0.0462	-292	0.55	0.66	8.4
292	711	2859	100237	3636	0.0628	-228	0.72	1.2	6.3
301	755	2895	101789	2115	0.0791	-167	0.84	2.0	4.2
PLA/α-tocopherol-4% (64.0 µm)									
284	181	2474	97873	4286	0.0548	-235	0.85	1.6	5.4
291	152	2517	99297	2698	0.0660	-178	0.98	2.5	3.9
302	156	3931	102333	1448	0.0880	-127	1.26	4.7	2.7
PLA/α-tocopherol-2% (82.4 µm)									
284	97	166	101700	465	0.0556	-25	1.07	24.3	0.44

a) From Bao *et al* - Ref. [130] (PLA98:2 with 4% crystallinity, casting).

b) From Auras *et al* - Ref.[129](PLA98%L, with 40 % crystallinity, extruded).

For all films, both permeability and diffusivity increase with temperature, while the opposite behaviour was found for solubility.

The incorporation of only 2 wt.% of BHT and TBHQ into PLA films, on average, decreases the CO_2 permeability by 44 % and 30 %, respectively, while the incorporation of α-tocopherol caused the opposite effect, increasing the permeability (Figure 73) This difference can be explained by SEM analysis where BHT and TBHQ enriched films revealed a more compact or integrated structure than the neat PLA (Figure 27). The presence of empty voids in α-tocopherol enriched films can explain the permeation behaviour and thus the increase in diffusivity and permeability for this film (Figure 74).

The incorporation of BHT and TBHQ in the PLA films increased the carbon dioxide solubility, while α-tocopherol does not produce a significant effect. (Figure 75).

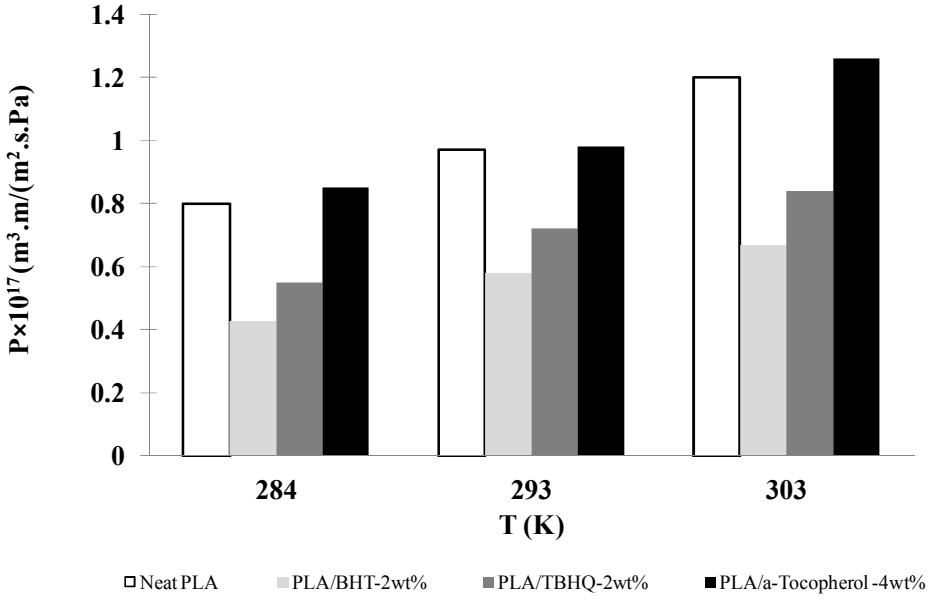

Figure 73 – Carbon dioxide permeability of antioxidants PLA films.

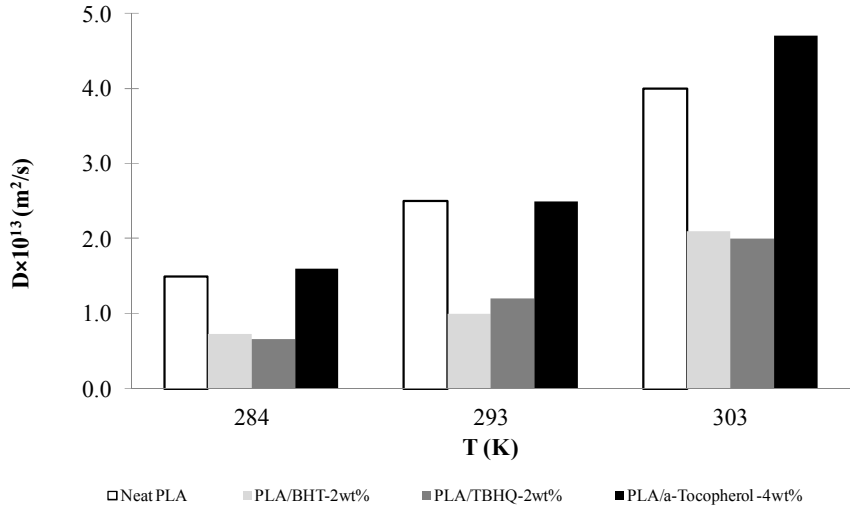

Figure 74 – Carbon dioxide diffusivity of antioxidants PLA films.

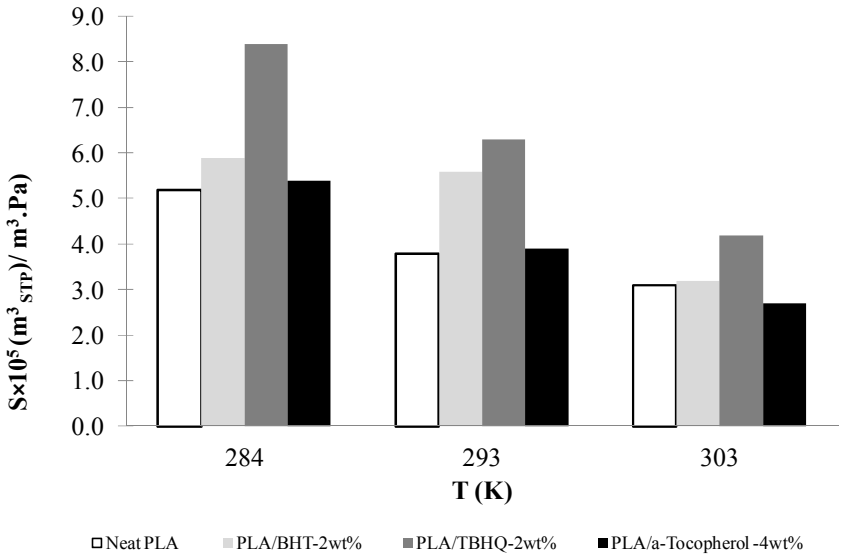

Figure 75 – Carbon dioxide solubility of antioxidants PLA films.

Many attempts were made to study the permeability of CO_2 in films containing 2 wt% of α-tocopherol, but the absence of time-lag for this concentration led us again to cast some doubts on the methodology used to make the membranes. Many different membranes were studied without observing a time-lag. However, the results could be obtained at higher concentrations of α-tocopherol and SEM images of the films are compared in Figure 76. The SEM image of the film enriched with 4 wt% of α-tocopherol, revealed that the size of the voids is smaller than in the film at 2 wt%, and that the film gained some homogeneity despite having areas similar to an orange peel appearance. The increase of the amount of α-tocopherol seemed to improve the morphological properties, that continued to be, nevertheless, still quite poor.

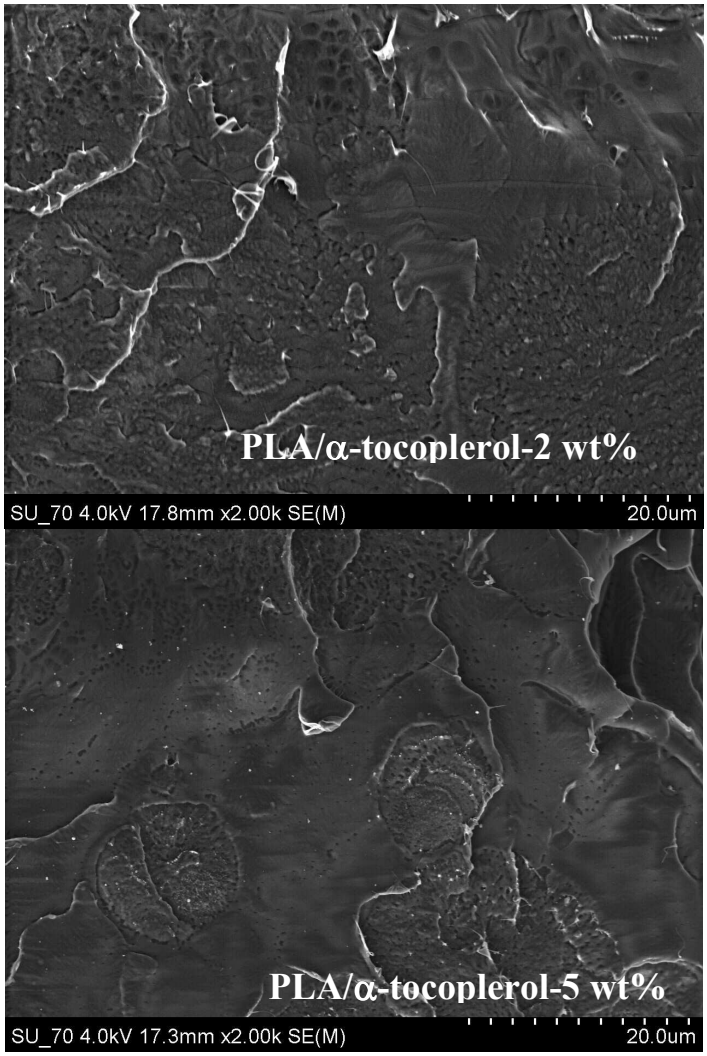

Figure 76 – SEM images of fracture surfaces of PLA based films containing 2 and 5 wt% of α-tocopherol.

The temperature dependence of CO_2 permeation properties for neat PLA and antioxidants enriched films, in the temperature range of 284 K - 303 K, is presented in Figure 77 to Figure 79. The activation energies for these properties are listed in Table 19.

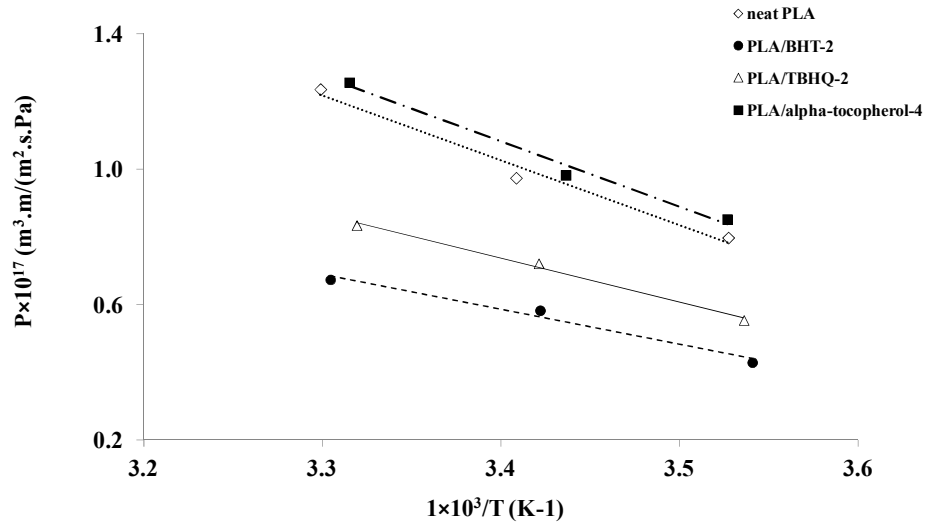

Figure 77 - Temperature dependence of CO_2 permeation in PLA with and without antioxidants. The lines represent the data fitting to an Arrhenius equation for PLA (.....), PLA/BHT-2 wt.% (- - - -), PLA/TBHQ-2 wt.% (—), PLA/α-tocopherol-4 wt % (— . —).

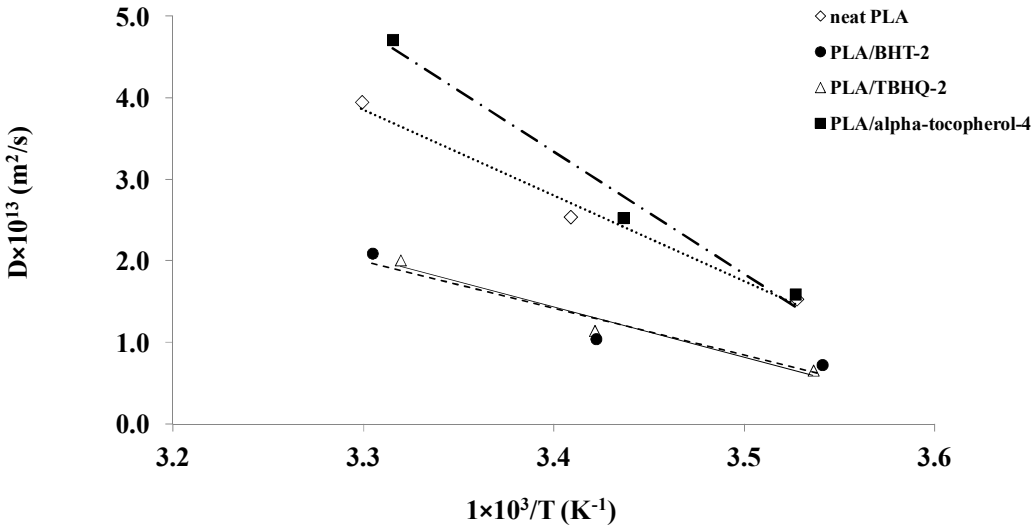

Figure 78 - Temperature dependence of CO_2 diffusivity in PLA with and without antioxidants. The lines represent the data fitting to an Arrhenius equation for PLA (.....), PLA/BHT-2 wt.% (- - - -), PLA/TBHQ-2 wt.% (—), PLA/α-tocopherol-4 wt % (— . —).

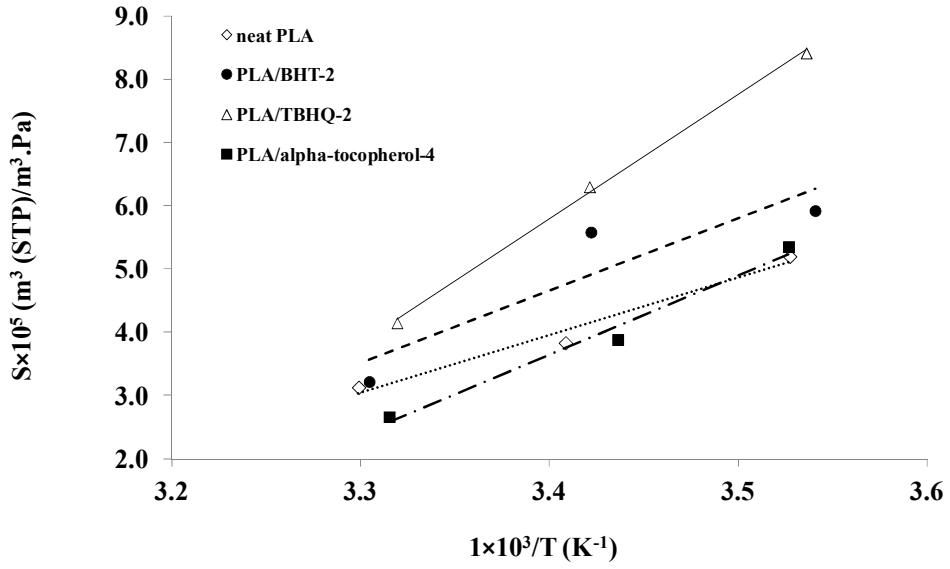

Figure 79 - Temperature dependence of CO_2 solubility in PLA with and without antioxidants. The lines represent the data fitting to an Arrhenius equation for PLA (.....), PLA/BHT-2 wt.% (- - - -), PLA/TBHQ-2 wt.% (—), PLA/α-tocopherol-4 wt % (— . —).

Table 19 - Activation energy for CO_2 permeability, diffusivity and solubility in neat PLA and enriched antioxidants.

Film	E_P (kJ/mol)	E_D (kJ/mol)	E_S (kJ/mol)
Neat PLA 98:2	15.9 (18.1) [a] (15.65) [b]	34.5 (36.3) [a]	-18.5 (-18.4) [a]
PLA/BHT-2%	15.9	37.3	-21.4
PLA/TBHQ-2%	15.8	42.7	-27.0
PLA/α-tocopherol-4%	15.4	42.7	-27.3
PLA/α-tocopherol-2%	-	-	-

a) From Bao *et al* - Ref. [130] (PLA98:2 with 4% crystallinity, casting)

b) From Auras *et al* - Ref.[129](PLA98%L, with 40 % crystallinity, extruded)

The obtained activation energies for CO_2 permeability, diffusivity and solubility in the neat PLA film were all in good agreement with the values reported by Bao *et al.* [130] and Auras *et al.* [129] The activation energies for CO_2 permeability for PLA/BHT-2 wt.%, PLA/TBHQ-2 wt% and PLA-4 wt.% α-tocopherol films were roughly the same as those obtained for neat PLA. The activation energy for CO_2 diffusivity increases 8 % for PLA/BHT-2 wt.%, and about 24 % for both PLA/TBHQ-2 wt% and PLA-4 wt.% α-

tocopherol films, relatively to neat PLA. The obtained activation energy for CO_2 solubility decrease about 16 % for PLA/BHT-2 wt.%, and decrease about 47 % for PLA/TBHQ-2 wt% and PLA-4 wt.% α-tocopherol films, relatively to neat PLA.

4.3.3. Oxygen permeation

In Table 20 the results obtained by time-lag technique for PLA based films are presented. Also, for neat PLA, are shown some data found in other works with PLA membranes containing a percentage of L-lactide near the PLA used in this work. The results for neat PLA film towards O_2 at 303 K are in good agreement with those reported by Auras *et al*. [129] and Bao *et al*.[130]

As expected, for the same membrane, at the same temperature, the time-lag is greater for carbon dioxide than for the oxygen. Surprisingly, the films with 2 wt% α-tocopherol did not show a significant time-lag for the carbon dioxide but showed a small time-lag for oxygen. An explanation for this change of behavior may be due the fact that α-tocopherol act as oxygen scavenger, and thus takes longer time to reach the equilibrium. This will be a hypothesis to investigate in the future.

Table 20 – Experimental data obtained from time-lag technique for oxygen in PLA films with and without antioxidants. Each result is an average of least three measurements.

T (K)	P_i (Pa)	P_f(Pa)	P_{feed} (Pa)	t_L (s)	Slope	Intercept	$P\times10^{18}$ (m^3. m/m^2.s.Pa)	$D\times10^{12}$ (m^2/s)	$S\times10^{6}$ ($m^3_{(STP)}.m^{-3}.Pa^{-1}$)
PLA (67.5 µm)									
284	17	464	98120	1043	0.0124	-12.8	1.9	0.67	2.9
293	20	599	102067	625	0.0176	-10.9	2.6 (6.2) [a]	1.2	2.2
303	34	455	100580	307	0.0232	-7.1	3.4 (1.9) [b]	2.3 (5.7) [b]	1.6 (0.37) [b]
PLA/BHT-2% (60.6 µm)									
282	28	118	101875	1875	0.00901	-17	1.2	0.33	3.82
292	26	370	98750	1223	0.0120	-15	1.4 (8.1) [a]	0.50	2.87
303	12	122	106767	783	0.0176	-14	2.2	0,78	2.82
PLA/TBHQ-2% (59.2 µm for 282 and 292 K and 65.0 µm for 302 K))									
283	99	254	99980	1163	0.0114	-13	1.6	0.52	3.10
292	145	378	101790	856	0.0161	-16	1.9 (5.9) [a]	0.64	3.06
302	15	437	102350	654	0.0210	-14	2.9	1.0	2.81
PLA/α-tocopherol-4% (64.0 µm)									
283	6	371	92610	921	0.0129	-12	2.09	0.74	2.82
293	16	301	96077	428	0.0218	-9	2.16	1.85	1.26
302	26	1169	99430	240	0.0298	-7	3.62	2.28	1.62
PLA/α-tocopherol-2% (82.4 µm)									
284	28	216	92737	776	0.0161	-12	3.4	1.5	2.3
294	66	572	92340	399	0.0293	-11	6.0	3.0	2.0
304	69	765	92340	112	0.0504	-6	9.9	11.3	0.96

a) From Jamshidian *et al* – Ref. [55] (PLA24-30%L, 20% crystallinity, films obtained from casting solution with 1 % antioxidant).

b) From Bao *et al* - Ref. [130] (PLA98,7 % L-lactide, 4% crystallinity, casting).

As observed for CO_2 permeation, the permeability and diffusivity of O_2 in the PLA films with and without antioxidants increased with temperature, while the solubility decreased, as expect. The O_2 permeation and solubility in PLA at 303 K are 1.7 times and 4 times higher those reported by Bao *et al.* [130], respectively and the diffusivity is about 2.5 times lower. These discrepancies may be due to differences in the crystallinity, because our films have about 45 % crystallinity and Bao *et al* [130] reported 4 % of crystallinity in their

films. The increased crystallinity of our films might have caused highly tortuous paths within the membrane and consequently a decrease of the diffusivity.

The incorporation of only 2 wt.% of BHT and TBHQ into PLA films, on average, decreases the O_2 permeability by 40 % and 19 %, respectively, while the incorporation of 4 wt.% of α-tocopherol into PLA films did not significantly affect the permeability towards O_2 from 283 K to 293 K, but increase for 303 K (Figure 80).

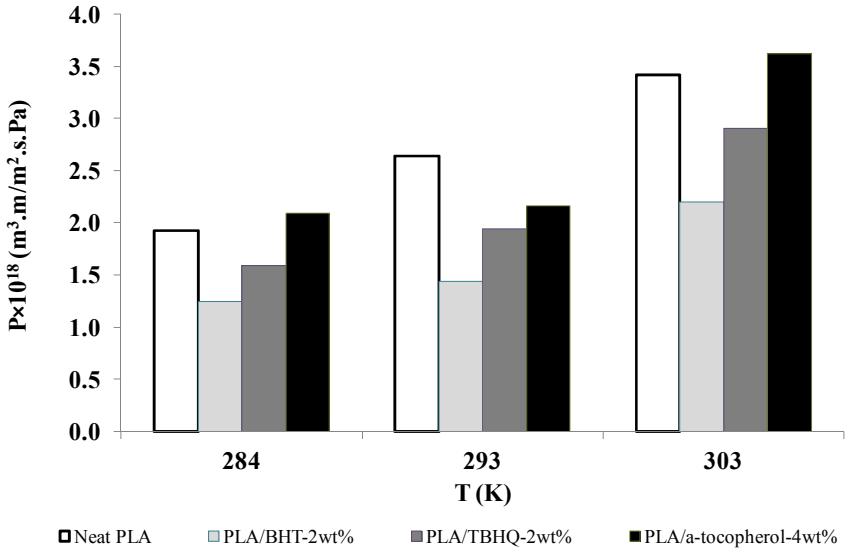

Figure 80 – Oxygen permeation of antioxidants PLA films.

The decrease in the O_2 permeability obtained for the PLA films with incorporated BHT and TBHQ can be attributed to their slow gas diffusion compared to the pure PLA film. A similarity in behaviour pattern between permeability and diffusivity is observed, and this result is consistent with the well known gas transport behaviour in dense polymer membranes. Although gas molecules dissolve into the polymer and diffuse through it, the differences in the gas permeability mainly arise from the diffusion differences of each gas component (Figure 81) in the polymer film since the solubilities tend to slightly increase or to be similar (Figure 82). Furthermore, SEM images revealed that films with 2 wt% of these antioxidants (Figure 27) present a better integrity than PLA. If their structure is more cohesive, and the diffusion of both carbon dioxide and oxygen is lower than in neat PLA, then these two antioxidants may be acting as fillers.

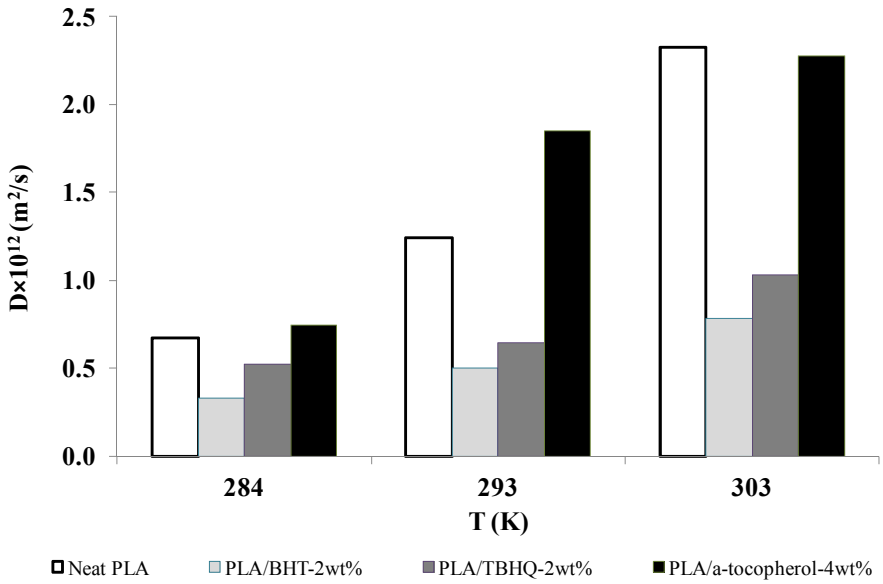

Figure 81 – Oxygen diffusivity of antioxidants enriched PLA based films.

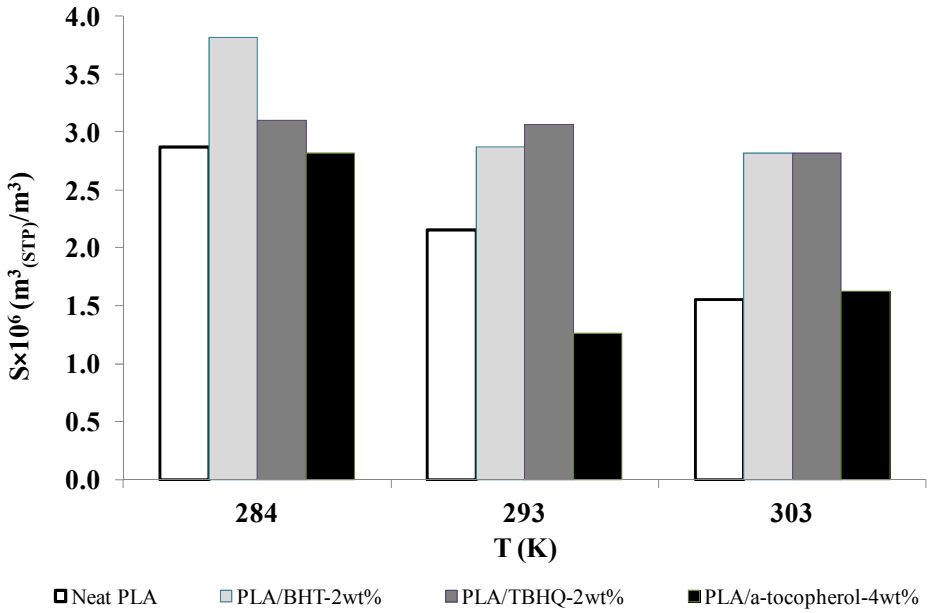

Figure 82 – Oxygen solubility of antioxidants PLA films.

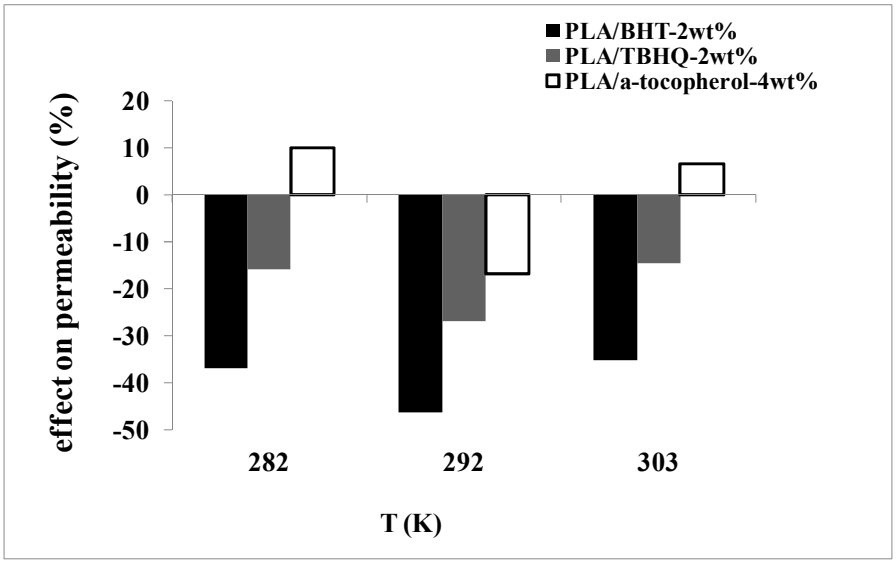

Figure 83 – Effect of each antioxidant on the O_2 permeability of antioxidants enriched in PLA-based films with the temperature.

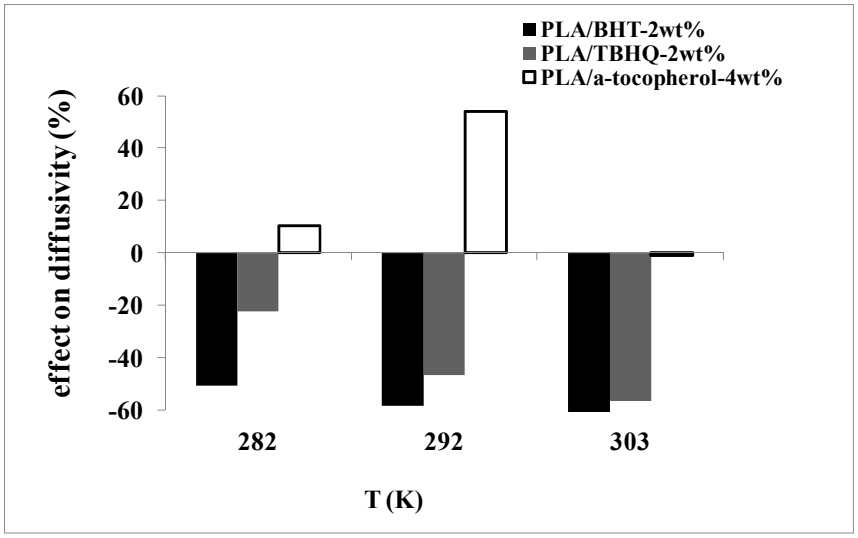

Figure 84 – Effect of each antioxidant on the O_2 diffusivity of antioxidants enriched in PLA-based films with the temperature.

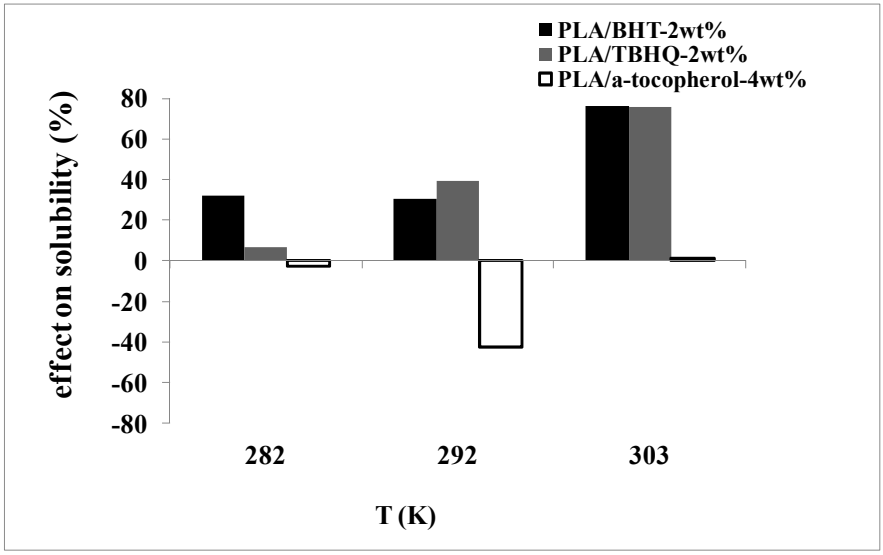

Figure 85 – Effect of each antioxidant on the O_2 diffusivity of antioxidants enriched in PLA-based films with the temperature.

The temperature dependence of O_2 permeation properties for neat PLA and antioxidants enriched films, in the temperature range of 284-303 K is presented in Figure 86 to Figure 88. The activation energies for these properties are listed in Table 21.

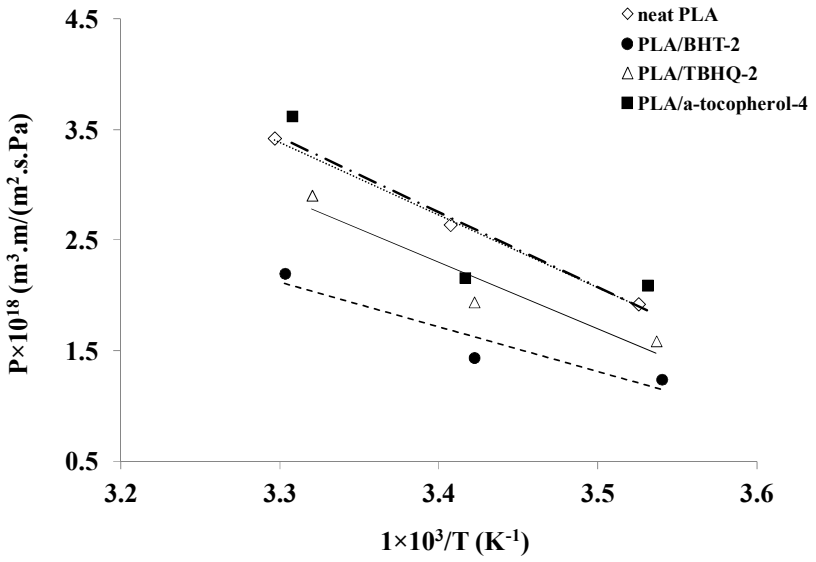

Figure 86 - Temperature dependence of O_2 permeation in PLA with and without antioxidants. The lines represent the data fitting to an Arrhenius equation for PLA (.....), PLA/BHT-2 wt.% (**- - - -**), PLA/TBHQ-2 wt.% (—), PLA/α-tocopherol-4 wt % (— **.** —).

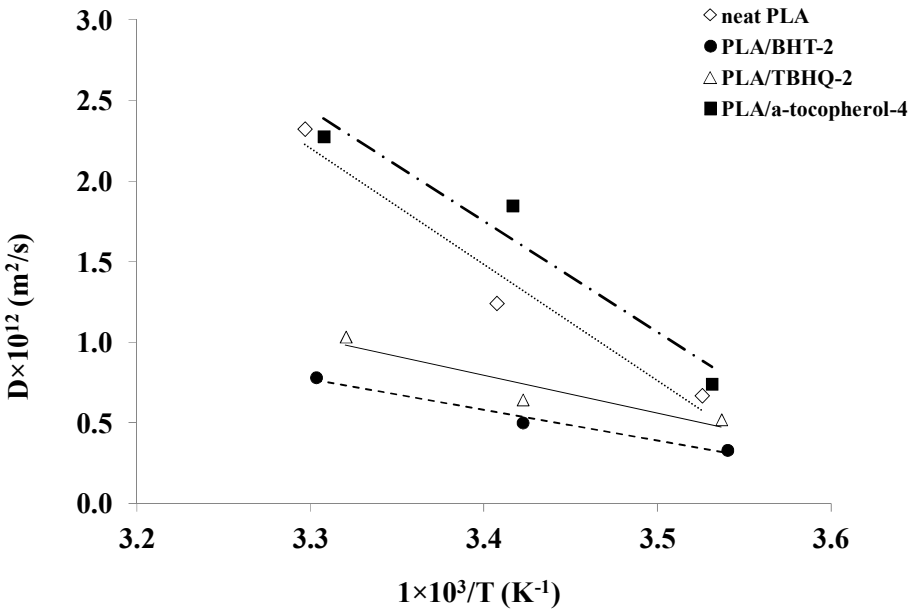

Figure 87 - Temperature dependence of O_2 diffusivity in PLA with and without antioxidants. The lines represent the data fitting to an Arrhenius equation for PLA (.....), PLA/BHT-2 wt.% (- - - -), PLA/TBHQ-2 wt.% (—), PLA/α-tocopherol-4 wt % (— . —).

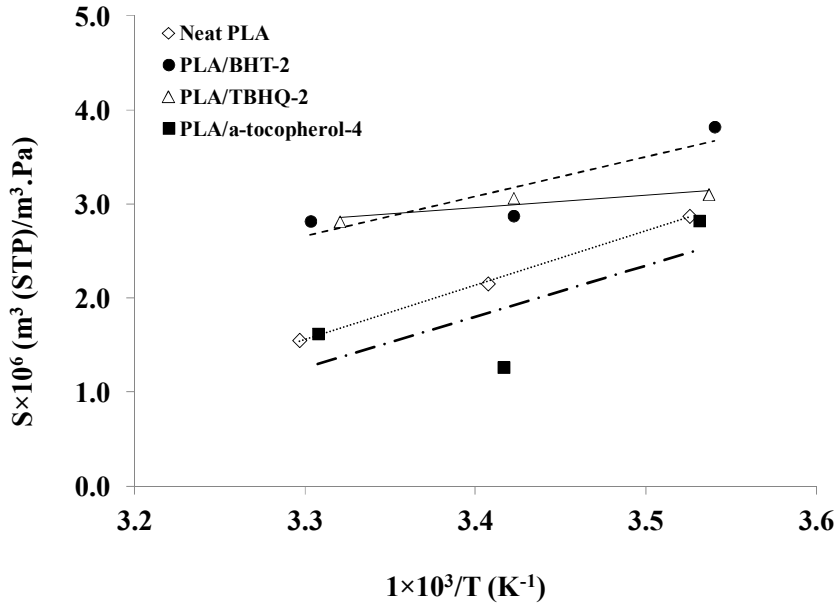

Figure 88 - Temperature dependence of O_2 solubility in PLA with and without antioxidants. The lines represent the data fitting to an Arrhenius equation for PLA (.....), PLA/BHT-2 wt.% (- - - -), PLA/TBHQ-2 wt.% (—), PLA/α-tocopherol-4 wt % (— . —).

It is visible a lack of linearity of the permeability with the temperature for the PLA membranes enriched with α-tocopherol and also for the solubility of both PLA enriched films with α-tocopherol and BHT. The same behaviour was also found by QCM technique, for the same antioxidants.

Table 21 - Activation energy for O_2 permeability, diffusivity and solubility in neat PLA ant enriched antioxidants.

Film	E_P (kJ/mol)	E_D (kJ/mol)	E_S (kJ/mol)
Neat PLA 98:2	21.0 (24.0) [a)]	45.2 (42.7) [a)]	-22.3 (-19.2) [a)]
PLA/BHT-2%	20.1	30.1	-10.7
PLA/TBHQ-2%	23.0	26.1	-3.7
PLA/α-tocopherol-4%	20.2	41.9	-20.9

a) From Bao *et al* - Ref. [130] (PLA98:2 with 4% crystallinity, casting).

The activation energies for O_2 permeability, diffusivity and solubility in the neat PLA films have the same order of magnitude of those determined by Bao *et al.* The incorporation of antioxidants into PLA films does not affect the activation energy for O_2 permeability, but a less endothermic diffusivity than that observed for the neat PLA was found for BHT and TBHQ. Also, the incorporation of 2 wt % of BHT or TBHQ into PLA films renders the oxygen solubility in PLA films a less exothermic process.

As found by QCM technique, at higher temperatures, the oxygen solubility in α-tocopherol enriched films increase. This behaviour is independent of the thermal treatment of the films, because in QCM the films were melted. Once more, the mobility of the polymeric chains must occur, and the increase of free volume promotes de solubility.

4.4. Conclusions

Carbon dioxide and oxygen are two of the main permeants studied in packaging application, because they may transfer from internal or external environment through the polymer package wall, influencing the quality and shelf-life of the food. The introduction of new packaging material PLA based as well its end-use application depend of its barrier

properties. The incorporation of only 2 wt % of BHT and TBHQ decreases the carbon dioxide permeability in average 44 % and 30 % and decrease the oxygen permeability by 40 % and 20 %, respectively. Although the barrier properties have been improved, the BHT or TBHQ-PLA based membranes have lower CO_2 and O_2 permeability coefficients than PS and PP but higher than PET, the most used to make plastic bottles for carbonated drinks due to good barrier to oxygen and carbon dioxide. Regarding to barrier properties of the PLA (Figure 89 and Figure 90), it could replaces a wide variety of synthetic polymers used in packaging industry, if not were its brittleness failure and low tensile elongation.

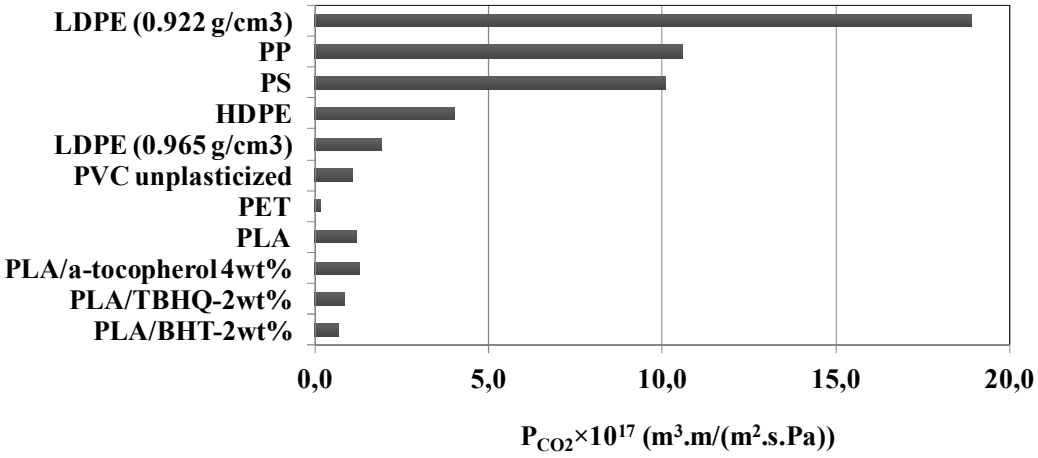

Figure 89 – Comparison of carbon dioxide permeability of antioxidants/PLA based membranes against the most widely polymers in food packaging industry. (adapted from Ref. 122).

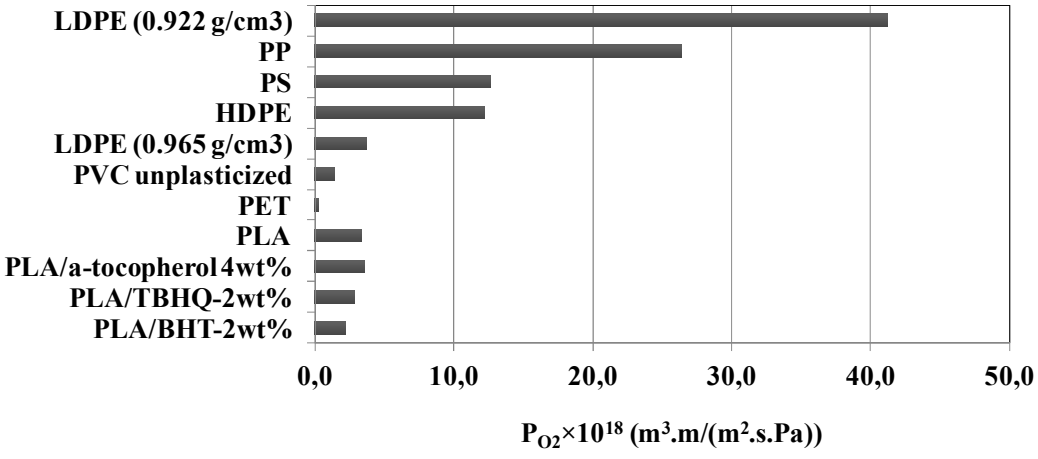

Figure 90 – Comparison of oxygen permeability of antioxidants/PLA based membranes against the most widely polymers in food packaging industry. (adapted from Ref. 122).

These results demonstrate the potential applicability of both antioxidants to produce antioxidants-PLA based films with applicability in food packaging. Nevertheless, the methodology to produce PLA/α-tocopherol based membranes needs to be improved in order to increase its homogeneity and compatibility between the antioxidant and the PLA matrix.

5. General Conclusions and Final Remarks

This work shows that it is possible to improve PLA's properties by the addition of chosen amounts of specific antioxidants. Here, PLA based membranes were additivated with synthetic (BHT and TBHQ) and natural (α-tocopherol) based antioxidants and further characterized for their final structural, morphological and barrier properties. This work demonstrates that PLA's properties can be enhanced by incorporation of antioxidants such as BHT and TBHQ. The addition of 10 wt% of each of these antioxidants to PLA films promotes the decrease of their Tg, which is important to improve the flexural properties of PLA. Based on this study, complementary studies, such as elastic modulus measurements, are needed in order to better understand this behaviour and deeply evaluate the impact of those antioxidants on the flexibility of TBHQ/PLA based films.

Regarding the introduction of α-tocopherol in PLA based membranes, new strategies are needed to enhance the compatibility between this antioxidant and the PLA matrix. Also, the yellowish colour of the PLA/α-tocopherol films needs to be investigated.

A time-lag apparatus was build during this thesis so that carbon dioxide and oxygen barrier properties of the several prepared films could be studied. Good agreement with literature data was obtained for pure PLA's films permeability towards carbon dioxide and oxygen. The incorporation of only 2 wt% of BHT and TBHQ in the PLA matrix can decrease the carbon dioxide permeability by 44 % and 30 % and the oxygen permeability by 40 % and 20 %, respectively. Films containing 4 wt% of α-tocopherol present carbon dioxide and oxygen permeability which are very similar to those of pure PLA.

It would be interesting to study PLA with higher molecular weight, since the Tg of PLA increases with molecular weight, the additivation of PLA with 2 wt% of antioxidants may not represent a problem, regarding the transition to the rubbery state.

Considering the good results obtained after incorporation of TBHQ into PLA, films enriched with TBHQ amounts approved by FDA should be investigated. However, it should be noted that this compound is prohibited in Canada and in the European Union which highlights the need for the use of natural based antioxidant alternatives. Since the compatibility between the α-tocopherol and the PLA matrix seems unlikely, based on the results obtained in this work, it should be interesting to find other potential candidates, such as rosemary extracts, which already revealed powerful antioxidant properties being able to simultaneously work as plasticizers.

6. References

1. Mülhaupt, R. Green Polymer Chemistry and Bio-based Plastics: Dreams and Reality. *Macromol. Chem. Phys.* **214,** 159–174 (2013).

2. Plastic Facts - Recycle Plastic. *Accessed on 29-04-2014* at <http://junkyard.recycleinme.com/recycle_plastic/default.aspx>

3. European plastics industry on the Commission's Green Paper on Plastic Waste in the Environment. *Accessed on 29-04-2014* at <http://www.plasticseurope.org/information-centre/press-room-1351/press-releases-2013/european-plastics-industry-on-the-commissions-green-paper-on-plastic-waste-in-the-environment.aspx>

4. Wu, G. & Li, J. Z. X. Triboelectrostatic separation for granular plastic waste recycling: A review. *Waste Manag.* **33,** 585–597 (2013).

5. Siracusa, V., Rocculi, P., Romani, S. & Rosa, M. D. Biodegradable polymers for food packaging: a review. *Trends Food Sci. Technol.* **19,** 634–643 (2008).

6. Plastics – the Facts 2012 An analysis of European plastics production , demand and waste data for 2011. *Accessed on 29-04-2014* at <http://www.plasticseurope.org/Document/plastics-the-facts-2012.aspx?Page=DOCUMENT&FolID=2>

7. Recycling Resources. at <http://www.ehso.com/recyclingfacts2.php>

8. Avérous, L. & Pollet, E. Biodegradable Polymers. *Environ. Silic. Nano-Biocomposites* (2012). doi:10.1007/978-1-4471-4108-2

9. Colomines, G., Ducruet, V., Courgneau, C., Guinault, A. & Domenek, S. Barrier properties of poly(lactic acid) and its morphological changes induced by aroma compound sorption. *Polym. Int.* **59,** 818–826 (2010).

10. Babu, R. P., O'Connor, K. & Seeram, R. Current progress on bio-based polymers and their future trends. *Prog. Biomater.* **2,** 8 (2013).

11. Avérous, L. & Pollet, E. Environmental Silicate Nano-Biocomposites. (2012). doi:10.1007/978-1-4471-4108-2

12. W. Baltus, D. Carrez, M. Carus, H. Kaeb, J. Ravenstijn, S. Z. Bio-based polymers - Production capacity will triple from 3.5 million tonnes in 2011 to nearly 12 million tonnes in 2020. *nova-Institute GmbH* 1–13 (2013). at <http://www.bio-based.eu/market_study/media/13-03-06PRMSBiopolymerslongnova.pdf>

13. Oliveira, N. S. *et al.* Gas sorption in poly(lactic acid) and packaging materials. *Fluid Phase Equilib.* **222-223,** 317–324 (2004).

14. Auras, R., Harte, B. & Selke, S. An overview of polylactides as packaging materials. *Macromol. Biosci.* **4,** 835–64 (2004).

15. *Poly(lactic acid): Synthesis, Structures, Properties, Processing, and Applications*. (John Wiley & Sons, 2010).

16. Balkcom, M., Welt, B. & Berger, K. Notes from the Packaging Laboratory : Polylactic Acid -- An Exciting New Packaging Material 1. 1–5 (2002).

17. Jonh R. Dorgan, Hans jJ. Lehermeier, L.-I. P. and J. C. Polylactides: Properties and Prospects of an Environmentally Benign Plastic from Renewaable Resources. *Macromol. Symp.* **66,** 55–66 (2001).

18. Siracusa, V. Food Packaging Permeability Behaviour: A Report. *Int. J. Polym. Sci.* **2012,** 1–11 (2012).

19. Hwang, S. W. *et al.* Migration of α-tocopherol and resveratrol from poly(L-lactic acid)/starch blends films into ethanol. *J. Food Eng.* **116,** 814–828 (2013).

20. Holm, V., Mortensen, G. & Risbo, J. Quality changes in semi-hard cheese packaged in a poly(lactic acid) material. *Food Chem.* **97,** 401–410 (2006).

21. Kilcast, D. & Subramaniam, P. *The stability and shelf-life of food*. (CRC Press LLC and Woodhead Publishing Limited, 2000).

22. Vermeiren, L., Devlieghere, F., van Beest, M., de Kruijf, N. & Debevere, J. Developments in the active packaging of foods. *Trends Food Sci. Technol.* **10,** 77–86 (1999).

23. López-Rubio, A. *et al.* Overview of Active Polymer-Based Packaging Technologies for Food Applications. *Food Rev. Int.* **20,** 357–387 (2004).

24. Ozdemir, M., Yurteri, C. U. & Sadikoglu, H. Physical polymer surface modification methods and applications in food packaging polymers. *Crit. Rev. Food Sci. Nutr.* **39,** 457–77 (1999).

25. Ozdemir, M. & Floros, J. D. Active food packaging technologies. *Crit. Rev. Food Sci. Nutr.* **44,** 185–93 (2004).

26. *Innovations in Food Packaging*. (Food Science and Technology, International Series, 2005).

27. Wessling, C., Nielsen, T. & Giacin, J. R. Antioxidant ability of BHT- and a -tocopherol- impregnated LDPE film in packaging of oatmeal. *J. Sci. Food Agric.* **81,** 194–201 (2001).

28. Wessling, C., Nielsen, T., Leufvén, A. & Jagertad, M. Retention of a-tocopherol in low-density polyethylene (LDPE) and polypropylene (PP) in contact with foodstuffs and food-simulating liquids. *J. Sci. Food Agric.* **1641,** 1635–1641 (1999).

29. Wessling, B. C., Nielsen, T. & Leufve, A. The Influence of a-Tocopherol Concentration on the Stability of Linoleic Acid and the Properties of Low-density Polyethylene. *Packag. Technol. Sci.* **13,** 19–28 (2000).

30. Auras, R. a., Harte, B., Selke, S. & Hernandez, R. Mechanical, Physical, and Barrier Properties of Poly(Lactide) Films. *J. Plast. Film Sheeting* **19,** 123–135 (2003).

31. Auras, R., Harte, B. & Selke, S. An overview of polylactides as packaging materials. *Macromol. Biosci.* **4,** 835–64 (2004).

32. Auras, R. a., Singh, S. P. & Singh, J. J. Evaluation of oriented poly(lactide) polymers vs. existing PET and oriented PS for fresh food service containers. *Packag. Technol. Sci.* **18,** 207–216 (2005).

33. Mulder, M. *Basic Principles of Membrane Technology*. 22–69 (Kluwer Academic Publishers incorporates, 2000).

34. Dury-Brun, C., Chalier, P., Desobry, S. & Voilley, A. Multiple Mass Transfers of Small Volatile Molecules Through Flexible Food Packaging. *Food Rev. Int.* **23,** 199–255 (2007).

35. *Polymer Crystallization Observations, Concepts and Interpretations*. (Springer-Verlag Berlin Heidelberg New York, 2003).

36. Ronova, I. a., Rozhkov, E. M., Alentiev, A. Y. & Yampolskii, Y. P. Occupied and Accessible Volumes in Glassy Polymers and Their Relationship with Gas Permeation Parameters. *Macromol. Theory Simulations* **12,** 425–439 (2003).

37. Liu, R. Y. F., And, A. H. & Baer, E. Free volume and oxygen transport in cold-drawn polyesters. *J. Polym. Sci. Part B Polym. Phys.* **42,** 493–504 (2004).

38. Lim, L.-T., Auras, R. & Rubino, M. Processing technologies for poly(lactic acid). *Prog. Polym. Sci.* **33,** 820–852 (2008).

39. Nanostructures, P., Bhardwaj, R. & Mohanty, A. K. Modification of Brittle Polylactide by Novel Hyperbranched. 2476–2484 (2007).

40. Ljungberg, N. & Wessl□n, B. The effects of plasticizers on the dynamic mechanical and thermal properties of poly(lactic acid). *J. Appl. Polym. Sci.* **86,** 1227–1234 (2002).

41. Martin, O. & Ave, L. Poly (lactic acid): plasticization and properties of biodegradable multiphase systems. **42,** 6209–6219 (2001).

42. Ahmed, J. & Varshney, S. K. Polylactides—Chemistry, Properties and Green Packaging Technology: A Review. *Int. J. Food Prop.* **14,** 37–58 (2011).

43. Muller, Daniel; Voigt, Wolfgang; Ghosh, J. Vitamin E - A New Choice for Polyolefin Stabilization. *Macromol. Symp.* **176,** 17–29 (2001).

44. Peltzer, M., Wagner, J. R. & Jiménez, a. Thermal characterization of UHMWPE stabilized with natural antioxidants. *J. Therm. Anal. Calorim.* **87,** 493–497 (2007).

45. Strandberg, C. & Albertsson, A.-C. Process efficiency and long-term performance of α-tocopherol in film-blown linear low-density polyethylene. *J. Appl. Polym. Sci.* **98,** 2427–2439 (2005).

46. Wessling, C.; Nielsen, T.; Leufven, A.; Jagerstad, M. Mobility of alpha-tocopherol and BHT in LDPE in contact with fatty food simulants. *Food Addit. Contam.* **16,** 709–715 (1998).

47. Dopico-García, M. S., López-Vilariñó, J. M. & Gonzalez-Rodríguez, M. V. Antioxidant content of and migration from commercial polyethylene, polypropylene, and polyvinyl chloride packages. *J. Agric. Food Chem.* **55,** 3225–31 (2007).

48. Granda-Restrepo, D., Peralta, E., Troncoso-Rojas, R. & Soto-Valdez, H. Release of antioxidants from co-extruded active packaging developed for whole milk powder. *Int. Dairy J.* **19,** 481–488 (2009).

49. Oral, E., Wannomae, K. K., Rowell, S. L. & Muratoglu, O. K. Diffusion of vitamin E in ultra-high molecular weight polyethylene. *Biomaterials* **28,** 5225–37 (2007).

50. Sasaki, M., Hosoya, N. & Saruhashi, M. Vitamin E modified cellulose membrane. *Artif. Organs* **24,** 779–89 (2000).

51. Renò, F., Aina, V., Gatti, S. & Cannas, M. Effect of vitamin E addition to poly(D,L)-lactic acid on surface properties and osteoblast behaviour. *Biomaterials* **26,** 5594–9 (2005).

52. Byun, Y., Kim, Y. T. & Whiteside, S. Characterization of an antioxidant polylactic acid (PLA) film prepared with α-tocopherol, BHT and polyethylene glycol using film cast extruder. *J. Food Eng.* **100,** 239–244 (2010).

53. Manzanarez-López, F., Soto-Valdez, H., Auras, R. & Peralta, E. Release of α-Tocopherol from Poly(lactic acid) films, and its effect on the oxidative stability of soybean oil. *J. Food Eng.* **104,** 508–517 (2011).

54. Ortiz-Vazquez, H., Shin, J., Soto-Valdez, H. & Auras, R. Release of butylated hydroxytoluene (BHT) from Poly(lactic acid) films. *Polym. Test.* **30,** 463–471 (2011).

55. Jamshidian, M. *et al.* Effects of synthetic phenolic antioxidants on physical, structural, mechanical and barrier properties of poly lactic acid film. *Carbohydr. Polym.* **87,** 1763–1773 (2012).

56. Hwang, S. W. *et al.* Poly(L-lactic acid) with added α-tocopherol and resveratrol: optical, physical, thermal and mechanical properties. *Polym. Int.* **61,** 418–425 (2012).

57. López-Rubio, A. *et al.* Overview of Active Polymer-Based Packaging Technologies for Food Applications. *Food Rev. Int.* **20,** 357–387 (2004).

58. Lehermeier, H. J., Dorgan, J. R. & Way, J. D. Gas permeation properties of poly (lactic acid). *J. Memb. Sci.* **190,** 243–251 (2001).

59. Gonçalves, C. M. B. *et al.* Effect of natural and synthetic antioxidants incorporation on the gas permeation properties of poly(lactic acid) films. *J. Food Eng.* **116,** 562–571 (2013).

60. Martin, O. & Averous, L. Poly (lactic acid): plasticization and properties of biodegradable multiphase systems. **42,** 6209–6219 (2001).

61. Shibata, M., Teramoto, N. & Inoue, Y. Mechanical properties, morphologies, and crystallization behavior of plasticized poly(l-lactide)/poly(butylene succinate-co-l-lactate) blends. *Polymer (Guildf).* **48,** 2768–2777 (2007).

62. Piorkowska, E., Kulinski, Z., Galeski, a. & Masirek, R. Plasticization of semicrystalline poly(l-lactide) with poly(propylene glycol). *Polymer (Guildf).* **47,** 7178–7188 (2006).

63. Jamshidian, M. *et al.* Structural, mechanical and barrier properties of active PLA–antioxidant films. *J. Food Eng.* **110,** 380–389 (2012).

64. Kaczmarek, H., Nowicki, M., Vuković-Kwiatkowska, I. & Nowakowska, S. Crosslinked blends of poly(lactic acid) and polyacrylates: AFM, DSC and XRD studies. *J. Polym. Res.* **20,** 91 (2013).

65. Chang, S.-M., Muramatsu, H., Nakamura, C. & Miyake, J. The principle and applications of piezoelectric crystal sensors. *Mater. Sci. Eng. C* **12,** 111–123 (2000).

66. V.M. Mecea. Is quartz crystal microbalance really a mass sensor. *Sensors Actuators A Phys.* **128,** 270–277 (2006).

67. Wakatsuki, N. and Kagawa, Y. Identification of the properties of a complex layer deposited on the surface of a quartz crystal microbalance (QCM) by the impedance measurement. *Meas. Sci. Technol.* 57–61 (2007).

68. Schrag, John L.; White, C. C. Theoretical predictions for the mechanical response of a model quartz crystal microbalance to two viscoelastic media: A thin sample layer and surrounding bath medium. *J. Chem. Phys.* **111,** 11192 – 11206 (1999).

69. Hellstrom, S. L. Introduction to Quartz Crystal Microbalance. *Accessed on 29-04-2014* at <http://large.stanford.edu/courses/2007/ph210/hellstrom2/Accessed 29-04-2014>

70. Rodahl, M., Krozer, A. & Kasemoa, B. Quartz crystal microbalance setup for frequency and Q-factor measurements in gaseous and liquid environments. *Rev. Sci. Instrum.* **66,** (1995).

71. Aubert, J. H. Solubility of carbon dioxide in polymers by the quartz crystal microbalance technique. *J. Supercrit. Fluids* **11,** 163–172 (1998).

72. Zhang, C., Wyatt, J. & Weinkauf, D. H. Carbon dioxide sorption in conventional and plasma polymerized methyl methacrylate thin films. *Polymer (Guildf).* **45,** 7665–7671 (2004).

73. Oliveira, N. S. *et al.* Carbon dioxide, ethylene and water vapor sorption in poly(lactic acid). *Fluid Phase Equilib.* **250,** 116–124 (2006).

74. Oliveira, N. S. *et al.* Gas solubility of carbon dioxide in poly(lactic acid) at high pressures. *J. Polym. Sci. Part B Polym. Phys.* **44,** 1010–1019 (2006).

75. Miura, K. *et al.* Solubility and adsorption of high pressure carbon dioxide to poly styrene . *Fluid Phase Equilib.* **144,** 181–189 (1998).

76. Feng, H. Modeling of vapor sorption in glassy polymers using a new dual mode sorption model based on multilayer sorption theory. *Polymer (Guildf).* **48,** 2988–3002 (2007).

77. Wang, J. & Kamiya, Y. Evaluation of Gas Sorption Parameters and Prediction of Sorption Isotherms in Glassy Polymers. *J. Memb. Sci.* **154,** (1999).

78. Favre, E., Nguyen, Q. T. & Nrel, J. The engaged species induced clustering (ENSIC) model : a unified mechanistic approach of sorption phenomena in polymers. *J. Mater. Sci.* **117,** 227–236 (1996).

79. http://www.doitpoms.ac.uk/tlplib/mechanical-testing/results1.php?printable=1. *Accessed on 29-04-2014* at <http://www.doitpoms.ac.uk/tlplib/mechanical-testing/results1.php?printable=1/Accessed 29-04-2014>

80. Siracusa, V. Food Packaging Permeability Behaviour: A Report. *Int. J. Polym. Sci.* **2012,** 1–11 (2012).

81. George, S. C. & Thomas, S. Transport phenomena through polymeric systems. *Prog. Polym. Sci.* **26,** 985–1017 (2001).

82. Hwang, S. W. *et al.* Migration of α-tocopherol and resveratrol from poly(L-lactic acid)/starch blends films into ethanol. *J. Food Eng.* **116,** 814–828 (2013).

83. Jamshidian, M., Tehrany, E. A. & Desobry, S. Release of synthetic phenolic antioxidants from extruded poly lactic acid (PLA) film. *Food Control* **28,** 445–455 (2012).

84. Oliveira, N. S. Solubilidade de gases em membranas poliméricas, Thesis. (2006).

85. Till, Derek E.; Ehntholt, Daniel J.; Reid, Robert C.; Schwartz, Patricia S.; Sidman, Kenneth R.; Schwope, Arthur D.; Whelan, R. H. Migration of BHT antioxidant from high density polyethylene to foods and food simulants. *Ind. Eng. Chem. , Prod. Res. Dev.* **21,** 106–113 (1982).

86. Schwope, Arthur D.; Till , Derek E.; Ehntholt, Daniel J.; Sidman, Kenneth R.; Whelan, Richard H.; Schwartz, Patricia S.; Reid, R. C. Migration of BHT from impact polystyrene to foods and food-simulating liquids. *Ind. Eng. Chem. Res.* **26,** 1668–1670 (1987).

87. Lundbäck, M., Hedenqvist, M. S., Mattozzi, A. & Gedde, U. W. Migration of phenolic antioxidants from linear and branched polyethylene. *Polym. Degrad. Stab.* **91,** 1571–1580 (2006).

88. Jeon, D. H., Park, G. Y., Kwak, I. S., Lee, K. H. & Hyun Jin Park. Antioxidants and their migration into food simulants on irradiated LLDPE film. *LWT - Food Sci. Technol.* **40,** 151–156 (2007).

89. Van Aardt, M., Duncan, S. E., Marcy, J. E., Long, T. E. & And, Sean Francis O'Keefe Sims, S. R. Release of antioxidants from poly(lactide-co-glycolide) films into dry milk products and food simulating liquids. *Int. J. Food Sci. Technol.* **42,** 1327–1337 (2007).

90. Soto-Cantú CD, Graciano-Verdugo AZ, Peralta E, Islas-Rubio AR, González-Córdova A, González-León A, S.-V. H. Release of butylated hydroxytoluene from an active film packaging to Asadero cheese and its effect on oxidation and odor stability. *J. Dairy Sci.* **91,** 11–19 (2008).

91. Schaich, K.M.; Obinata, N; Yam, K. Delivering natural antioxidants via controlled release packaging. in *Acta Hortic.* **778,** 53–64 (2006).

92. Peltzer M, Wagner J, J. A. Migration study of carvacrol as a natural antioxidant in high-density polyethylene for active packaging. *Food Addit. Contam. Part A. Chem. Anal. Control. Expo. Risk Assess.* **26,** 938–946 (2009).

93. Gemili, S., Yemenicioğlu, A. & Altınkaya, S. A. Development of antioxidant food packaging materials with controlled release properties. *J. Food Eng.* **96,** 325–332 (2010).

94. Contini C, Valzacchi S, O'Sullivan M, Simoneau C, Dowling DP, M. F. Overall migration and kinetics of release of antioxidant compounds from citrus extract-based active packaging. *J. Agric. Food Chem.* **61,** 12155–12163 (2013).

95. Miller, Jane C.; Miller, J. N. *Statistics for Analytical Chemistry*. 233 (New York: Ellis Horwood PTR Prentice Hall, 1993).

96. Sajilata, M. G., Savitha, K., Singhal, R. S. & Kanetkar, V. R. Scalping of Flavors in Packaged Foods. *Compr. Rev. Food Sci. Food Saf.* **6,** 17–35 (2007).

97. Nielsen, T. & Jägerstad, M. Flavour scalping by food packaging. *Trends Food Sci. Technol.* **5,** 353–356 (1994).

98. Van Willige, R., Schoolmeester, D., Van Ooij, A., Linssen, J. and Voragen, A. Influence of Storage Time and Temperature on Absorption of Flavor Compounds from Solutions by Plastic Packaging Materials. *J. Food Sci.* **67,** 2023–2031 (2002).

99. Nakatsuka, T. Polylactic Acid-Coated Cable. *Fujikura Tech. Rev.* 39–46 (2011).

100. Burdick & Jackson solvents. Dielectric Constant. *Accessed on 29-04-2014* at <http://macro.lsu.edu/howto/solvents/Dielectric Constant .htm/>

101. Colomines, G., Ducruet, V., Courgneau, C., Guinault, A. & Domenek, S. Barrier properties of poly(lactic acid) and its morphological changes induced by aroma compound sorption. *Polym. Int.* **59,** 818–826 (2010).

102. Auras, R. B. H. and S. S. Sorption of ethyl acetate and d-limonene in poly(lactic) polymers. *Jounal Sci. Food Agric.* **86,** 648–656 (2006).

103. Hamouda, S. Ben, Nguyen, Q. T., Langevin, D., Schaetzel, P. & Roudesli, S. Fine characterization of the ethylene and ethane sorption in poly(amide 12-block-tetramethylenoxide) copolymer/AgBF4 membranes. *Eur. Polym. J.* **42,** 2994–3005 (2006).

104. Pinnau, I. & Toy, L. G. Solid polymer electrolyte composite membranes for olefin/paraffin separation. *J. Memb. Sci.* **184,** 39–48 (2001).

105. Kim, J. Olefin-induced dissolution of silver salts physically dispersed in inert polymers and their application to olefin/paraffin separation. *J. Memb. Sci.* **241,** 403–407 (2004).

106. Choi, H. W. *et al.* Highly selective facilitated transport membranes for isoprene/n-pentane separation. *J. Memb. Sci.* **279,** 403–409 (2006).

107. Kim, H. S. *et al.* Multi-functional zwitterionic compounds as new membrane materials for separating olefin?paraffin mixtures. *Green Chem.* **9,** 599 (2007).

108. Yoshino, M. *et al.* Olefin / paraffin separation performance of asymmetric hollow fiber membrane of 6FDA / BPDA – DDBT copolyimide. *J. Memb. Sci.* **212,** 13–27 (2003).

109. Shimazu, A. ;T. M. M. M. I. Relationships between chemical structures and solubility, diffusivity, and permselectivity of 1,3-butadiene and n-butane in 6FDA-based polyimides. *J. Polym. Sci. Part B Polym. Phys.* **37,** 2941–2949 (1999).

110. *Membrane Engineering for the Treatment of Gases*. 85–89 (RSC Publishing, 2000).

111. Staudt-Bickela, C. & Korosb, W. J. Olefin/paraffin gas separations with 6FDA-based polyimide membranes. *J. Memb. Sci.* **170,** 205–214 (2000).

112. Oliveira, N. S. *et al.* Gas solubility of carbon dioxide in poly(lactic acid) at high pressures: Thermal treatment effect. *J. Polym. Sci. Part B Polym. Phys.* **45,** 616–625 (2007).

113. Nair, L. S. & Laurencin, C. T. Biodegradable polymers as biomaterials. *Prog. Polym. Sci.* **32,** 762–798 (2007).

114. Compan, V. ;L. F. D. C. I. H. M. L.-G. R. On the crystallinity effect on the gas sorption in semicrystalline linear low density polyethylene (LLDPE). *J. Polym. Sci. Part B Polym. Phys.* **45,** 1798–1807 (2007).

115. Liu, L., Chakma, A. & Feng, X. Sorption, diffusion, and permeation of light olefins in poly(ether block amide) membranes. *Chem. Eng. Sci.* **61,** 6142–6153 (2006).

116. Wind, J. D., Paul, D. R. & Koros, W. J. Natural gas permeation in polyimide membranes. *J. Memb. Sci.* **228,** 227–236 (2004).

117. Safarik, D. J. & Eldridge, R. B. Olefin / Paraffin Separations by Reactive Absorption : A Review. *Ind. Eng. Chem. Res.* **5885,** 2571–2581 (1998).

118. Syrtsovaa, D. *et al.* Removing of light hydrocarbons from gas mixtures using polymeric composite membranes based on poly(1-trimethylsilylpropyne). *Desalination* **200,** 253–255 (2006).

119. Afeefy, H. Y. L., J. F.; Stein, S. E. National Institute of Standards and Tecy. *Gaithersbg. MD, 20899*

120. Tayeb, M. R. Gas separation characteristics of polymer blend membranes, Thesis. (2004).

121. Flaconnèche, B., Martin, J. & Klopffer, M. H. Transport Properties of Gases in Polymers : Experimental Methods. *Oil Gas Sci. Technol.* **56,** 245–259 (2001).

122. *Food Packaging and Preservation*. (Aspen Publishers, Inc, 1994).

123. Baker, R.W.; Wijmans, J. G. The solution-diffusion model: a review. *J. Memb. Sci.* **107,** 1–21 (1995).

124. Ismail, Ahmad Fauzi , Hasbullah, Hasrinah; Mustafa, Azeman; Kusworol, T. D. . Understanding the solution-diffusion mechanism in gas separation membrane for engineering students. in *Reg. Conf. Eng. Educ. RCEE 2005* 12–13 (2005).

125. Auras, Rafael A; Tanprasert, K. Permeation of water vapor , carbon dioxide , and oxygen in polymeric materials . *Sch. Packag. Michigan State Univ.* (2002).

126. Mendes, Adélio M.; Brandão, Lúcia; Madeira, L. M. Mass transport on composite dense PDMS membranes with palladium nanoclusters. *J. Memb. Sci.* **288,** 112–122 (2007).

127. Taveira, P., Mendes, A. & Costa, C. On the determination of diffusivity and sorption coefficients using different time-lag models. *J. Memb. Sci.* **221,** 123–133 (2003).

128. Rutherford, S. W. & Do, D. D. Review of time lag permeation technique as a method for characterisation of porous media and membranes. *Adsorption* **3,** 283–312 (1997).

129. Auras, R. a., Harte, B., Selke, S. & Hernandez, R. Mechanical, Physical, and Barrier Properties of Poly(Lactide) Films. *J. Plast. Film Sheeting* **19,** 123–135 (2003).

130. Bao, L. *et al.* Gas permeation properties of poly(lactic acid) revisited. *J. Memb. Sci.* **285,** 166–172 (2006).

131. Santos, J. C. Study of New Adsorbents and Operation Cycles for Medical PSA Units - Thesis. (2005).

Appendix A

A.1.1 – Measurement of the volumes of the tanks

The size of the permeate tank was measured using the gas expansion method, which entails expanding fixed amount of gas to or from the permeate tank, while monitoring the pressure change. By repeating the same gas expansion procedure with and without a calibration volume in either thanks involved, and using the ideal gas law, one can easily obtain the volume of the permeate tank.

For determining the volume of the tanks, were carried out the following steps:

a) Perform vacuum in both tanks, initially empty;
b) Close de valve between the tanks A and B (see Figure 91);
c) Introduce nitrogen in tank A until a given pressure, P_A, is reached;
d) Open de valve between tank A and tank B, and record the equilibrium pressure;
e) Performing the above steps at least 10 times.

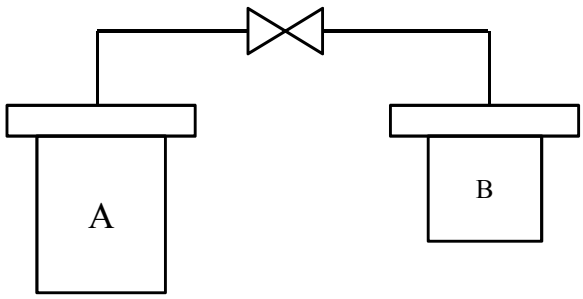

Figure 91 - Empty tanks.

Note: this figure was adapted from Ref.131

In the step a), the number of moles remaining after the evacuation is given by the following expression:

$$n_A^0 + n_B^0 = \frac{P^0 \left(V_A + V_B\right)}{RT} \quad \textbf{(30)}$$

where n is the number of moles of the gas, V_A the volume of tank A, V_B, volume of tank B, P^0 the pressure for initial conditions, R the universal gas constant and T the absolute temperature.

The number of moles of the gas, n, that was introduced in tank A, in step c), is given by the following expression

$$n_A = \frac{(P^A - P^0)V_A}{RT} \quad \textbf{(31)}$$

After opening the valve between the two tanks, a new equilibrium is reached, P^{AB}, and the number of moles of the gas in both tanks is given by:

$$n_A^e + n_B^e = \frac{P^{AB}(V_A + V_B)}{RT} \quad \textbf{(32)}$$

As,

$$n_A^e + n_B^e = n_A + n_A^0 + n_B^0 \quad \textbf{(33)}$$

The combination of equations (30), (31), (32) and (33), allows to obtain the following relation between the tank's volume:

$$\frac{V_A}{V_B} = \frac{P^{AB} - P^0}{P^A - P^{AB}} = \beta_1 \quad \textbf{(34)}$$

Then, the tank B is filled with spheres of glass, which were previously weight, as shown in Figure 92 .

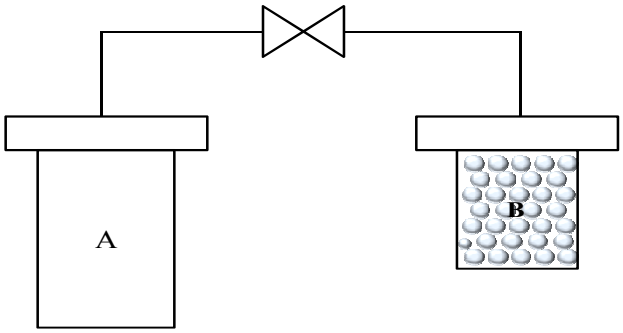

Figure 92 - Tank A empty and tank B with spheres of glass.

Note: this figure was adapted from Ref.[131]

Carried out the previous steps a) to e) but now with the tank B filled with spheres of glass, which have a volume V^S, determinates from the relationship between the density of the glass and the mass of the spheres.

The number of moles of gas inside the tanks, in beginning, is given by:

$$n_A^0 + n_B^0 = \frac{P^0\left(V_A + V_B - V_S\right)}{RT} \quad \textbf{(35)}$$

The number of moles of the gas, *n*, that was introduced in tank A, in step c), is given by the following expression:

$$n_A = \frac{(P_A - P^0)V_A}{RT} \quad \textbf{(36)}$$

After opening the valve between the two tanks, the number of moles of the gas both tanks is given by:

$$n_A^e + n_B^e = \frac{P^{AB}\left(V_A + V_B - V_S\right)}{RT} \quad \textbf{(37)}$$

Therefore,

$$n_A^e + n_B^e = n_A + n_A^0 + n_B^0 \quad \textbf{(38)}$$

Combining the equation (35) to (38), one obtains the relation between the two tank's volumes:

$$\frac{V_A}{V_B - V_S} = \frac{P^0 - P^{AB}}{P^{AB} - P_A} = \beta_2 \quad \textbf{(39)}$$

Solving the system of equations composed by equations (34) and (39), the volume of each tank is given by following equations:

$$V_B = \frac{\beta_2}{\beta_2 - \beta_1} V_S \quad \textbf{(40)}$$

and

$$V_A = \frac{\beta_1 \beta_2}{\beta_2 - \beta_1} V_S \quad \textbf{(41)}$$

Applying the above equations to our system, the following results were obtained:

$\beta_1 = 0{,}7498$;

$\beta_2 = 1{,}6691$;

$V_S = 2{,}51 \times 10^{-5}\ m^3$;

V_A (permeate volume) $= 34{,}19 \times 10^{-6}\ m^3$;

The procedure for calculating the measurement uncertainty was based on the law on propagation of uncertainty, and the principally sources of uncertainty identified were:

Source	Type	Standard uncertainty	Used to uncertainty calculation
Repeatability β_1	A	$u_x = \frac{s}{\sqrt{n}}$	yes
Repeatability β_2	A	$u_x = \frac{s}{\sqrt{n}}$	yes
$V_S = m_{spheres} / \rho_{glass}$ (ρ_{glass}=2515,94 kg/m^3) ($m_{spheres}$ = 0,0633 kg)	A	$u_x = \frac{s}{\sqrt{n}}$	yes
Uncertainty of calibration of pressure sensor	B	$u_x = \frac{U_{calibration}}{2}$	No

A.1.2 – Calibration of the temperature sensor

The sensor used for monitoring the temperature had a output signal in ohm. For the conversion to Celsius degrees, was used a thermocouple calibrated in accredited laboratory. The relationship between the output signal of the sensor used to monitoring the temperature of the permeability system and the thermocouple calibrated traceable to international standards is shown in

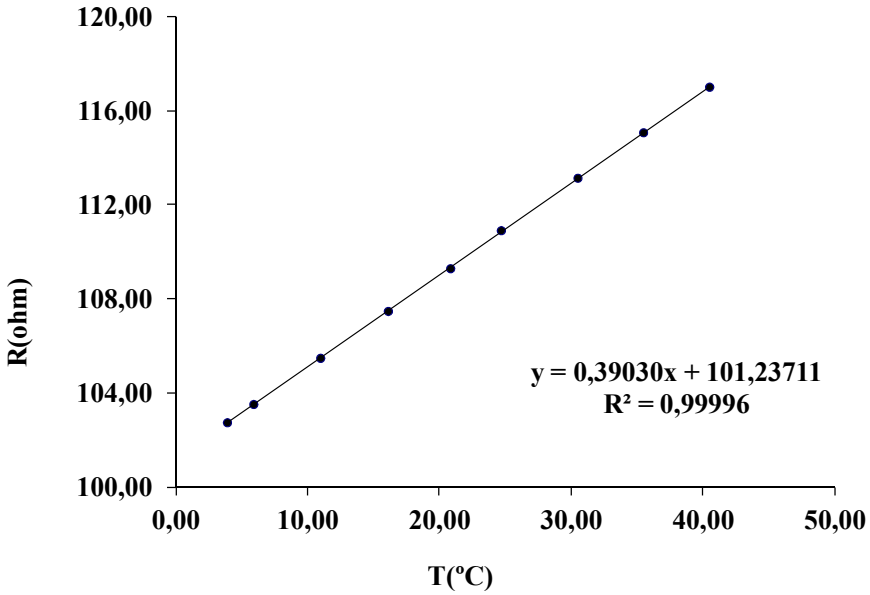

Figure 93 – Relationship between output signal of the temperature sensor and a standard thermocouple.